

Design and Development of a High Capacity 20K Pulse Tube Cryocooler

By
Avi Friedman

A thesis submitted in partial fulfillment of
the requirements for the degree of

Master of Science
(Mechanical Engineering)

at the
UNIVERSITY OF WISCONSIN – MADISON
2015

This page intentionally left blank

Approved By

Professor Franklin K. Miller

Date

Professor John M. Pfotenhauer

Date

This page intentionally left blank

Abstract

For future space exploration missions it is important to be able store cryogenic propellants for long periods of time, in particular storing liquid hydrogen which has a boiling point of 20.28K. Currently, there is a lack of high capacity, light weight, and highly efficient cryogenic cooling systems. The objective of this research has been the development of a two-stage pulse tube cryocooler with a 1W or larger cooling capacity at 20K. To accomplish this, the researchers at the University of Wisconsin are working with the Georgia Tech Cryo Lab. It has been the responsibility of the University of Wisconsin researchers to do the mechanical design, the design of the transition regions and to build and test a two stage 20K pulse tube cryocooler. To ensure that the cooler wouldn't fail when pressurized the mechanical design was done following the ASME pressure vessel code and using finite element analysis, a full set of mechanical drawings was created using Solidworks. A pores flow study was conducted using ANSYS Fluent which showed that transition regions are needed in order for the cooler to fully utilize its heat exchangers and regenerators. Multiple flow studies were done to optimize the design of these transition regions. Once the design of the cooler was done the cooler was manufactured and instrumented by the researchers. The instrumentation was read by a LabVIEW code and analyzed using MATLAB and Excel. After the first round of testing to two stage PTC reached a no load temperature of 121K. The underperformance of the cooler can be predominately attributed to a lack of acoustic power provided by the compressor. The acoustic power can be greatly improved by slightly increasing the frequency of the compressor. The failure to reach 20K is also due to poor packing of the regenerator. Alteration of the PTC and the compressor is ongoing and will hopefully drastically improve the performance of the cooler.

Acknowledgements

Franklin and Jim, I've learned more from meeting with the two of you then I did in my entire undergraduate career. Franklin, your ability to quickly come up with a back of the envelope calculation that is representative of an extremely complex engineering problem never ceases to amaze and inspire me. Jim, I truly enjoyed spending hours with you learning how a pulse tube cryocooler actually works and I hope to someday replicate the way that you analyze whether a system is actually buildable or not. John, thank you for giving Franklin, Jim, and me so much guidance for the past two years. Sandy and Greg, the thermodynamics and heat transfer courses that you guys teach are two of the best courses that I have ever taken.

Thank you to all of my lab mates and MANY undergrads. Not only have you helped me with my course work and my research but you've made my time in Madison a lot of fun.

Last thanks to the fam: Mom, Unki Dave, Mariss, Z-man double quick, and Bri I'll see y'all soon!

Table of Contents

Abstract.....	i
Acknowledgements.....	ii
List of Figures.....	v
List of Tables.....	vii
Nomenclature.....	i
1. Introduction.....	1
1.1 Objective.....	1
1.2 The Stirling Cryocooler.....	2
1.2.1 The Regenerator.....	3
1.2.2 The Cryogenic Stirling Cycle.....	6
1.4 Pulse Tube Cryocooler.....	8
1.4.1 Designing a PTC.....	9
1.3.2 Advantages of a PTC.....	11
2. Mechanical Design of Two Stage Pulse Tube.....	12
2.1 Introduction.....	12
2.2 Overall System.....	12
2.3 Preexisting Lab Setup.....	15
2.3.1 Compressor.....	16
2.3.2 Aftercooler.....	16
2.3.3 Conical Adaptor.....	17
2.4 Heat Flow through the Cooler.....	18
2.4.1 Common Heat Exchanger.....	19
2.4.2 75K Bus Bar.....	20
2.5 1 st Stage Pulse Tube Cryocooler.....	21
2.5.1 1 st Stage Regenerator.....	22
2.5.2 1 st Stage Cold Heat Exchanger.....	23
2.5.3 1st Stage Pulse Tube.....	24
2.5.4 Top 300K Heat Exchanger.....	25
2.5.5 1 st Stage Inertance Network.....	27
2.6 2 nd Stage Pulse Tube Cryocooler.....	28
2.6.1 Precooler Design.....	28

2.6.2	Bottom 75K Heat Exchanger	29
2.6.3	2 nd Stage Regenerator	30
2.6.4	20K Cold Heat Exchanger	32
2.6.5	2 nd Stage Pulse Tube	33
2.6.6	Top 75K Heat Exchanger.....	35
2.6.7	2 nd Stage Inertance Network	36
3.	Modeling the Transition Regions.....	37
3.1	Introduction	37
3.2	20K Heat Exchanger Transition Region	37
3.3	Top 2 nd Stage Transition Region.....	45
3.4	Transition Zones in the 1st Stage	47
4.	2 nd Stage Pulse Tube Cryocooler Testing	49
4.1	Introduction	49
4.2	Preliminary Testing.....	50
4.2.1	Hydrostatic Pressure Testing	50
4.2.2	Leak Testing.....	51
4.3	Experimental Setup and Data Collection	52
4.3.1	Keeping the 2 nd Stage Hot Heat Exchangers at 75K.....	52
4.3.2	Reducing Heat Transfer to the Surroundings.....	56
4.3.3	Instrumentation	61
4.3.4	Data Acquisition	62
4.4	Data Analysis	66
4.4.1	Determining the Mass Flow.....	66
4.4.2	Phase Angle between Mass Flow and Pressure	67
4.5	Results, Troubleshooting, and Conclusions	71
5.	Full PTC Testing.....	75
5.1	Introduction	75
5.2	Experimental Setup and Data Collection	76
5.3	Results	78
5.4	Conclusions and Recommendations.....	80
	References.....	82
	Appendix A: Mechanical Drawings.....	83
	Appendix B: ESS and MATLAB Code	104

List of Figures

Figure 1.1: NASA's cryogenic propellant storage tank (NASA 2013)	1
Figure 1.2: (a) Stirling cycle cooler (b) P-V diagram of an idealized Stirling cryogenic cycle 3	
Figure 1.3: Specific heat of regenerator materials (a) (Klein 2012) (b) (Alar 2013).....	5
Figure 1.4: Cycle of a Stirling type cryocooler.....	7
Figure 1.5: Diagram of the PTC	8
Figure 1.6: AC circuit analogy representing a PTC.....	9
Figure 2.1. The two-stage PTC	15
Figure 2.2: The aftercooler	17
Figure 2.3: The unfilled conical adaptor.....	18
Figure 2.4: 75K heat flow in the two stage PTC.....	19
Figure 2.5: Steady state 3D conduction model of the common heat exchanger.....	20
Figure 2.6: Temperature rise over the bus bar as a function of cross sectional area	21
Figure 2.7: Tongue and groove arrangement used for an indium seal.....	22
Figure 2.8: The regen loader and pistons.....	23
Figure 2.9: Common HX (left) is the bottom 75K HX (right) is the 1 st stage cold HX	24
Figure 2.10: The 1 st stage PT and top 300K heat exchanger	24
Figure 2.11: The top 300K heat exchanger and transition region.....	25
Figure 2.12: Temperature the 300K HX based on power dissipation and water velocity	27
Figure 2.13: 1 st stage reservoir.....	28
Figure 2.14: Design of the 2 nd stage regenerator	31
Figure 2.15: Thermal conductivity of copper as a function of temperature and purity	33
Figure 2.16: The 2 nd stage pulse tube, 20K heat exchanger, and 2 nd stage regenerator.....	34
Figure 2.17: 3D conduction model of the top 75K heat exchanger	35
Figure 2.18: (a) VCR to NPT connection (b) 2 nd stage inertance network and 75K bus bar .	36
Figure 3.1: Geometry used to model the 2 nd stage PT to 20K heat exchanger transition	38
Figure 3.2: Mesh used to model the 2 nd stage PT to 20K heat exchanger transition	38
Figure 3.3: Flow field between the 2 nd stage PT and the 20K heat exchanger	39
Figure 3.4: Velocity profiles in the 20K heat exchanger and 2 nd stage regenerator	40
Figure 3.5: Mesh for (a) ½ cm void (b) ¼ cm void (c) ¼ cm conical void	41
Figure 3.6: Flow fields in the 20K HX (a) ½ cm (b) ¼ cm (c) ¼ cm conical void	42
Figure 3.7: Velocity profile in 20K HX (a) ½ cm (b) ¼ cm (c) ¼ cm conical void	43
Figure 3.8: Streamlines for fluid entering at the 2 nd stage regenerator	44
Figure 3.9: Transition zone between the 2 nd stage PT and 20K heat exchanger	45
Figure 3.10: (a) Geometry (b) mesh and (c) results of the 75K top hot HX transition region	46
Figure 3.11: Transition zone between the 2 nd stage PT and the top 75K heat exchanger	47
Figure 3.12: Transition zone between the 1 st stage cold heat exchanger and the 1 st stage PT	48

Figure 3.13: Transition zone between the top 300K HX and the 1 st stage inertance tube.....	48
Figure 4.1: 2 nd stage PTC.....	49
Figure 4.2: Hydrostatic pressure test	51
Figure 4.3: Part used to attach copper straps to other components.....	53
Figure 4.4: Temperature distribution in thermal buses	55
Figure 4.5: Top and bottom thermal buses	55
Figure 4.6: Cryogenic Dewar.....	56
Figure 4.7: Conductivity of air in a vacuum (Barron 1985)	57
Figure 4.8: Percent improvement due to number of Mylar sheets.....	58
Figure 4.9: Experiment covered in MLI	58
Figure 4.10: Shielding of 20K HX.....	60
Figure 4.11: Spectral Distribution at 75K.....	60
Figure 4.12: Thermal Program: (a) the front panel (b) the block diagram	64
Figure 4.13: Mechanical program: (a) the front panel (b) the block diagram	65
Figure 4.14: Mass flow through the 2 nd stage PTC as a function of the current.....	67
Figure 4.15: Results and corresponding Fourier series (a) P1 (b) L.....	69
Figure 4.16: Results and Fourier transform (a) P1 (b) L	70
Figure 4.17: Cool down of the 2 nd Stage PTC	71
Figure 4.18: Pressure and stroke as a function of frequency	72
Figure 4.19: The transfer-line	73
Figure 5.1: (a) Separate 1 st stage and 2 nd stage PTC (b) two stage PTC.....	75
Figure 5.2: Locations of instrumentation used for the two stage PTC	77
Figure 5.3: Stroke and pressure ratio of the compressor with two stage PTC mounted.....	78
Figure 5.4: Cooling Curve for the two stage PTC	79
Figure 5.5: Pressure and mass flow as a function of frequency.....	81

List of Tables

Table 2.1: Specifications for the flanges and Tubes	13
Table 2.2: Critical Parameters for Compressor.....	16
Table 3.1: Vertex locations for Figure 3.1	38
Table 3.2: Regenerator Test Section Boundary and Region Definitions.....	38
Table 3.3: Porous Zone Parameters for the 20K Heat Exchanger and Regenerator.....	39
Table 3.4: Vertex locations for Figure 3.10.....	46
Table 3.5: Test Section Boundary and Region Definitions	46
Table 4.1: GM Cooling Curve	52
Table 4.2: Location of Each Sensor.....	61
Table 4.3: Pressure Drop and Mass Flow over the Precooler.....	74

Nomenclature

A	Cross-sectional area
A_p	Area of piston
A_s	Surface area
C_2	Internal resistance
C	Capacitance
C_C	Capacitance of compressor
C_{CHX}	Capacitance of cold HX
C_{HHX}	Capacitance of hot HX
C_{PT}	Capacitance of PT
C_R	Capacitance of regenerator
C_V	Capacitance of reservoir
C_{THX}	Capacitance of top HX
D_p	Particle diameter
\dot{E}	Acoustic power
\dot{E}_e	Experimental acoustic power
\dot{E}_{SAGE}	Models acoustic power
h	Heat transfer coefficient
i	$\sqrt{-1}$
k	Thermal conductivity
L	Inertance
L_I	Inertance of inertance tube
l	Length
\dot{m}	Mass flow
P	Pressure
P_a	Pressure amplitude
P_e	Electrical Power
P_m	Mean pressure
P_{max}	Maximum pressure
PR	Pressure ratio
q	Heat flow
R	Gas constant for helium
R_C	Resistance in compressor
R_{CHX}	Resistance of cold HX
R_e	Electrical Resistance
R_{HHX}	Resistance of hot HX
R_I	Resistance of inertance tube
R_i	Resistance from node i-1
r_i	Inside radius
r_o	Outer radius
R_R	Resistance of regenerator
R_{THX}	Resistance of top HX
R_v	Resistance due to viscous effects
s	Displacement

s_0	Peak Displacement
T	Temperature
T_0	Temperature of the GM cooler
T_∞	Temperature of the cooling water
T_C	Temperature at the cold end
T_H	Temperature at the hot end
T_i	Temperature of the nodes
T_n	Temperature of the HX
t	Time
th	Thickness
V	Volume
V_e	Voltage
v	Velocity

Greek

α	Viscous resistance
γ	Specific heat ratio
δ_v	Viscous penetration depth
Δ	Change of a variable
ε	Emissivity
λ	Wavelength
μ	Viscosity
Π	Perimeter
ρ	Density
ρ_m	Mean density
σ_{all}	Allowable stress of the material
ϕ	Void fraction
$\phi_{P\dot{m}}$	Phase between P and \dot{m}
ω	Angular frequency

1. Introduction

1.1 Objective

For future space exploration missions it is necessary to be able to refuel when not on earth. Therefore, it is important to be able store propellants for long periods of time using a device like the one in Figure 1.1, in particular storing liquid hydrogen which has a boiling point of 20.28K and is about 870 times as dense as gaseous hydrogen at room temperature. However, there is a lack of high cooling capacity, low temperature, and highly efficient cryogenic cooling systems. The current state-of-the-art 20K pulse tube cryocoolers (PTC) have a cooling capacity of 1W and a specific power of 180 W/W (produce 1W of cooling for 180W of electrical input). However for future exploration 20K cryocoolers with a cooling capacity of at least 20W and a specific power of approximately 100 W/W will be required (NASA 2013). The high cooling capacity is required to offset the parasitic loads due to conduction and radiation heat loads. This will decrease loss due to boil off. The objective of this research is to design and build a two-stage PTC with a 3W or larger cooling capacity at 20K. This technology also has potential applications in sensor cooling, magnetic resonance imaging machines (MRI), and super conductors.

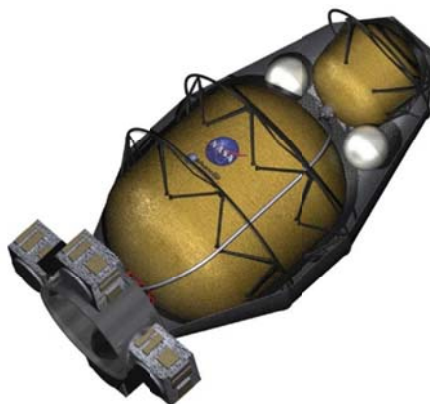


Figure 1.1: NASA's cryogenic propellant storage tank (NASA 2013)

To design and develop a high capacity 20K PTC, the researchers at the University of Wisconsin are working with the Georgia Institute of Technology Cryogenics Lab. It is the responsibility of the University of Wisconsin to do the mechanical design, including the design of the transition regions between sections of the cooler, and to build and test the two stage 20K PTC. The researchers at Georgia Tech were responsible for the majority of the thermal fluid modeling which was done using SAGE and REGEN. The following thesis is an in depth description of the work that was accomplished by the researchers at the University of Wisconsin and is organized in chronological order. It includes a description of the mechanical design process, the fabrication, testing and instrumentation of both individual components and the entire system, the design of the transition regions and the results from the testing. This chapter will give the reader a basic understanding of how the system works.

1.2 The Stirling Cryocooler

To understand how a PTC works it is necessary to understand how the Stirling cryogenic cycle works, since the cycle and components of the two systems are very similar. The Stirling cooler and P-V cycle diagram are shown in Figure 1.2. The cooler consists of two linear compressors: one at the hot end of the cooler and the other at the cold end. Also, at the hot end there is a heat exchanger which rejects heat. At the cold end there is a cold heat exchanger which accepts heat from the load. The heat accepted by the cold heat exchanger is the cooling power for the cooler. The last component needed for the Stirling cryogenic cycle is the regenerator which is located in-between the hot and cold heat exchangers. It is desirable to use a working fluid that behaves as an ideal gas for Stirling type cycles. Helium has the lowest critical temperature and therefore is used for low temperature coolers.

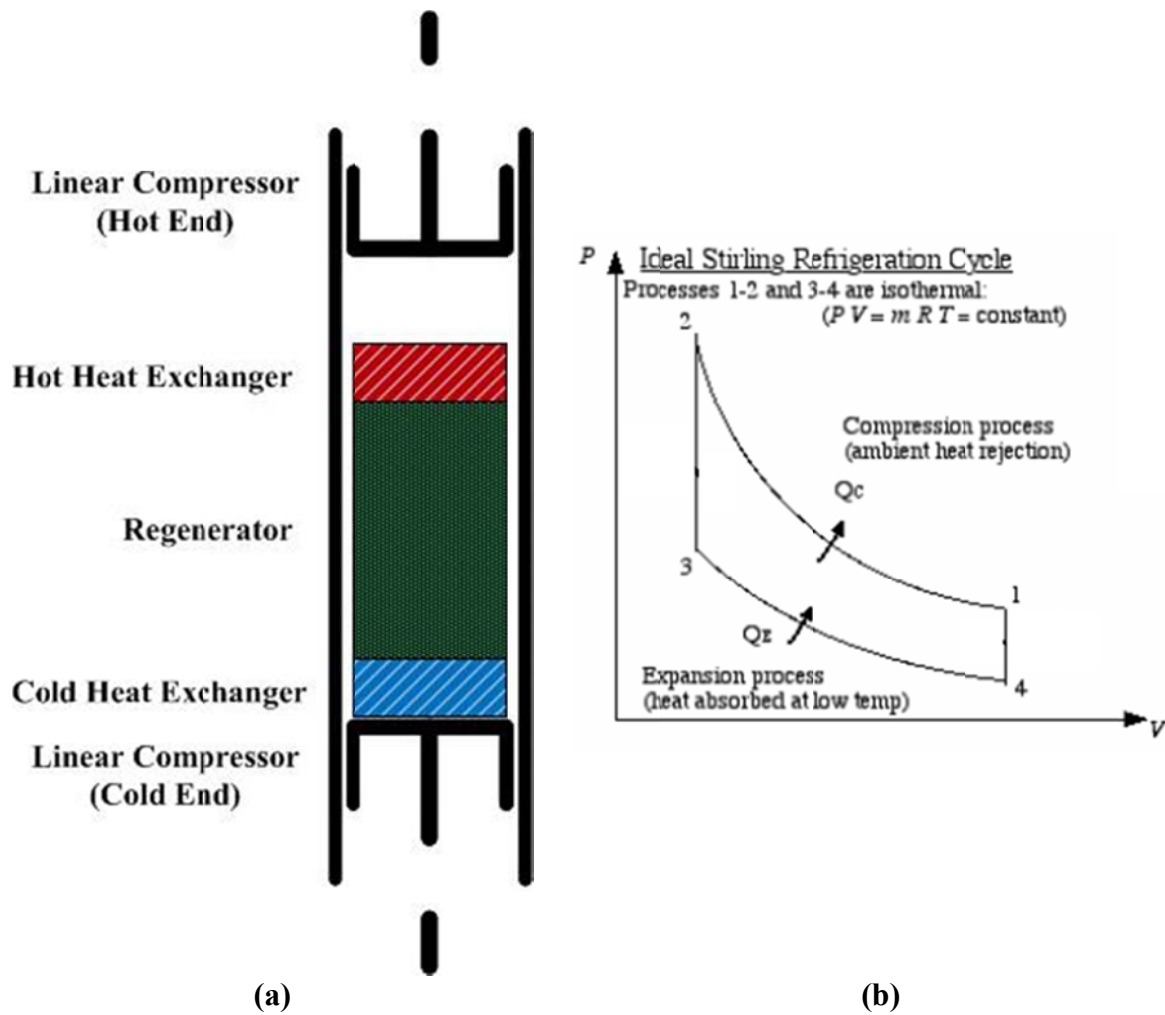


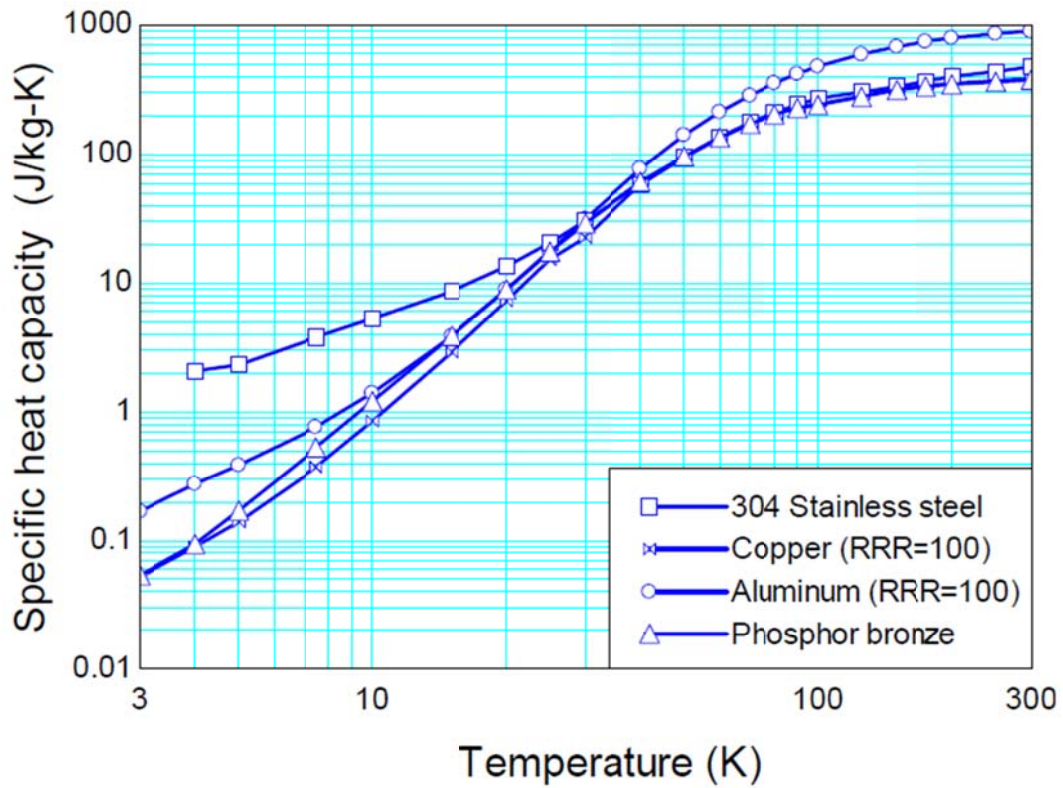
Figure 1.2: (a) Stirling cycle cooler (b) P-V diagram of an idealized Stirling cryogenic cycle

1.2.1 The Regenerator

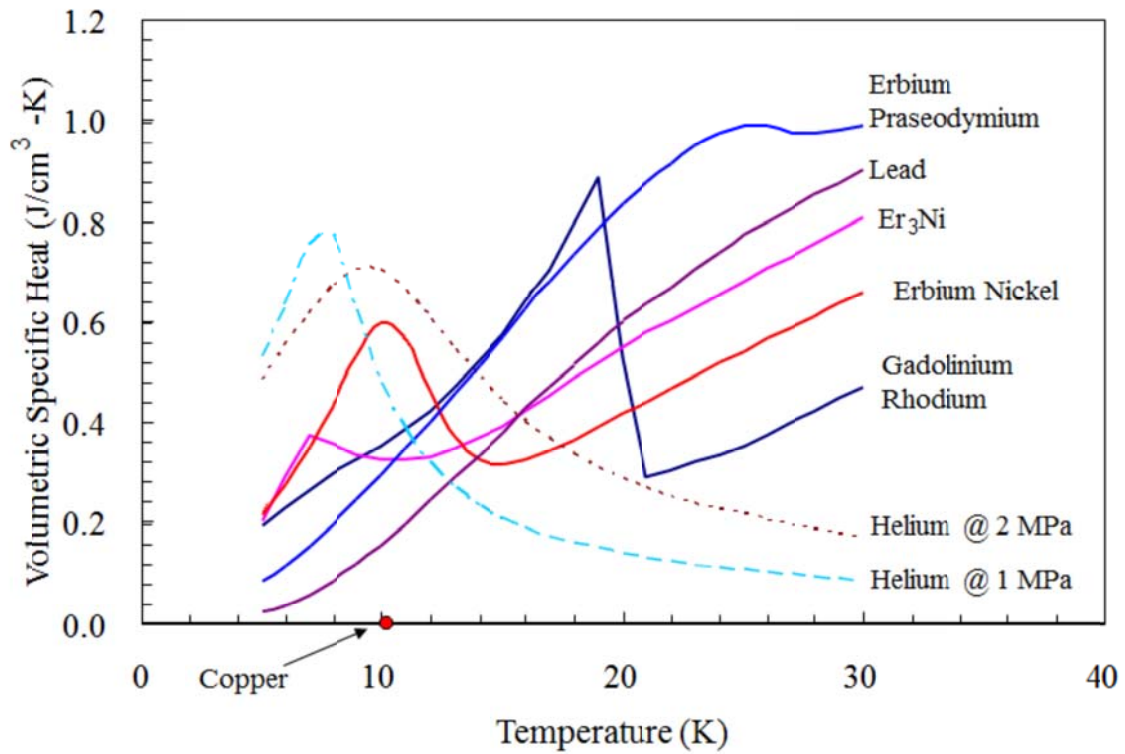
The regenerator is a solid-to-fluid heat exchanger where the hot and cold fluids occupy the same space at different times. When the working fluid goes from the hot end to the cold end the regenerator matrix accepts energy. Conversely, when the fluid goes from the cold end to the hot end, the regenerator matrix rejects energy into the fluid. Since the regenerator is in-between the hot and cold end of the cooler it has a very large axial temperature gradient.

The regenerator is made up of a porous material with a high specific heat capacity at the regenerator operating temperature. A high specific heat is important so that the matrix temperature will stay relatively constant when the fluid passes through. Unfortunately, the specific heat of most solids decrease drastically with temperature, as shown in Figure 1.3a. Therefore unique materials are used for regenerators at very low temperatures as shown in Figure 1.3b (Note: the units of specific heat are different in Figure 1.3 a and b). The unique aspect of the 20K PTC lies in the design of the 2nd stage regenerator which operates between 75K-20K. The matrix in this regenerator is a packed bed of 50% Erbium and 50% Praseodymium (ErPr) 45 μ m, particles. By changing the ratio of the particles, the specific heat of the matrix can be optimized for the temperature at which the regenerator operates.

The 20K PTC also has two other regenerators that operate from 300K-75K and are composed of 400 stainless steel mesh screens. All of the regenerators used in this project were designed by the Georgia Tech Cryo Lab using REGEN. REGEN is a numerical tool developed by NIST to model the performance of regenerators at cryogenic temperatures.



(a)



(b)

Figure 1.3: Specific heat of regenerator materials (a) (Klein 2012) (b) (Alar 2013)

1.2.2 *The Cryogenic Stirling Cycle*

The following is a step by step description of how the cryogenic Stirling cycle operates:

State 1 to 2 (Compression): At state one all the fluid is at the hot end (assuming a negligible void volume in the regenerator). Then, the linear compressor on the hot end compresses the fluid. The compression occurs isothermally due to the heat rejection through the hot heat exchanger. This increases the pressure in the cooler while keeping the temperature at T_H .

State 2 to 3 (Hot-to-Cold Blow): In this step the working fluid is shuttled from the hot end to the cold end in an isochoric process. The fluid goes through the regenerator where the regenerator matrix accepts energy carried by the fluid. When the fluid reaches the end of the regenerator it is at the temperature of the cold heat exchanger (T_C).

State 3 to 4 (Expansion): At state three all the fluid is at the cold end assuming a negligible void volume in the regenerator. Then, the linear compressor on the cold end expands the fluid, the expansion occurs isothermally due to the heat transfer at the cold heat exchanger. The heat transfer that occurs is the cooling capacity of the cooler per cycle. This step also brings the pressure inside the cooler back to its original pressure.

State 4 to 1 (Cold-to-Hot Blow): In the final step of the Stirling cryogenic cycle the fluid is shuttled from the cold end to the hot end in an isochoric process. The fluid goes through the regenerator where the regenerator matrix rejects energy to the fluid. When the fluid reaches the end of the regenerator it is at the temperature of the hot heat exchanger (T_H). A diagram showing this cycle is shown in Figure 1.44.

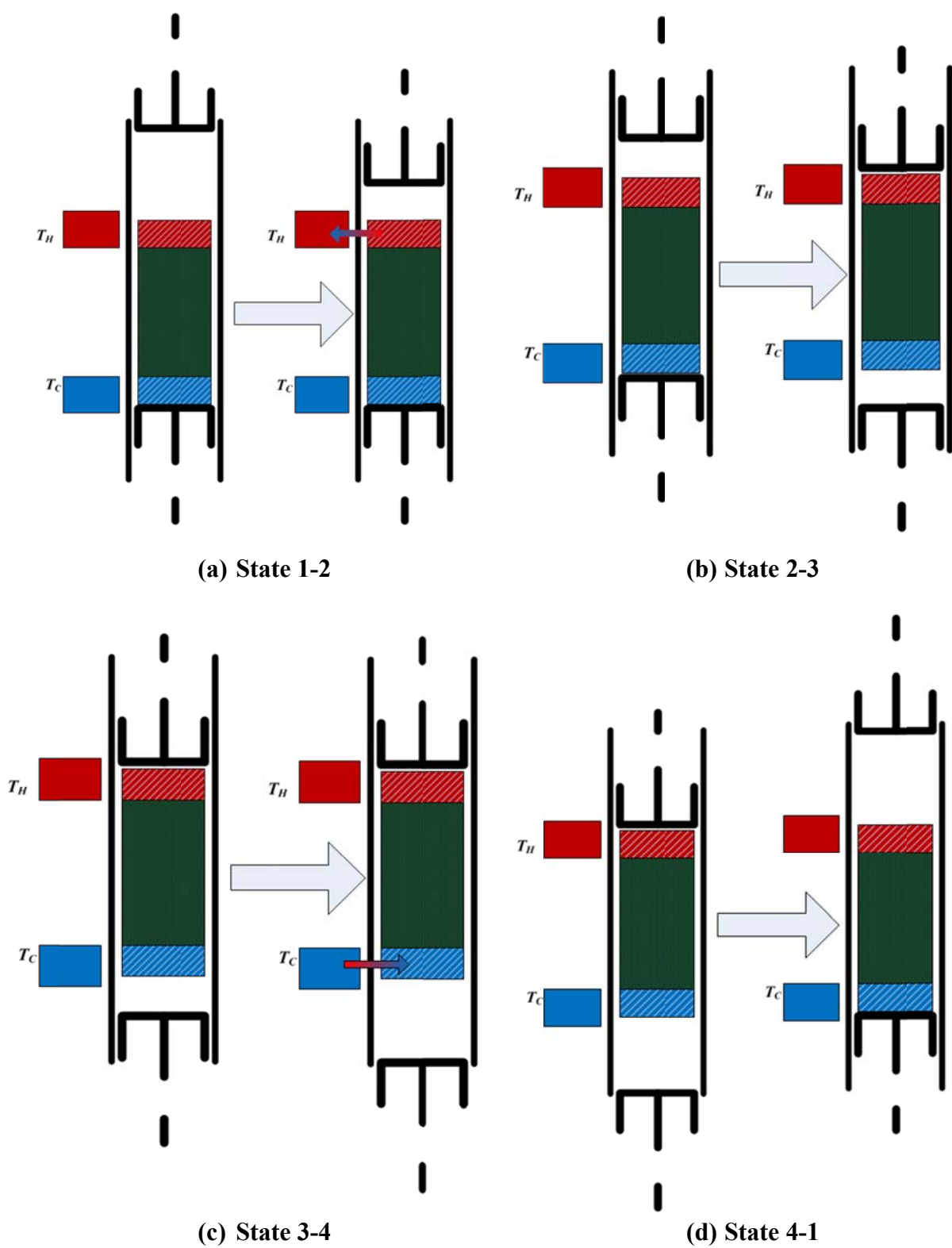


Figure 1.4: Cycle of a Stirling type cryocooler

1.3 Pulse Tube Cryocooler

As discussed above, the pulse tube cryocooler being designed follows the cryogenic Stirling cycle. However, the mechanical piston at the cold end is replaced by a pulse tube, a hot heat exchanger, an inertance tube and a reservoir as shown in Figure 1.5. The fluid in the pulse tube has a very uniform velocity profile and therefore acts as a fluid piston. Since the pulse tube's fluid piston can't be directly controlled like a mechanical piston in a compressor, the pressure and mass flow are kept in the correct phase by setting the geometry of an inertance tube. At the end of the inertance tube is a large reservoir which simulates an infinitely large open space. The reservoir is used to ensure that there are no reflections back into the pulse tube. The hot heat exchanger located in-between the pulse tube and the inertance tube is used to reject all the extra heat due to the addition of the pulse tube system. Since the pulse tube is in-between the cold heat exchanger and the second hot heat exchanger there is a significant temperature gradient in the pulse tube.

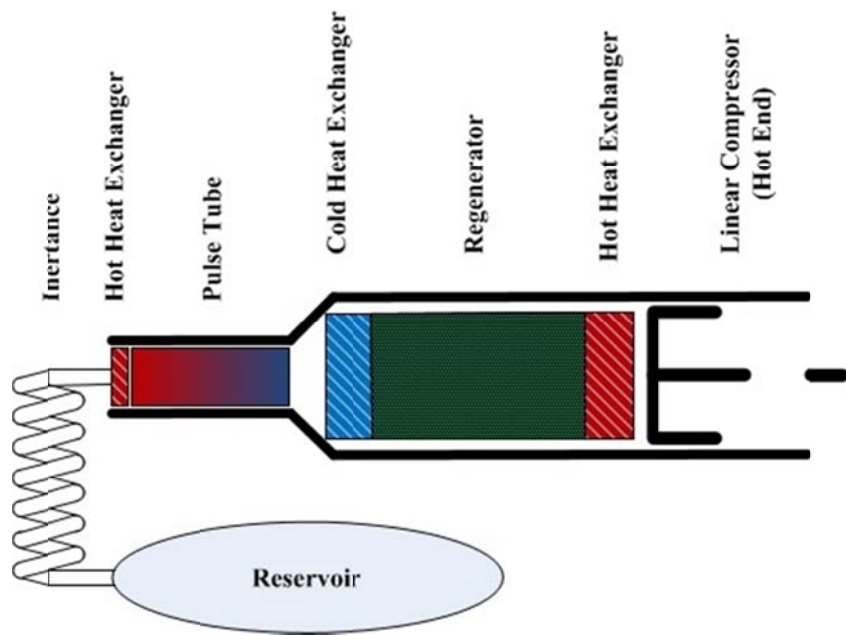


Figure 1.5: Diagram of the PTC

1.3.1 Designing a PTC

This section covers basic PTC design in order for the reader to have a qualitative understanding of what changing different parameters of the PTC will do. This is accomplished by using an AC circuit analogy shown in Figure 1.6. Each component of the PTC is modeled as an impedance which controls the AC component of the mass flow and the pressure. To determine the value of the impedance the technique outlined in chapters 4 and 5 of Greg Swift's book *Thermoacoustics* was employed (Swift 2002). This technique models the pressure and mass flow as complex phasors. There are three parameters that make up the impedance: compliance, inertance and resistance. The values of these parameters depend on the geometry of the part being modeled and the working fluid.

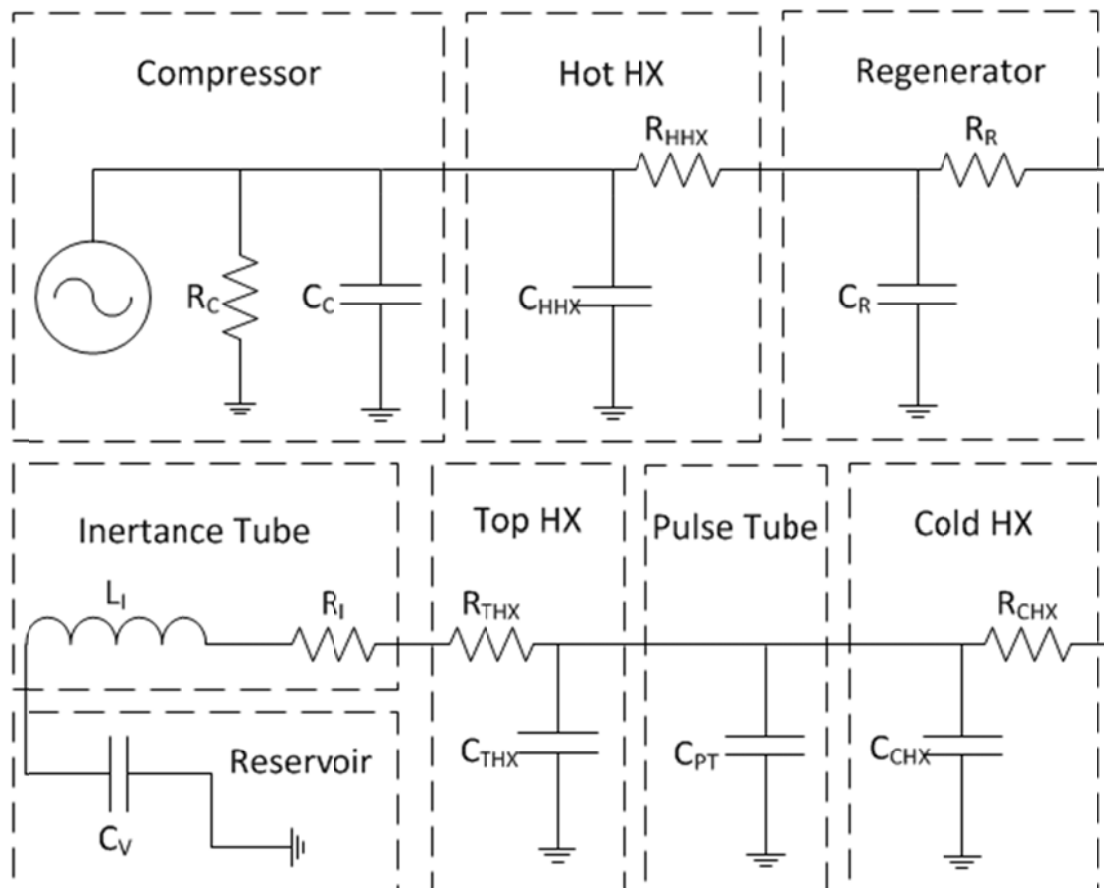


Figure 1.6: AC circuit analogy representing a PTC.

The compliance of a component determines the change in the mass flow through that component but does not change its pressure as shown in equation [1.1] where \mathbf{P} is the complex value of pressure, ω is the angular frequency, C is the compliance and $\Delta\dot{\mathbf{m}}$ is the complex value for the change in mass flow.

$$\mathbf{P} = -\frac{1}{i\omega C}\Delta\dot{\mathbf{m}} \quad [1.1]$$

The compliance of a part is a function of the volume (V) of the part, and the specific heat ratio (γ), density (ρ_m), and mean pressure (P_m) of the working fluid. Equation [1.2] is used to find the compliance of each component of the cooler.

$$C = \frac{V\rho_m}{\gamma P_m} \quad [1.2]$$

The inertance and the resistance due to viscous effects, change the pressure through the section being modeled as shown in equation [1.3]. Where $\Delta\mathbf{P}$ is the complex change in pressure, L is the inertance, and R_v is the resistance due to viscosity.

$$\Delta\mathbf{P} = -(i\omega L + R_v)\dot{\mathbf{m}} \quad [1.3]$$

The inertance is a function of the length (l) and cross-sectional area (A) of the part being modeled as shown in equation [1.4].

$$L = \frac{l}{A} \quad [1.4]$$

When the part being analyzed has a very large surface area relative to the cross-sectional area, viscous effects must be included. This is done by using a resistor (R_v) with a value derived from equation [1.5]. Where Π is the perimeter, l is the length, and A is the cross-sectional area, μ is viscosity, and δ_v is the viscous penetration depth, shown in equation [1.6].

$$R_v = \frac{\mu \Pi \Delta x}{A^2 \delta_v \rho_m} \quad [1.5]$$

$$\delta_v = \sqrt{2\mu/\omega\rho_m} \quad [1.6]$$

By calculating the compliance, inertance and resistance through the PTC phase information between the pressure and the mass flow can be determined which is useful in both design and testing the PTC.

1.3.2 Advantages of a PTC

The main advantage of the pulse tube cryocooler over other types of cryocoolers is that there are no moving parts at the cold end. This is desirable because any contaminants that get into the cooler will make it to the cold end and will either solidify or liquefy which could be detrimental to the performance and durability of a cooler if there is a mechanical piston at the cold end. Durability is extremely important in space applications because of how inaccessible a cooler is once it is launched. The absence of a mechanical piston also reduces the vibration and the electromagnetic interference.

2. Mechanical Design of Two Stage Pulse Tube

2.1 Introduction

The goal of the mechanical design was to implement the thermodynamic design created by Georgia Tech. The design had to be able to withstand 400psi on the inside of the cryocooler while also remaining leak tight in a high vacuum environment. In addition, it was advantageous to have a modular design which made it easy to remove and replace different components of the system. The following explains the detailed mechanical design of the two-stage pulse tube cryocooler.

2.2 Overall System

To ensure that the cooler would be safe to operate, the thickness of the flanges and the number of bolts needed for each flange was determined using Section VIII, Division I, Appendix 2 of the ASME Boiler and Pressure Vessel code. The code uses P_{max} , the flange and gasket material properties, the diameter of the flange, the bolt circle, and the type of bolts.

In order to make sure that the tubes can withstand the maximum internal pressure, the ASME Boiler and Pressure Vessel Code was also employed (Section VIII, Division I, Paragraph UG27). The code assumes that the tubes acts as a thin-walled pressure vessels, thus to calculate the thickness (th) equation [2.1] was used.

$$th = \frac{(P_{max}r_i)}{\sigma_{all} - 0.6P_{max}} \quad [2.1]$$

Where P_{max} is the maximum pressure, r_i is the inside radius of the tube and σ_{all} is the allowable stress of the material. This equation was used for all of the thin-walled tubes in the system where P_{max} is set at 450psi, which is slightly higher than the actual maximum pressure

of 400psi. The tubes are 304L-stainless steel so σ_{all} is 16ksi according to Section II-D of the Pressure Vessel Code.

Finite element analysis (FEA) was also employed using SolidWorks SimulationXpress in order to verify the mechanical design. FEA provides the factor of safety for each part when under 450psi. SimulationXpress allows parts to be quickly updated and reanalyzed if needed. The program also shows the areas of highest stress concentrations. The thicknesses of the flanges/tubes, bolt size and the corresponding factor of safety are shown in Table 2.1. Each flange is held in place with eight bolts.

Table 2.1: Specifications for the flanges and Tubes

Part #	Part	Type of Bolt (in)	Thickness (in)	Factor of Safety
0.1	Conical Adaptor	½ - 20	N/A	4.10
0.2	Adaptor Top Flange	½ - 20	1.250	3.26
0.3	Common Heat Exchanger	¼ - 28	N/A	29.5
1.1	1 st Regen Shell	N/A	0.065	3.43
1.2	1 st Regen Top Flange	¼ - 28	0.375	9.02
1.3	1 st PT Bottom Flange	¼ - 28	0.500	5.24
1.4	1 st PT Shell	N/A	0.049	4.19
1.5	300K HX	¼ - 28	0.787	20.1
1.6	1 st Transition Region	¼ - 28	1.000	17.2
2.1	Precooler Shell	N/A	0.039	2.75
2.2	Precooler Top Flange	¼ - 28	0.375	5.07
2.3	2 nd Regen Bottom Flange	¼ - 28	0.375	5.07
2.4	2 nd Regen Shell	N/A	0.039	2.87
2.5	2 nd Regen Top Flange	¼ - 28	0.375	5.07
2.6	20K HX	¼ - 28	0.750	12.3
2.7	2 nd PT Shell	N/A	0.039	6.73
2.8	2 nd PT Flange	#10-24	0.250	3.22
2.9	75K HX	#10-24	0.591	44.5
2.10	2 nd Transition Region	#10-24	0.750	6.20

Figure 2.1 shows the solid model of the complete assembly of the two-stage PTC with all the components labeled (the 1st stage inertance network is not shown). The 1st stage PTC is the right portion of the figure and the 2nd stage PTC is at the left. A set of mechanical drawings

has been created for the two-stage cryocooler and are included in Appendix A:

Mechanical Drawings.

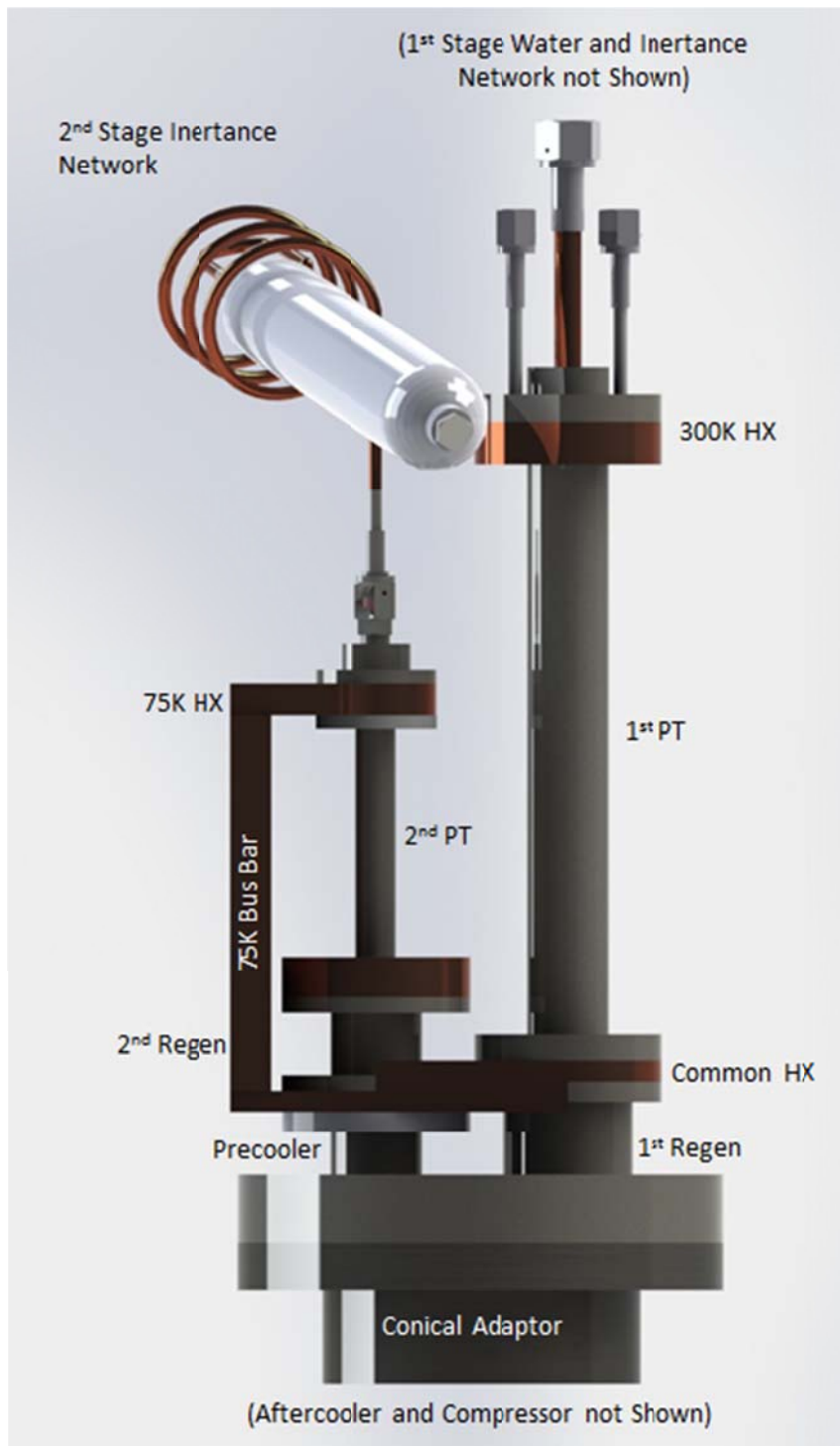


Figure 2.1. The two-stage PTC

2.3 Preexisting Lab Setup and Conical Adaptor

Both the compressor and aftercooler were in place before the cooler was designed. Therefore the cooler design was based on the capabilities of these two components. The conical adaptor was designed to connect the two stage PTC to the aftercooler and compressor.

2.3.1 Compressor

The compressor is a 77AS 2S241W “Light” water cooled pressure wave generator made by Q-Drive. The critical parameters for the compressor can be seen in Table 2.2. The peak pressure and the mass flow provided by the compressor are controlled by changing the current supplied to the compressor. The frequency for the compressor can also be set.

Table 2.2: Critical Parameters for Compressor

Maximum Rated Current	16 amps per motor
Max Operating Stroke	20 mm p-p
Area of piston (A_p)	$9.144 \times 10^{-3} \text{ m}^2$
Resistance	15.5 Watt/Bar
Volume	0.89 Liter

2.3.2 Aftercooler

Since the compressor increases the pressure of the helium the temperature of the helium also increases. Therefore is important to cool the helium in order for it to enter the conical adaptor at or below the ambient temperature. The aftercooler is a cross flow heat exchanger, as shown in Figure 2.2, where the blue arrows represent the flow of the cooling water and the red arrow represents the flow of helium. The helium is transported through 199 5.5” long, 0.095” diameter tubes which run parallel to one another. The cooling water passes over these tubes 4 times.

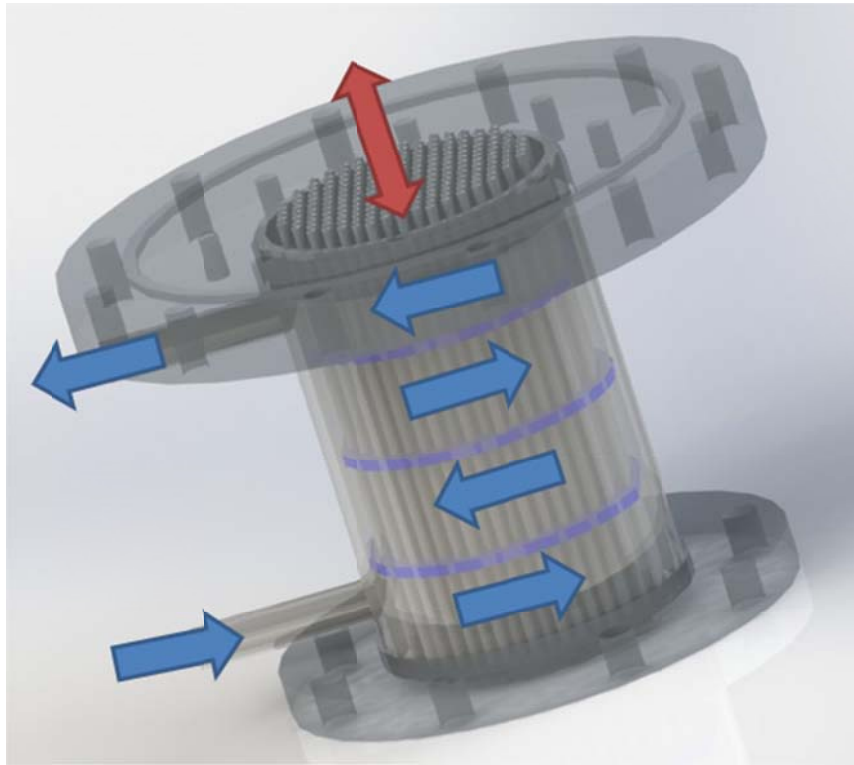


Figure 2.2: The aftercooler

2.3.3 Conical Adaptor

The maximum diameter of a flange that can be bolted to the aftercooler is 6". Unfortunately, the diameter of the bottom flange of the two stage PTC had to be 9" due to the size of the 1st stage regenerator and precooler. Therefore, the conical adaptor shown in Figure 2.3 was designed. To enable a smooth transition between the aftercooler and the PTC the conical adaptor was sized so that it does not cover any of the aftercooler tubes, the precooler, and the 1st stage regenerator.

Since the conical adaptor is located below the precooler and 1st stage regenerator, heat is rejected into it. Therefore it needs to transport this energy to the aftercooler to stay at room temperature. To do this, the adaptor was filled with 60 mesh copper screens to conduct energy from the precooler and the 1st stage regenerator into the aftercooler.

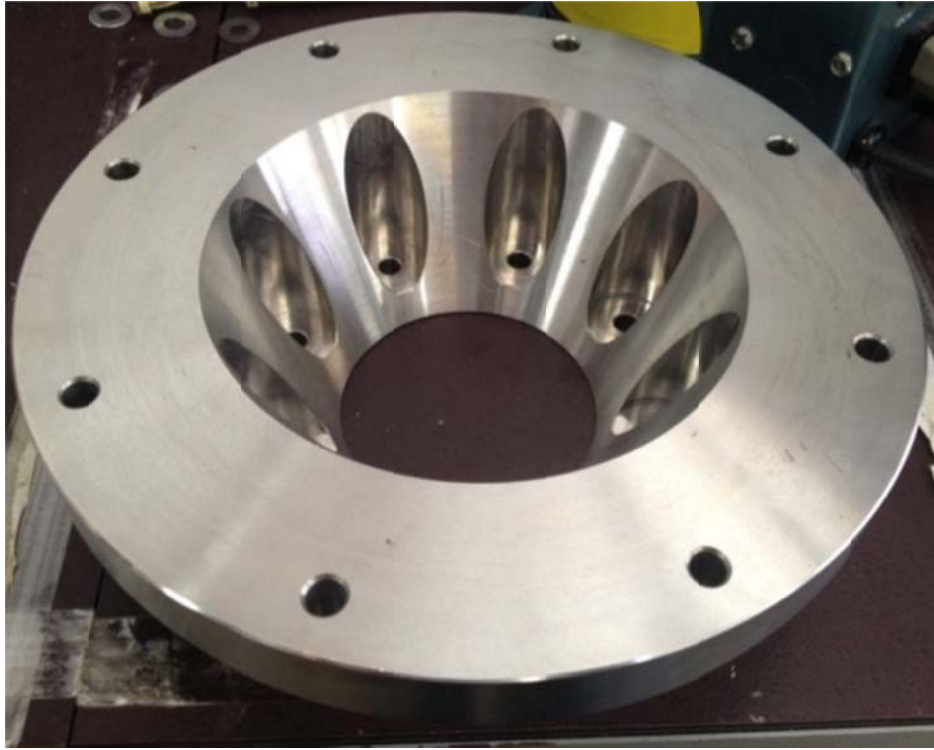


Figure 2.3: The unfilled conical adaptor

The top of the conical adaptor connects to the adaptor top flange which is where the precooler and 1st stage regenerator are located. O-rings are used to seal the conical adaptor to the aftercooler and to the adaptor top flange because this component is operated at room temperature.

2.4 Heat Flow through the Cooler

The following section outlines the heat transfer analysis on the thermal network from the top 75K heat exchanger to the cold heat exchanger of the 1st stage PTC, shown in Figure 2.4. The thermal network consists of the top 75K heat exchanger thermally connected to the common heat exchanger by a bus bar. The common heat exchanger consists of the bottom 75K heat exchanger of the 2nd stage PTC and the cold heat exchanger of the 1st stage PTC.

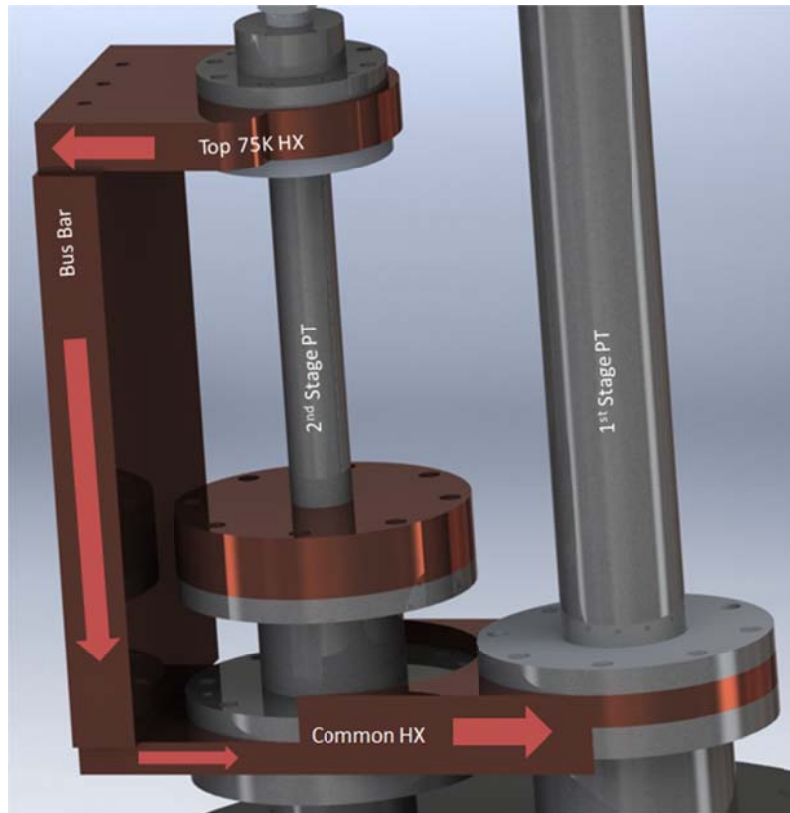


Figure 2.4: 75K heat flow in the two stage PTC

2.4.1 Common Heat Exchanger

The common heat exchanger consists of the 1st stage cold heat exchanger, the bottom 2nd stage 75K heat exchanger and a connection for the bottom of the 75K bus bar. It is important to know the change in temperature between the two heat exchangers in order to ensure that this thermal link adequately satisfies the requirements of the SAGE model. This was done by using SolidWorks Simulationxpress thermal modeling software. Using the SAGE model to predict boundary conditions, the 1st stage cold heat exchanger was fixed to accept 90W, the power input from the bus bar was 11W, and the bottom 75K heat exchanger was fixed at 75K. The result of this simulation is shown in Figure 2.5. The figure shows that the 1st stage heat exchanger will need to be at about 60K to keep the second stage at 75K which agrees with the sage model and therefore this is an acceptable design for common heat exchanger.

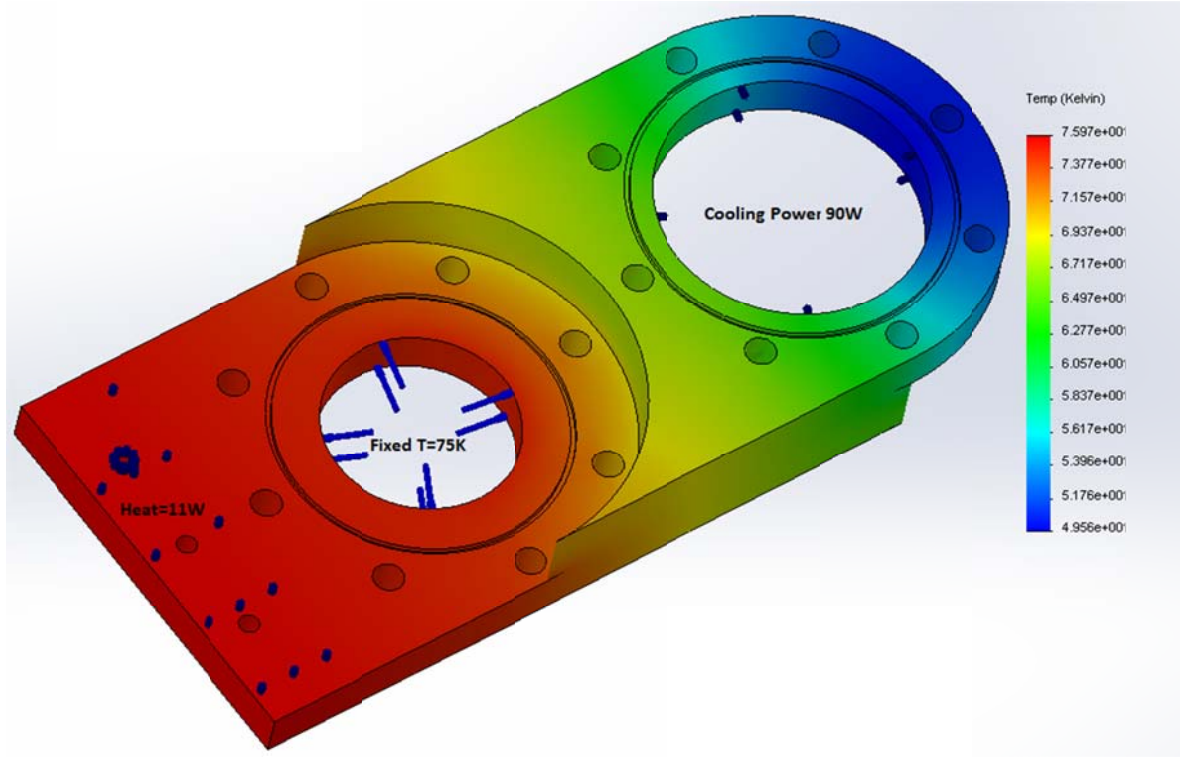


Figure 2.5: Steady state 3D conduction model of the common heat exchanger

2.4.2 75K Bus Bar

The top and bottom heat exchangers of the 2nd stage PTC need to be maintained at 75K. To achieve this, the 1st stage PTC's cold heat exchanger was thermally anchored to the bottom 2nd stage 75K heat exchanger via the common heat exchanger, which was connected to the top 2nd stage 75K heat exchanger with the thermal bus. The thermal bus was sized based on the heat loads provided from the SAGE model (11W for the top HX) along with equation [2.2]. The EES code used for this calculation can be seen in Appendix B: ESS and MATLAB Code.

$$q = \frac{A}{l} \int_{T_C}^{T_H} k(T) dT \quad [2.2]$$

Where q is the thermal load from the top heat exchanger, A is the cross sectional area of the thermal bus, l is the length from the top heat exchanger to the bottom heat exchanger, T_b is

the temperature at the bottom of the bus bar (76K from the SolidWorks simulationxpress common heat exchanger model), T_t is the temperature at the top of the bus bar, and $k(T)$ is the thermal conductivity of copper as a function of temperature. Using this equation, the temperature difference between the top and bottom heat exchanger is plotted as a function of cross sectional area as shown in Figure 2.6. A thermal bus with a cross sectional area of 3in^2 was selected because a temperature difference of 2K should not have a large effect on the performance of the cooler.

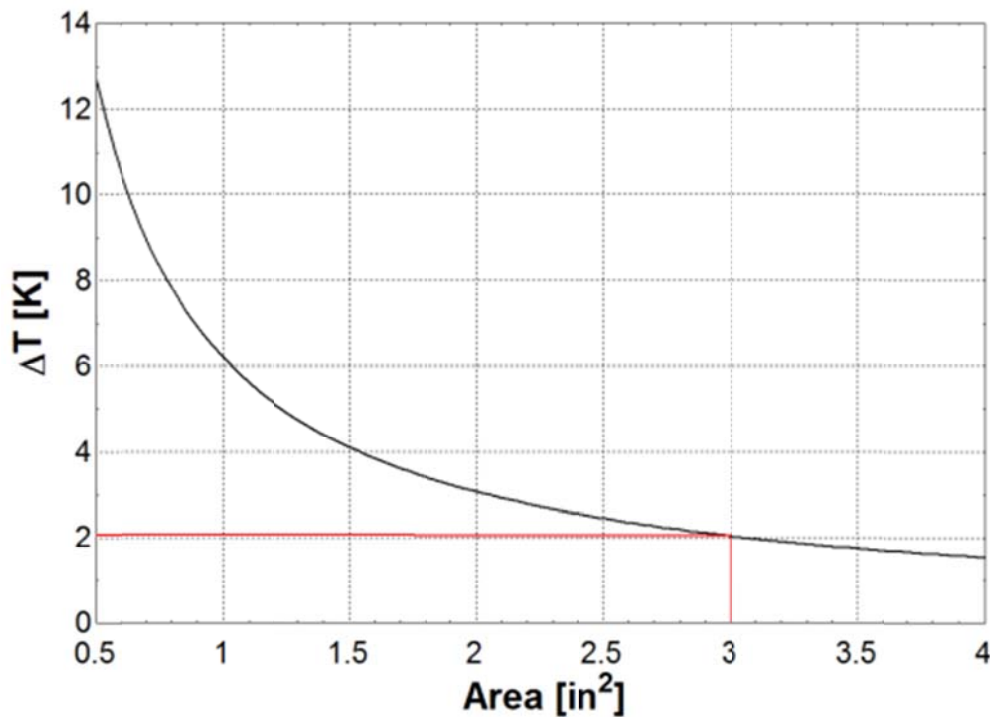


Figure 2.6: Temperature rise over the bus bar as a function of cross sectional area

2.5 1st Stage Pulse Tube Cryocooler

The 1st stage PTC cools from room temperature to 75K and provides the cooling power for the 2nd stage PTC. It consists of a regenerator, cold heat exchanger, pulse tube, hot heat exchanger and an inertance network. The following section outlines the design of these components.

2.5.1 1st Stage Regenerator

The regenerator used in the 1st stage is made from a stainless steel shell and is filled with 1300, 400 mesh 0.001” diameter wire stainless steel screens. The shell was made from an off-the-shelf tube with an inner diameter of 2.245” and a wall thickness of 0.065”. It is rated for 540psi and was cut to a length of 2.850” . The bottom of the regenerator is welded to the adaptor flange which is then bolted to the conical adapter, and is sealed with an O-ring. The top of the regenerator is welded to the 1st stage regenerator top flange which is bolted to the 1st stage cold heat exchanger and sealed using an indium ring inside a tongue and groove arrangement as shown in Figure 2.7. Indium is used because at cryogenic temperatures rubber O-rings fail. The tongue and groove design will ensure that the indium will stay in-between the flange and the heat exchanger when the cooler is under high pressure.

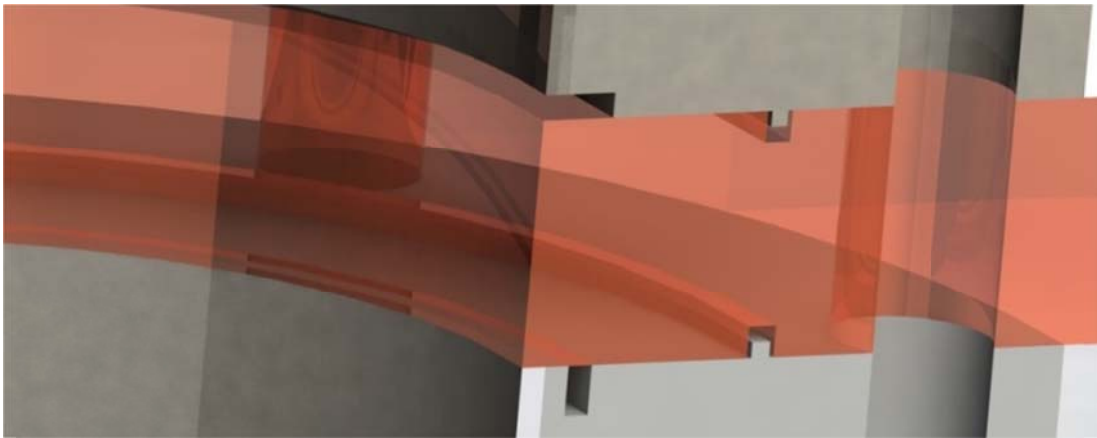


Figure 2.7: Tongue and groove arrangement used for an indium seal

To pack the screens in the 1st stage regenerator the regen loader, shown in Figure 2.8, was used. The regen loader was bolted to the adaptor top flange. Each screen was placed into the regenerator shell and compressed with a piston. Once all the screens were in, a 12 mesh 0.023” wire diameter screen was press fitted in the regenerator shell on top of the screens to

keep them from popping out. On the other side of the regenerator, the 1st stage cold heat exchanger keeps the screens from escaping.

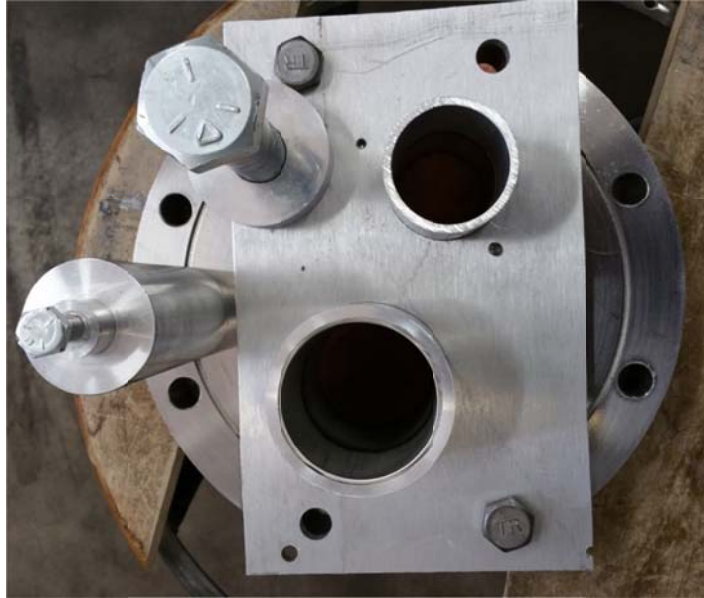


Figure 2.8: The regen loader and pistons

2.5.2 1st Stage Cold Heat Exchanger

The 1st stage cold heat exchanger is part of the common heat exchanger. It has an inner diameter 2.245" and was filled with 37, 100 mesh copper screens. The copper screens were soldered into the heat exchanger to make sure that they are secure and able to stop the screens in the 1st stage regenerator from bursting out of the top.

To solder the screens, the inner diameter of the cold heat exchanger was tinned. Then flux was put on the edge of screens and they are individually placed into the heat exchanger and compressed with a piston. The whole configuration was then heated up while still being compressed which caused the solder to wick slightly into the screens. This process was repeated until the screens were fully connected to the outside of the heat exchanger. The finished common heat exchanger is shown in Figure 2.9. The heat exchanger is in-between

the 1st stage top regenerator flange and the 1st stage pulse tube bottom flange. There is a tongue and groove indium seal between these components.



Figure 2.9: Common HX (**left**) is the bottom 75K HX (**right**) is the 1st stage cold HX

2.5.3 1st Stage Pulse Tube

The 1st stage PT is made from off the shelf seamless stainless steel tubing with an inner diameter of 1.402" and a thickness of 0.049". The tubing is rated for 1,000psi. The pulse tube is 11.138" and is welded to the 1st stage PT bottom flange and brazed to the top 300K heat exchanger as shown in Figure 2.10.



Figure 2.10: The 1st stage PT and top 300K heat exchanger

Since the pulse tube has a much smaller inner diameter than the cold heat exchanger, the 1st stage PT bottom flange has a $\frac{1}{4}$ cm conical void volume which acts as a transition region. The design of this transition region and the proof for the need of a transition region is outlined in chapter 3.

2.5.4 Top 300K Heat Exchanger

According to the SAGE model, the top 300K heat exchanger rejects 140W at 300K. Since the heat exchanger is in vacuum, cooling water was run around the outside of the screen pack (39, 60 mesh screens with 0.0075" wire diameter) to absorb energy from the helium creating a helium to water heat exchanger, as shown in Figure 2.11. The screen pack was soldered into the heat exchanger following the method outlined in section 2.5.2 1st Stage Cold Heat Exchanger. The heat exchanger was bolted to the transition region and sealed using two O-rings, one in between the water and the helium, and one in between the water and the bolt circle. The tubes for the water network and the inductance are brazed into the transition region.

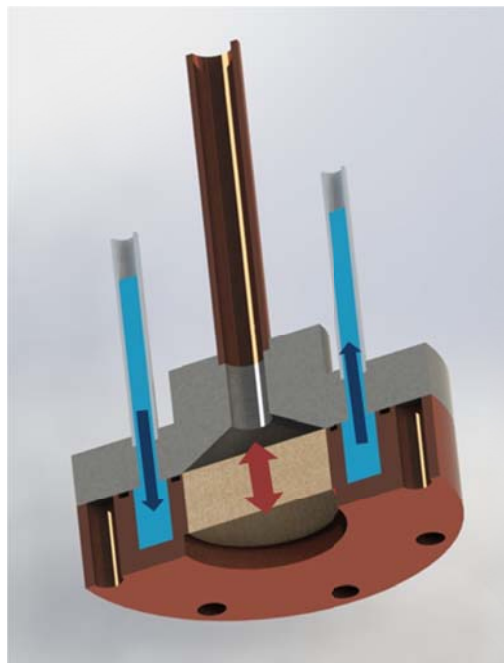


Figure 2.11: The top 300K heat exchanger and transition region

The cooling water is at 293.7K and has a volumetric flowrate of roughly 0.3L/s, which corresponds to a flow velocity of 2.2m/s. The flowrate was determined by timing how long it took to fill a 3.5 liter vessel. To find the temperature of the helium going through the screens, equation [2.3] was used. This equation assumes that the screen pack is isothermal. The EES code used for this calculation can be found in Appendix B: ESS and MATLAB Code.

$$T = q \left(\frac{\ln(r_o/r_i)}{2\pi tk} + \frac{1}{A_s h} \right) + T_\infty \quad [2.3]$$

Where T is the helium temperature, q is the heat that the heat exchanger rejects, r is the inner and outer radius, t is the thickness, k is the thermal conductivity of copper, A_s is the surface area of the wall on the inside of the water channel, h is the water's heat transfer coefficient and T_∞ is the temperature of the cooling water.

The heat transfer coefficient for the water was determined from the Reynold's number and the Prandtl number using the external flow correlation for turbulent flow around a cylinder (Nellis 2009). Since the flow is turbulent, the dominant heat transfer mechanism is the viscous sublayer, which is minimally affected by the top, bottom, and outer wall of the cooling channel. Hence this situation can be modeled by assuming turbulent flow around a cylinder.

The flow velocity and the power dissipation from the helium are the largest uncertainties when calculating the temperature of the helium. Therefore, a surface plot was created from equation [2.3] by varying both the velocity of the flow and the power dissipation, as shown in Figure 2.12. From this plot, it can be assumed that the temperature will range from 301K to 311K proving that this heat exchanger design works.

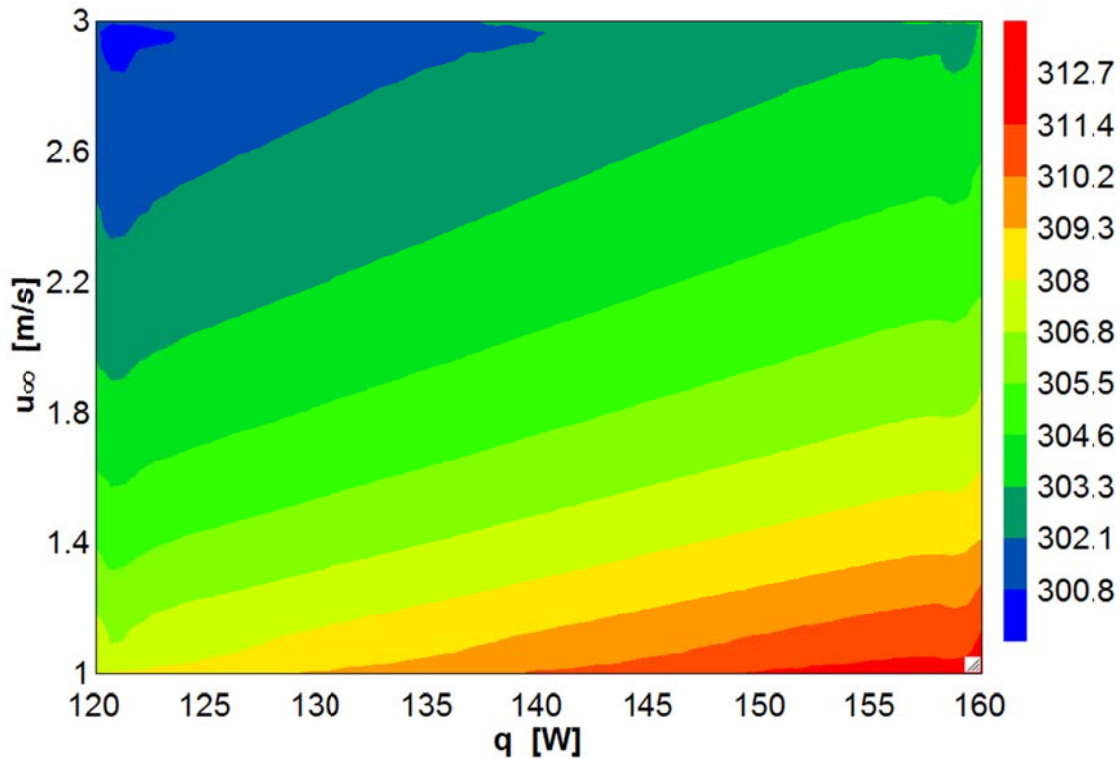


Figure 2.12: Temperature the 300K HX based on power dissipation and water velocity

2.5.5 1st Stage Inertance Network

To control the phase angle between the mass flow and the pressure, an inertance network is used. The inertance network consists of a 3.6L steel reservoir rated for 2,015psi and an inertance tube that is 2.182m long, with an inner diameter of 0.37", a thickness of 0.065 and a pressure rating of 1,400psi.

The inertance tube was brazed to the 1st stage top transition region which was bolted to the top 300K heat exchanger. The inertance tube was then welded to a KF 40 flange where it leaves vacuum space and is connected to the reservoir via a Swagelok fitting. To ensure that the inertance tube can be easily changed, each spot where there is a permanent connection (ie. a weld or braze) there is also a VCR connection.

The reservoir was specified to be 2.5L in the SAGE model, however this size was not commercially available and since the reservoir acts as an infinite volume increasing its size had no effect on the performance of the cooler. The reservoir is not only connected to the inertance tube but can also be pumped on directly by a vacuum pump as shown in Figure 2.13. This was done because it would have been difficult to clean out such a large volume when pumping through the rest of the cooler.



Figure 2.13: 1st stage reservoir

2.6 2nd Stage Pulse Tube Cryocooler

The 2nd stage PTC spans the temperature gap from 75K to 20K and is responsible for the cooling capacity of the two stage PTC at 20K. It consists of a precooler, two hot heat exchangers (75K), a regenerator, a cold heat exchanger (20K), a pulse tube, and an inertance network. The following section outlines the design of these components.

2.6.1 Precooler Design

The precooler has an inner diameter of 4.175cm, a thickness of 1mm and is 6.144cm long. It is filled with 1150, 350 mesh stainless steel screens. Since the specified shell dimensions are

not standard, the closest standard size stainless steel seamless tubing, OD:1.75"(4.445cm) th:0.065"(1.651mm) was compared to the specified tube. Conduction through the shell from the aftercooler at 300K (T_H) to the bottom hot heat exchanger at 75K (T_C) may be a problem. The size of this heat leak was found using equation [2.4] for both the specified tube ($A=1.28\text{cm}^2$, $q=4.51\text{W}$) and the standard tube ($A=2.22\text{cm}^2$, $q=7.83\text{W}$). A thermal conductivity of $k=9.6\text{W/m-K}$, was assumed to be constant for this temperature range because it varies the same for each case. Using the standard size tubing would conduct 3.32W more than the specified size, therefore the specified size was custom made. The ASME pressure vessel code required a minimum thickness of 0.597mm. Since the tube has a wall thickness of 1mm it should not fail.

$$q = \frac{kA}{l}(T_H - T_C) \quad [2.4]$$

The precooler shell is welded to two flanges that are bolted to the bottom 75K heat exchanger and the conical adaptor. The precooler top flange was designed to have an outer diameter of 3.5" and a thickness of 0.375". The connection between the precooler top flange and the bottom 75K heat exchanger is sealed using indium. The screens are packed using the regen loader in the same way that the 1st stage regenerator was packed, as discussed in section 2.5.1

1st Stage Regenerator.

2.6.2 Bottom 75K Heat Exchanger

The bottom 75K heat exchanger is part of the common heat exchanger. It has an inner diameter of 4.175cm (1.644") and is filled with 75, 145 mesh copper screens with a wire diameter of 0.0022". The copper screens are soldered into the heat exchanger, using the method discussed in section 2.5.2 1st Stage Cold Heat Exchanger, to make sure that the

screens are secure and to stop the screens in the precooler from bursting out through the top. The heat exchanger is connected to the precooler top flange and the bottom 2nd stage regenerator flange. There is a tongue and groove indium seal between these components.

2.6.3 2nd Stage Regenerator

The 2nd stage regenerator is 4.175cm long, has an inner diameter of 4.175cm and a thickness of 1mm. It is filled with ErPr 45um spheres as specified in the SAGE model. The 2nd stage regenerator is made up of four parts: two flanges, the regenerator tube, and the regenerator pellets. The shell was designed and manufactured the same way as the precooler shell.

Since the second stage regenerator is filled with powder, the flanges were designed in a unique way in order to contain the powder while simultaneously allowing helium to pass in and out of the regenerator. The design includes 400 mesh screens, used to contain the pellets, backed by 60 mesh screens, used to support the 400 mesh screens and minimize vibration. An indium ring at the screen edge prevents the particles from escaping at the perimeter. The whole assembly fits in a pocket machined into the regenerator flanges. The indium rings are heated during assembly so they stick to the 400 mesh screen. Then the ring is compressed when the regenerator is bolted into place. The design is shown in Figure 2.14. The two flanges were made so they can be bolted to the bottom 75K heat exchanger and 20K heat exchanger while being leak tight at 400 psi. This is accomplished using indium to seal the interface.

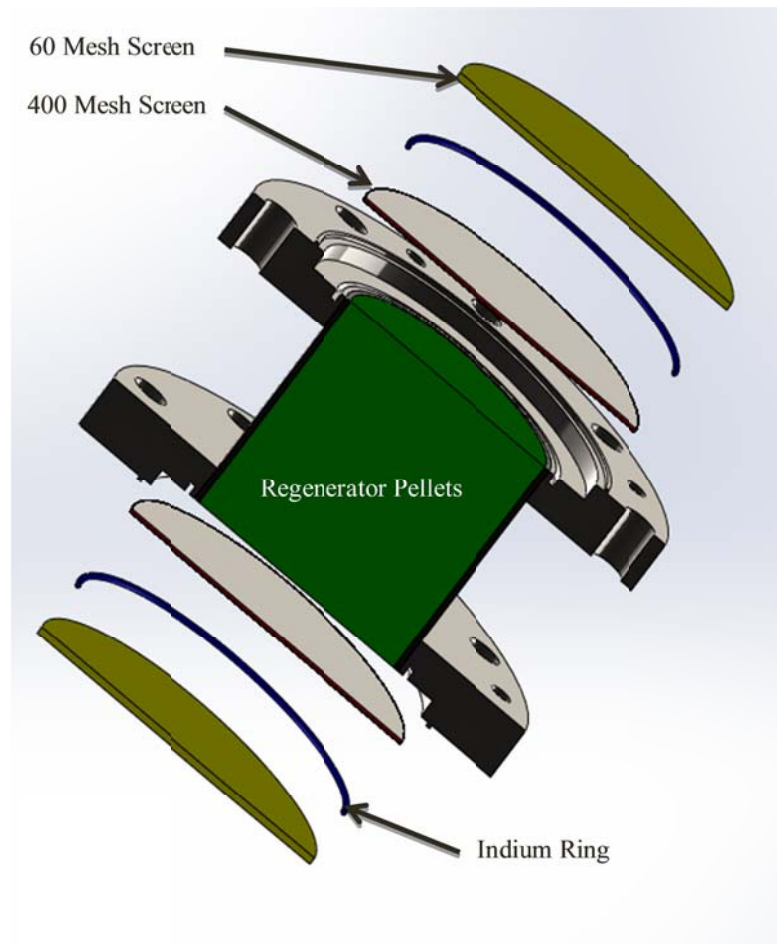


Figure 2.14: Design of the 2nd stage regenerator

In order to contain the powder both the assembly procedures and the design are important. If the powder is in an unstable configuration (i.e., the powder particles are stacked in an unstable fashion) then the possibility exists that, over time, the oscillating gas will cause particles to realign in a more stable configuration, resulting in voids. Such voids could let the powder begin to move, which would likely lead to wearing of the containment screens and eventual escape of the powder. Therefore, the powder was packed slowly while gently vibrating the regenerator to ensure a stable packing configuration. Once the packing was done the entire regenerator assembly was vibrated for 3hrs as a test to confirm that the powder would not escape.

2.6.4 20K Cold Heat Exchanger

The 20K heat exchanger is made of copper 101 (OFHC Copper). It has an inner diameter of 4.175cm, a thickness of 1cm, and is filled with copper screens. There is a transition region between the pulse tube and 20K heat exchanger in order to insure well distributed flow through these components. The transition region is discussed in Modeling the Transition Regions.

At cryogenic temperatures the thermal conductivity of copper varies greatly as shown in Figure 2.15 (Sanchez 1990). The 20K heat exchanger offers the opportunity to take advantage of this feature because the thermal conductivity of 110 copper is about 400W/m-K and the thermal conductivity of 101 copper is about 1000 W/m-K at this temperature. Since the heat load will be at the edge of the cold heat exchanger it is advantageous to have as small of a temperature gradient through the copper as possible.

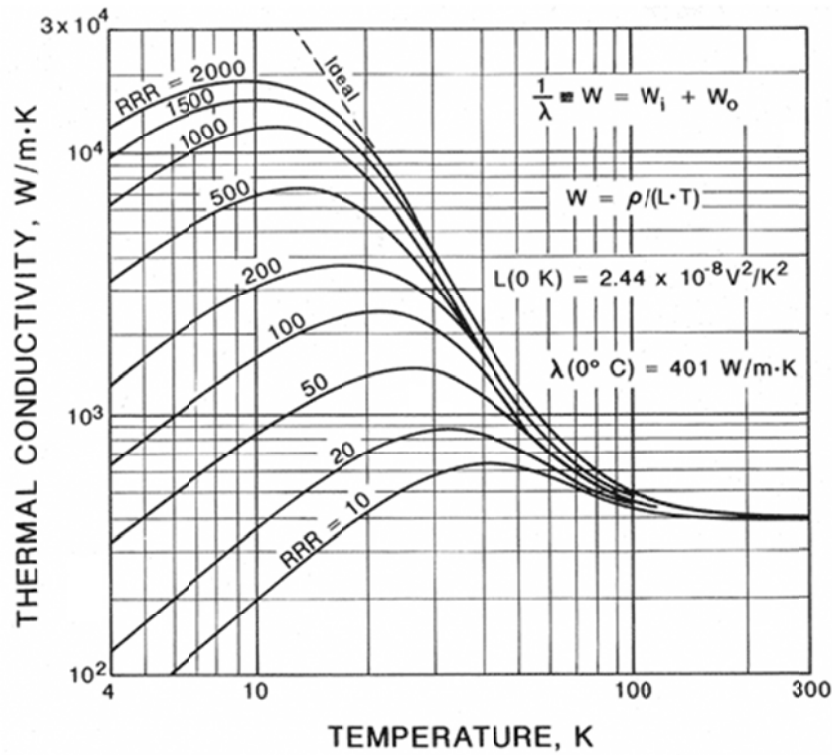


Figure 2.15: Thermal conductivity of copper as a function of temperature and purity
To find the temperature gradient (ΔT) in the copper, equation [2.5] is used

$$q = \frac{2\pi L k \Delta T}{\ln r_2/r_1} \quad [2.5]$$

Where q is the expected cooling power (3W), L is the length of the heat exchanger (1.635cm), k is the thermal conductivity of copper (400W/m-K or 1000W/m-K depending on the type of copper) and r_1 and r_2 are the inner and outer radius of the heat exchanger. This equation gives a temperature gradient of 0.12K for 110 copper and 0.048K for 101 copper. Copper 101 was selected because it wasn't that much more expensive than copper 110.

2.6.5 2nd Stage Pulse Tube

The 2nd stage PT is an off the shelf piece of seamless stainless steel tubing brazed into the 101 copper piece that contains the transition region and the 20K heat exchanger. It is 4.740"

long, has an inner diameter of 0.68", a thickness of 0.035" and is rated for 1,500psi. These dimensions are very close to the model which specified an inner diameter of 0.677" (0.4% error) and a thickness of 0.039" (11.1% error). The thickness error actually improves the performance of the cooler because it reduces the conductive loss through the pulse tube from the top 75K heat exchanger to the 20K heat exchanger. The pulse tube is connected to the top 75K heat exchanger with a flange that has a diameter of 2.25" and is 1/4" thick as shown in Figure 2.16. This connection is sealed using indium due to the low temperature.



Figure 2.16: The 2nd stage pulse tube, 20K heat exchanger, and 2nd stage regenerator

2.6.6 Top 75K Heat Exchanger

The 75K heat exchanger is made out of copper 110 and has an inner diameter of 1.72cm (the same as the pulse tube), a thickness of 1.5cm, and is filled with 126, 150 mesh copper screens. The heat exchanger is thermally connected to the common heat exchanger via the 75K bus bar. To ensure that this heat exchanger maintains an adequate temperature, a 3D conduction model was created in SolidWorks SimulationXpress, as shown in Figure 2.17. This shows that the maximum temperature in the heat exchanger is 79K which is very close to the SAGE model's assumption of 80K.

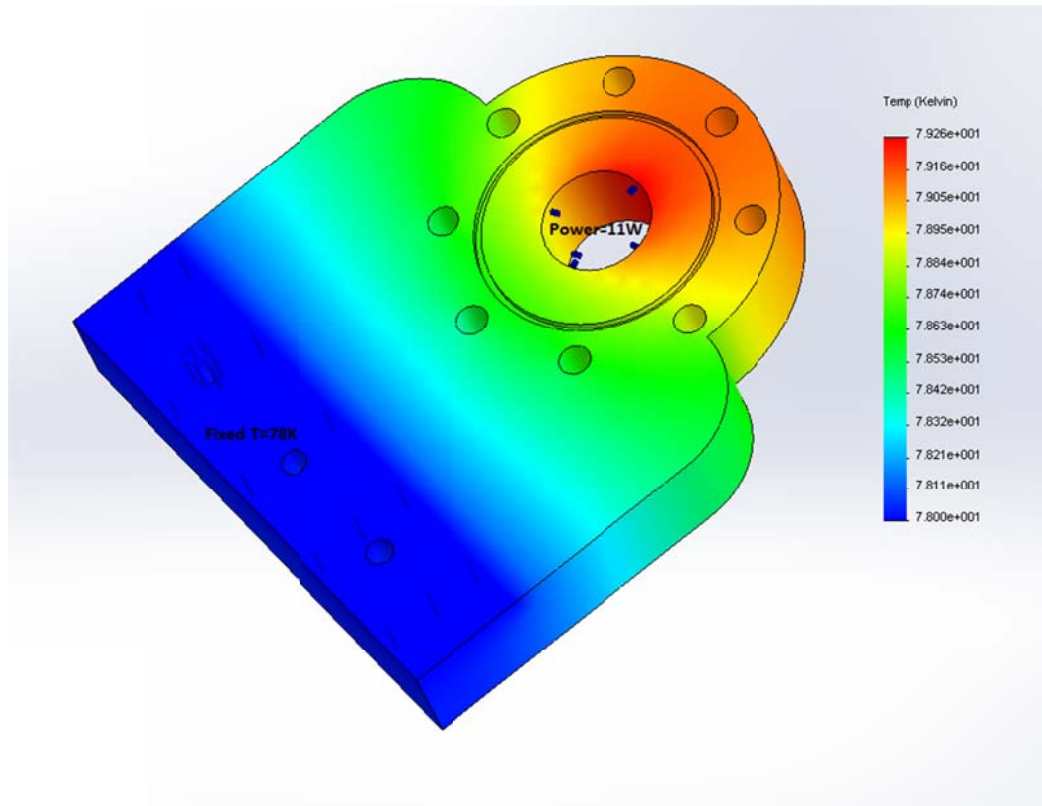


Figure 2.17: 3D conduction model of the top 75K heat exchanger

Due to the change in cross sectional area between the heat exchanger and inertance tube, there is a transition region between these components to insure well distributed flow. The transition region is discussed in Modeling the Transition Regions.

2.6.7 2nd Stage Inertance Network

The 2nd stage inertance network consists of a 0.5L stainless steel reservoir and an inertance tube that is 0.952m long, has an inner diameter of 0.152", a thickness of 0.049", and is rated for 2,200psi. The inertance tube is connected to the transition region and to the reservoir using NPT to VCR connections as shown in Figure 2.18a. Stycast 1266 epoxy is used to seal the NPT connections because at the conditions that the cooler is being run at (400psi helium on the inside and high vacuum on the outside) both thread tape and SWAK have a lot of difficulty keeping the system leak tight.

According to the SAGE model small fluctuations in the temperature of the inertance network can have large effect on the performance of the PTC. Therefore, the inertance network is held at 75K by strapping it to the 75K bus bar as shown in Figure 2.18b.



(a)



(b)

Figure 2.18: (a) VCR to NPT connection (b) 2nd stage inertance network and 75K bus bar

3. Modeling the Transition Regions

3.1 Introduction

There are four interfaces in the PTC where the diameter drastically changes. Those are between: the 2nd stage cold heat exchanger and the 2nd stage PT, the top 75K heat exchanger and the 2nd stage inertance tube, the 1st stage cold heat exchanger and the 1st stage PT, the 300K heat exchanger and the 1st stage inertance tube. It is of some concern that the large change in diameter could result in less effective heat exchangers and regenerators and cause jetting through the pulse tube. This chapter outlines the design and importance of each transition region.

3.2 20K Heat Exchanger Transition Region

When the working fluid goes from the 2nd stage PT to the 20K heat exchanger there is a sudden increase in cross-sectional area, which, without resistance, would result in two recirculation zones. This would drastically decrease the performance of both the 20K heat exchanger and the 2nd stage regenerator. However, since both the heat exchanger and the regenerator have large resistances due to the copper screens and ErPr pellets, it is necessary to model the flow through them using computational fluid dynamics (CFD).

The geometry of the transition from the pulse tube to the heat exchanger is shown in Figure 3.1. This geometry is for a 2D axisymmetric model. The locations of each vertex are shown in Table 3.1. The definition of each boundary and region are shown in Table 3.2. Once the geometry was created the model was meshed with 988 nodes. The mesh is shown in Figure 3.2.

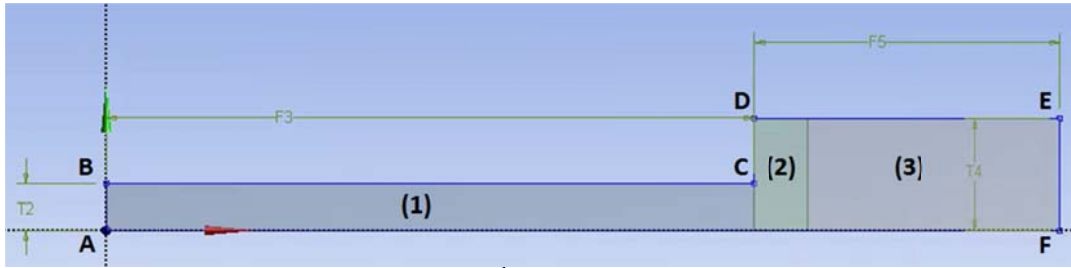


Figure 3.1: Geometry used to model the 2nd stage PT to 20K heat exchanger transition

Table 3.1: Vertex locations for Figure 3.1

Vertex	X Location (cm)	Y Location (cm)
A	0.0000	0.0000
B	0.0000	0.8600
C	12.0400	0.8600
D	12.0400	2.0875
E	18.6150	2.0875
F	18.6150	0.0000

Table 3.2: Regenerator Test Section Boundary and Region Definitions

Boundary/Region	Definition
Line AB	Mass Flow Inlet
Line BC	Wall
Line CD	Wall
Line DE	Wall
Line EF	Pressure Outlet
Line FA	Axis of Symmetry
Region 1	Pulse Tube (Open Fluid Zone)
Region 2	20K heat exchanger (Porous Fluid Zone)
Region 3	Regenerator (Porous Fluid Zone)

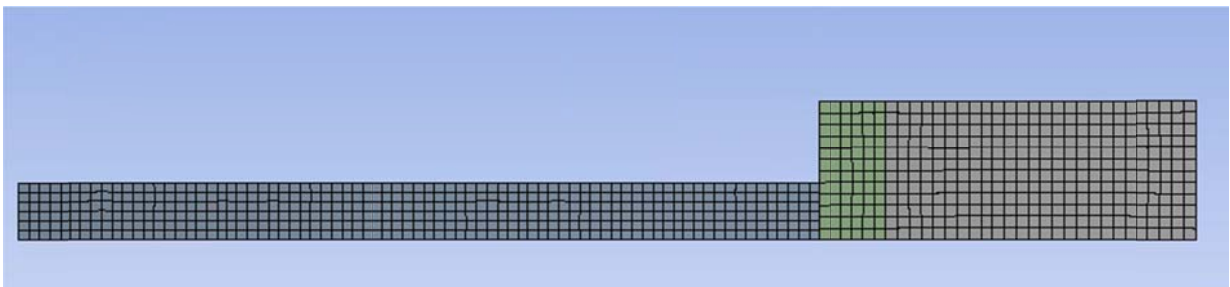


Figure 3.2: Mesh used to model the 2nd stage PT to 20K heat exchanger transition

The mesh was then exported to Fluent where it was fully defined and solved. The working fluid was helium with 20K properties. Three regions were set to accurately simulate the open volume in the pulse tube, the screens in the 20K heat exchanger, and the powder in the

regenerator. The resistances in the heat exchanger and the regenerator was modeled using the porous zone feature. The parameters are shown in Table 3.3, in which viscous resistance is $1/\alpha$ and internal resistance is C_2 . Resistance parameters for 250 mesh screens could not be found, so characteristics for 325 mesh screens were used as an approximation (Clearman 2007). Resistance parameters for the packed bed were found by manipulating the Ergun Equation—which expresses the friction factor in a packed bed—into equations [3.1] and [3.2] where D_p is particle diameter and ϕ is void fraction (FLUENT 2006). The results of this simulation are shown in Figure 3.3.

$$\alpha = \frac{D_p^2}{150} * \frac{\phi^3}{(1 - \phi)^2} \quad [3.1]$$

$$C_2 = \frac{3.5}{D_p} * \frac{(1 - \phi)}{\phi^3} \quad [3.2]$$

Table 3.3: Porous Zone Parameters for the 20K Heat Exchanger and Regenerator

20K HX (Porosity= 0.766)	$1/\alpha$ [1/m²]	C_2 [1/m]
Axial	47000	2.35e+10
Radial	98600	6.8e+09
Regenerator (Porosity=0.640)	2.966e+10	96130

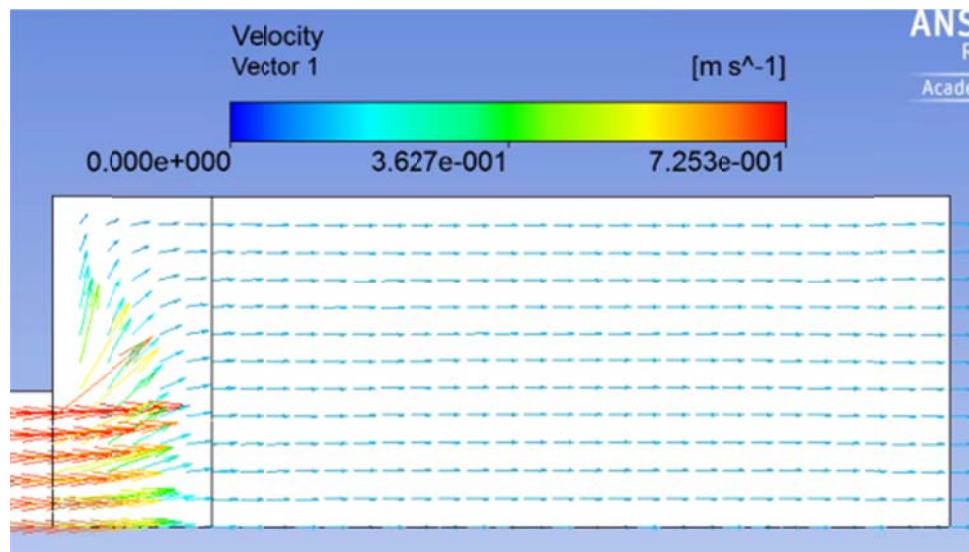


Figure 3.3: Flow field between the 2nd stage PT and the 20K heat exchanger

Five velocity profiles were taken: $\frac{1}{4}$ cm into the heat exchanger, $\frac{1}{2}$ cm into the heat exchanger, $\frac{3}{4}$ cm into the heat exchanger, at the interface of the heat exchanger and regenerator, and a $\frac{1}{2}$ cm into the regenerator. These profiles can be seen in Figure 3.4. Since the flow becomes mostly developed at the interface between the heat exchanger and the regenerator, the volume of the heat exchanger is not being fully utilized and, therefore, a transition region needs to be present.

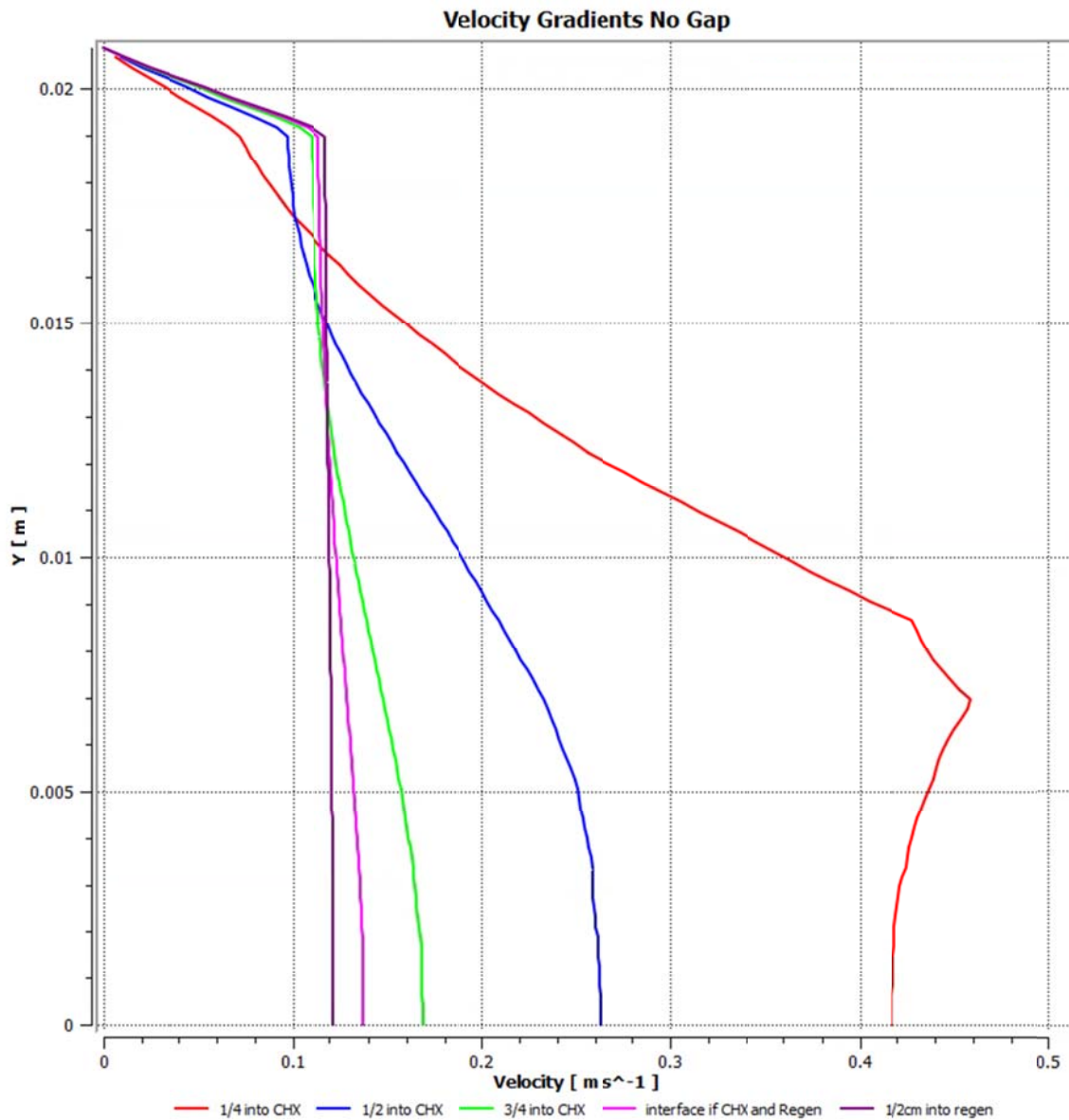


Figure 3.4: Velocity profiles in the 20K heat exchanger and 2nd stage regenerator

The results of the previous simulation inspired a new CFD study that provides the dimensions of an open transition region in-between the pulse tube and the heat exchanger that causes the flow to be uniform when entering the heat exchanger. Three different geometries were tested: a $\frac{1}{2}$ cm void volume in-between the pulse tube and the heat exchanger, a $\frac{1}{4}$ cm void volume, and a $\frac{1}{4}$ cm conical void volume. The meshes for the three different simulations are shown in Figure 3.5; the boundary conditions and region definitions are the same as they were in the previous study and the void volume is simulated as an open region.

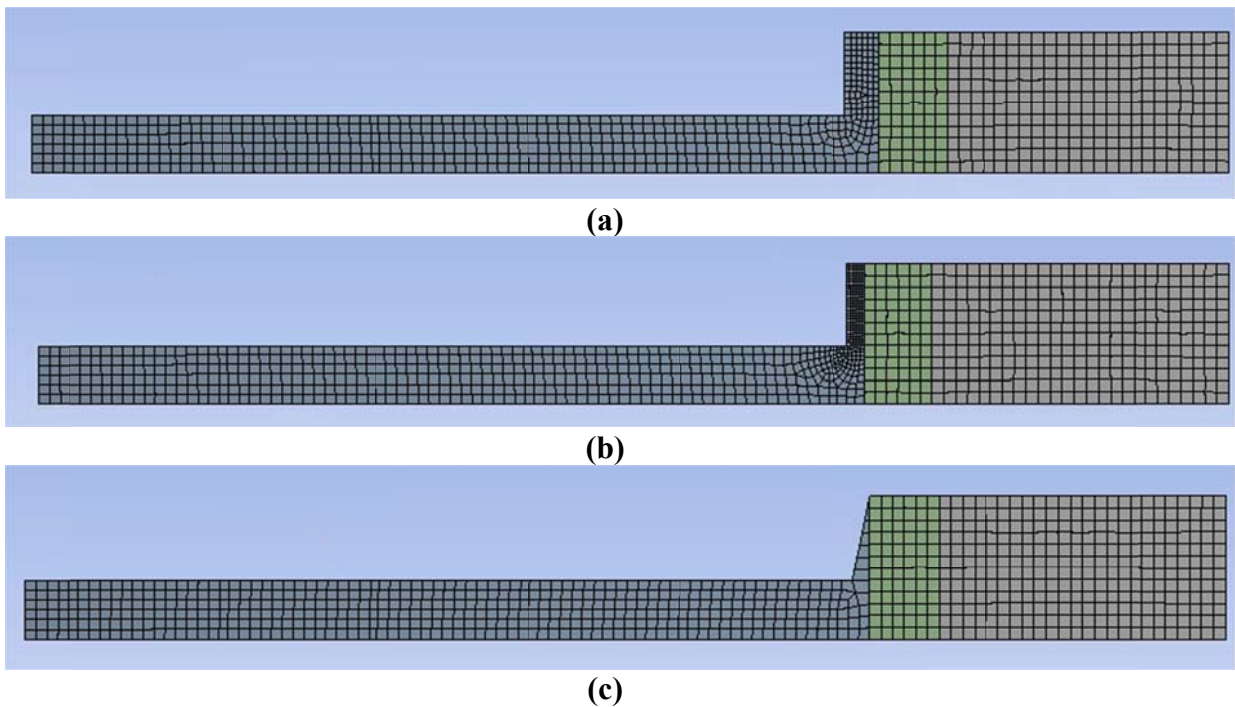


Figure 3.5: Mesh for (a) $\frac{1}{2}$ cm void (b) $\frac{1}{4}$ cm void (c) $\frac{1}{4}$ cm conical void

The flow fields for each simulation are shown in Figure 3.6. Velocity profiles of the simulations are taken at the interface between the void volume and the heat exchanger and $\frac{1}{4}$ cm into the heat exchanger as shown in Figure 3.7.

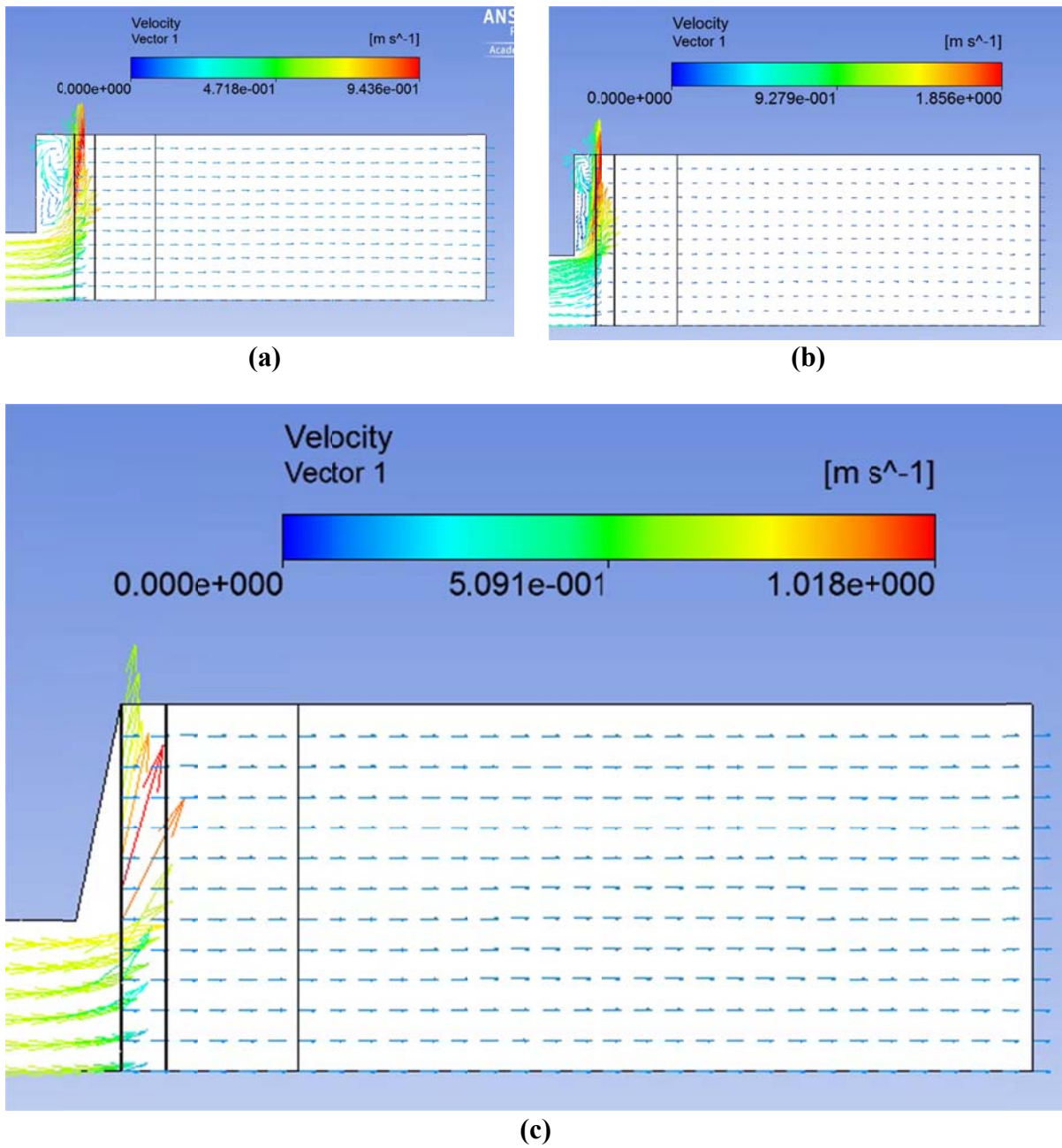
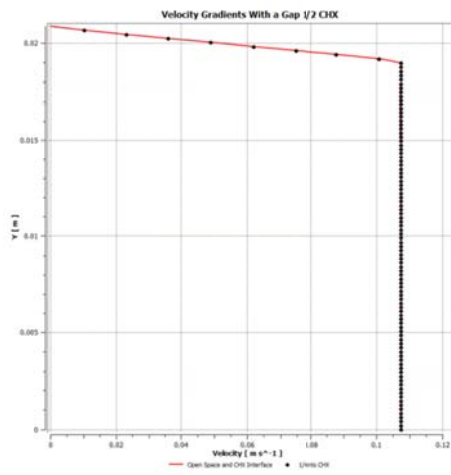
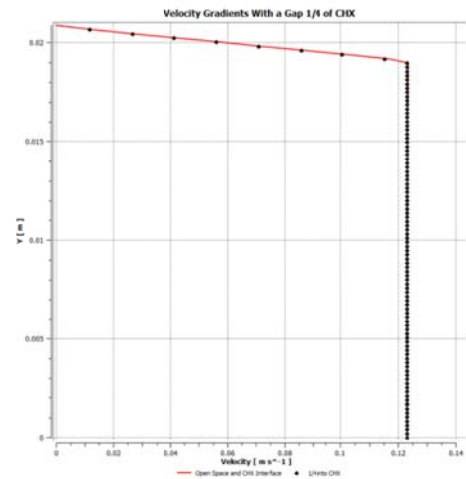


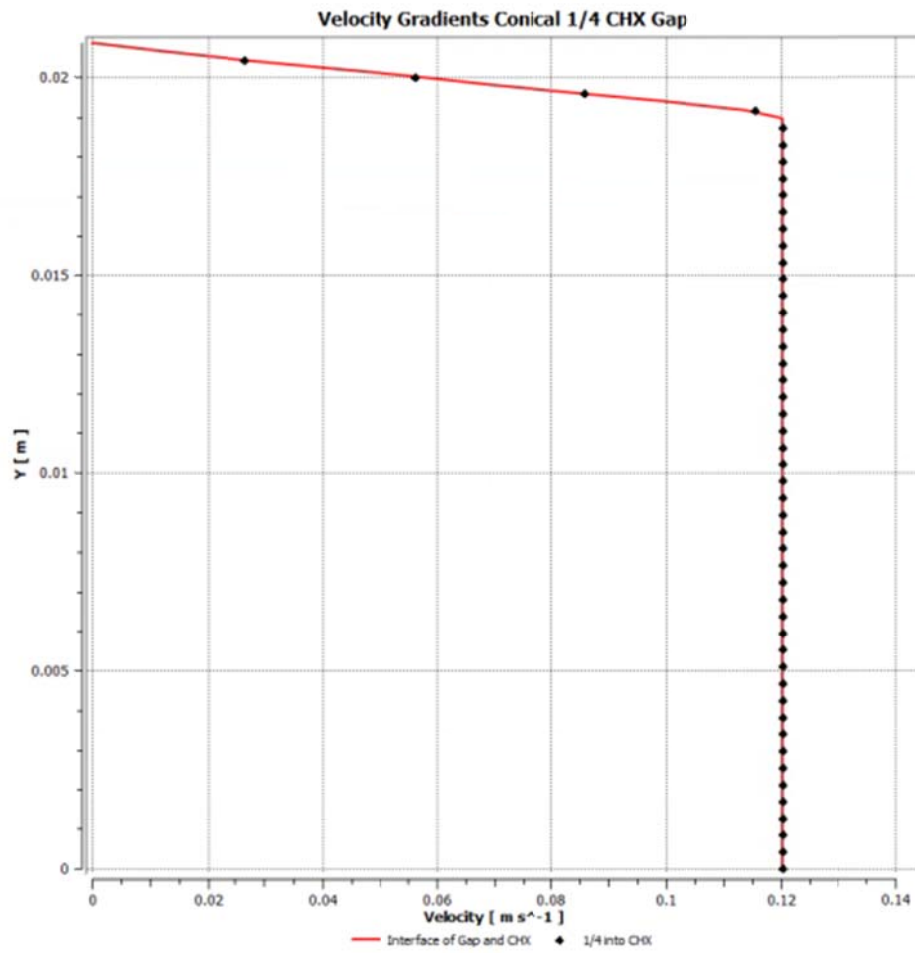
Figure 3.6: Flow fields in the 20K HX (a) $\frac{1}{2}$ cm (b) $\frac{1}{4}$ cm (c) $\frac{1}{4}$ cm conical void



(a)



(b)



(c)

Figure 3.7: Velocity profile in 20K HX (a) 1/2 cm (b) 1/4 cm (c) 1/4 cm conical void

The results from the three void volume simulations suggest that any of these designs would cause the velocity profile to be fully developed once fluid enters the 20K heat exchanger. Thus, the $\frac{1}{4}$ cm conical void volume design was chosen because it has the smallest volume and no recirculation zones.

To make sure that the $\frac{1}{4}$ cm conical void volume was a good choice, the simulation was rerun with the flow going in the opposite direction. The results from this simulation are shown in Figure 3.8. From this figure, it can be seen that the flow going through the void volume and into the pulse tube is uniform. Therefore, this design was selected for the transition zone between the 2nd stage PT and the 20K heat exchanger. The transition zone was implemented in the copper plate, above the 20K heat exchanger, as shown in Figure 3.9.

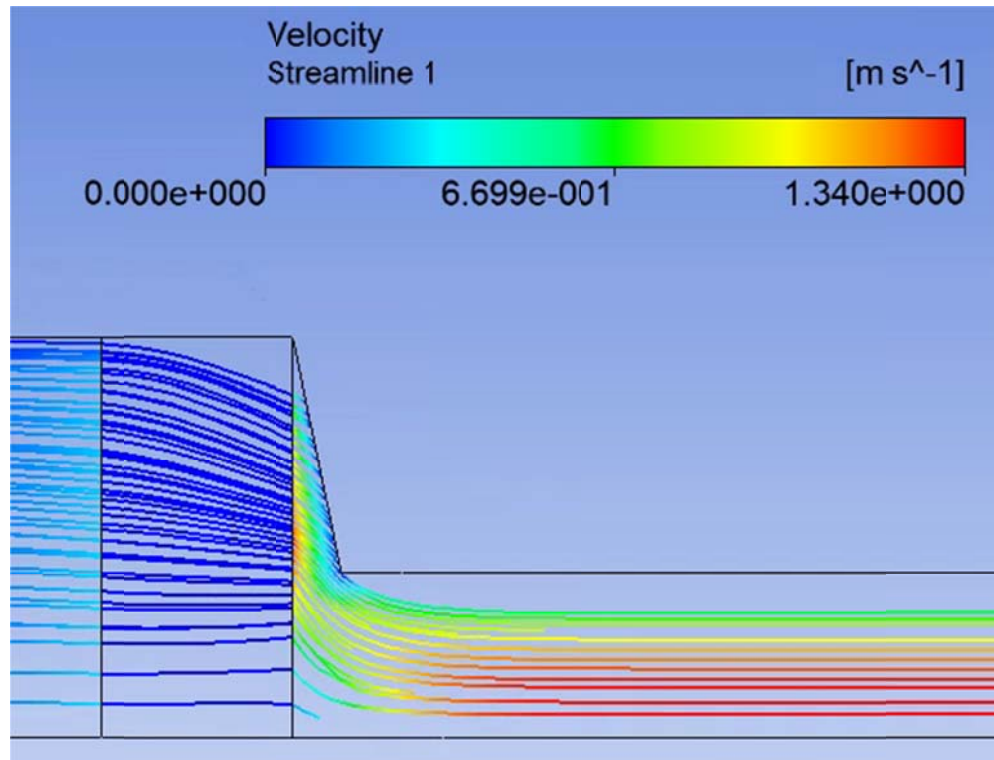


Figure 3.8: Streamlines for fluid entering at the 2nd stage regenerator

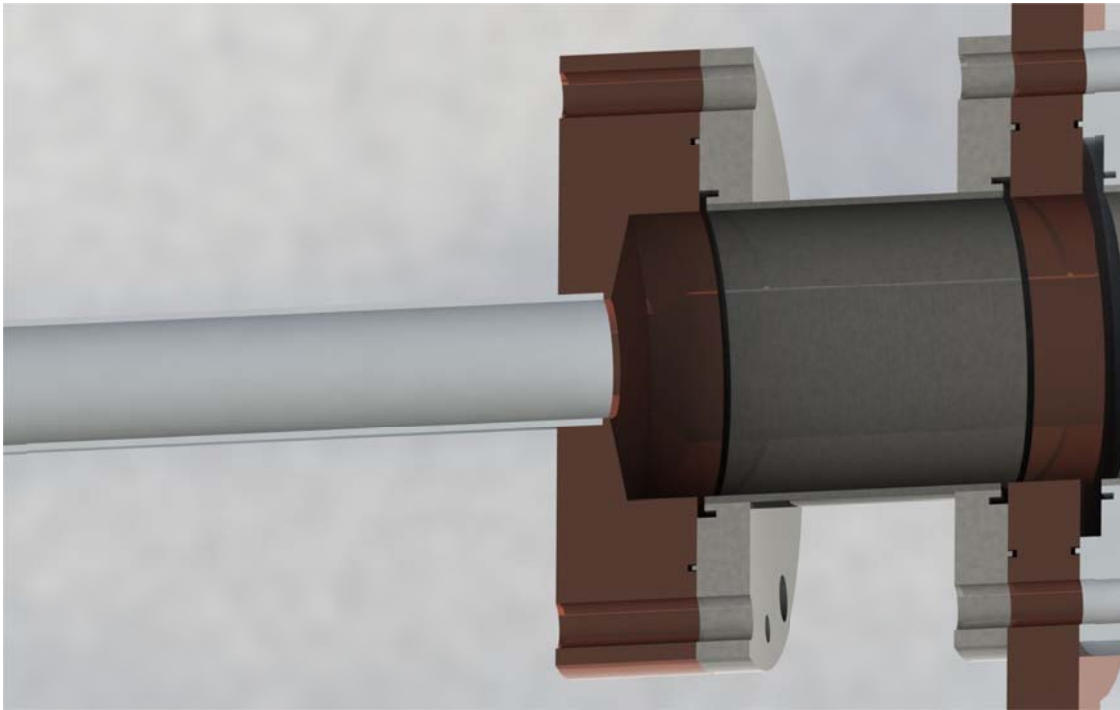


Figure 3.9: Transition zone between the 2nd stage PT and 20K heat exchanger

3.3 Top 2nd Stage Transition Region

A similar analysis was conducted for the transition zone between the top of the 2nd stage inertance tube and the 75K top hot heat exchanger. The geometry and mesh of the transition from the inertance tube to the heat exchanger are shown in Figure 3.10a and b. Due to the results of the previous simulation, the geometry used in modeling this transition is similar to that used for the transition zone between the 2nd stage PT and the 20K heat exchanger. The geometry being used is for a 2D axisymmetric model. The locations of each vertex are shown in Table 3.4 and the definition of each boundary and region are shown in Table 3.5. The working fluid was helium with 75K properties. The two zones were set to accurately simulate the open volume in the inertance tube and the mesh screens in the heat exchanger. The results of this simulation are shown in Figure 3.10c.

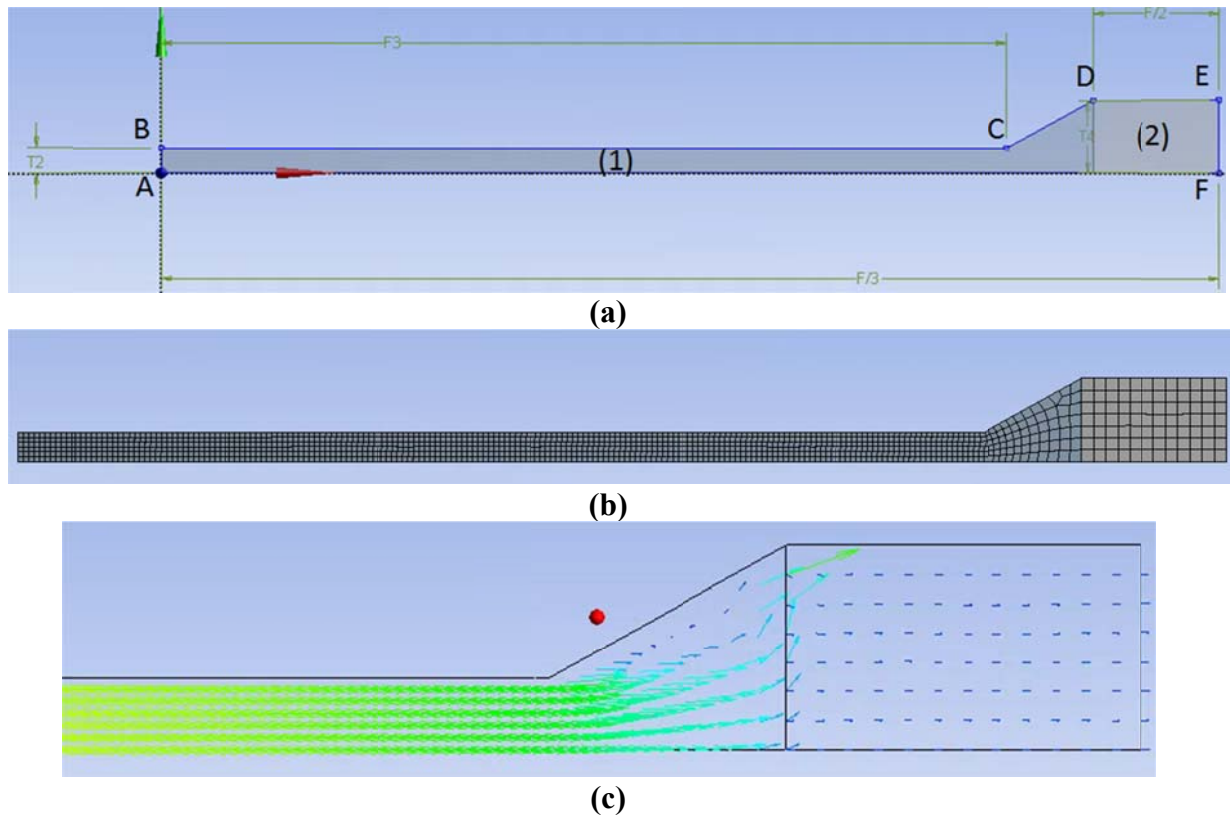


Figure 3.10: (a) Geometry (b) mesh and (c) results of the 75K top hot HX transition region

Table 3.4: Vertex locations for Figure 3.10

Vertex	X Location (cm)	Y Location (cm)
A	0.0000	0.0000
B	0.0000	0.3000
C	10.0000	0.3000
D	11.0000	0.8600
E	12.5000	0.8600
F	12.5000	0.0000

Table 3.5: Test Section Boundary and Region Definitions

Boundary/Region	Definition
Line AB	Mass Flow Inlet
Line BC	Wall
Line CD	Wall
Line DE	Wall
Line EF	Pressure Outlet
Line FA	Axis of Symmetry
Region 1	Inertance Tube (Open Fluid Zone)
Region 2	HHX (Porous Fluid Zone)

This transition region was implemented by adding a flange in-between the inertance tube and the 75K heat exchanger as shown in Figure 3.11. The flange acts as both the transition region and a link from the inertance tube to the heat exchanger because the flange has a $\frac{1}{4}$ " NPT attachment above the transition region. Since the transition region is relatively small and it is on the hot end of the pulse tube, it should have a small effect on the overall performance of the cryocooler.



Figure 3.11: Transition zone between the 2nd stage PT and the top 75K heat exchanger

3.4 Transition Zones in the 1st Stage

There are two transition zones in the 1st stage PTC. The first is between the 1st stage cold heat exchanger and the 1st stage PT. This is due to a change in inner diameter from 2.245" to 1.402". The second is between the top 300K heat exchanger and the 1st stage inertance tube due to a change in inner diameter from 1.402" to 0.37". The design of these two transition regions follows the same methodology used in the design of the 2nd stage transition regions.

Therefore, a $\frac{1}{4}$ cm conical void was machined into the 1st stage PT bottom flange and the top transition region, as shown in Figure 3.12 and Figure 3.13.

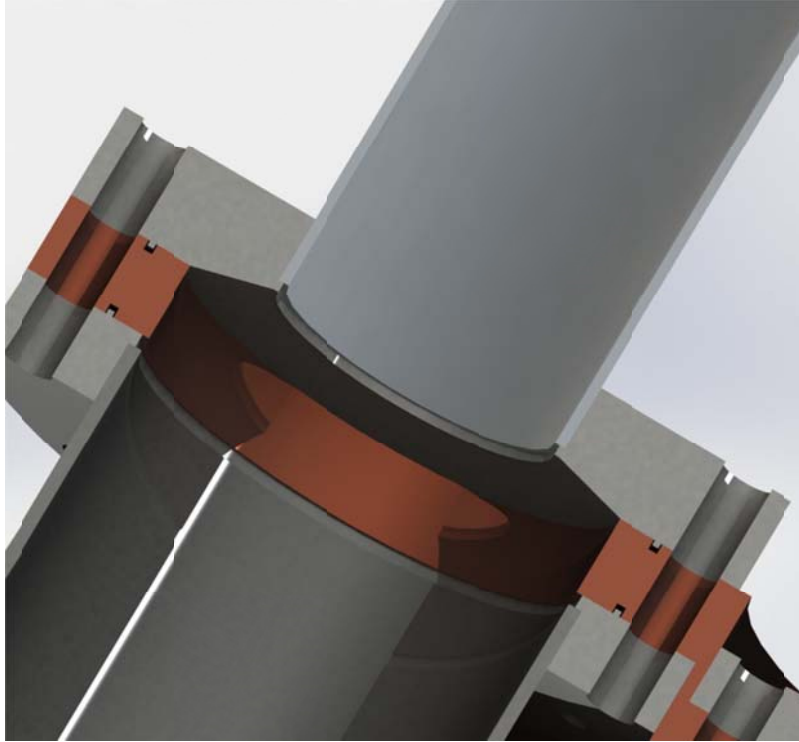


Figure 3.12: Transition zone between the 1st stage cold heat exchanger and the 1st stage PT

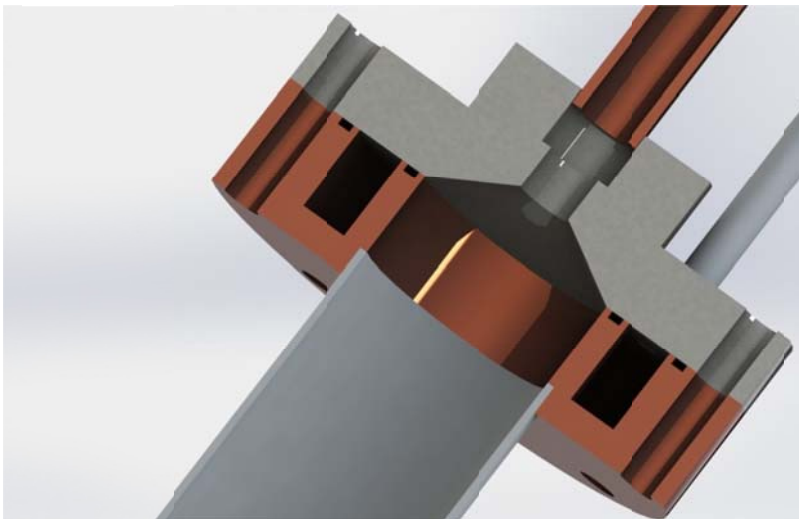


Figure 3.13: Transition zone between the top 300K HX and the 1st stage inertia tube

4. 2nd Stage Pulse Tube Cryocooler Testing

4.1 Introduction

In order to reduce experimental uncertainty and validate the model more systematically, the 2nd stage PTC (75K to 20K) was built and tested first, followed by the building the simpler 1st stage PTC (300K to 75K). This was done to verify that the 2nd stage PTC performs as expected without having to account for the complications of the 1st stage PTC. Instead of using the cooling power from the 1st stage PTC, the two 75K heat exchangers on the 2nd stage are maintained at 75K using a commercial GM cooler. The 2nd stage PTC is shown in Figure 4.1 (Note: A blank-off flange is bolted to the precooler and an NPT plugs the transition region). This chapter discusses the preliminary testing, the experimental set up, the testing, and the data analysis of the 2nd stage PTC.

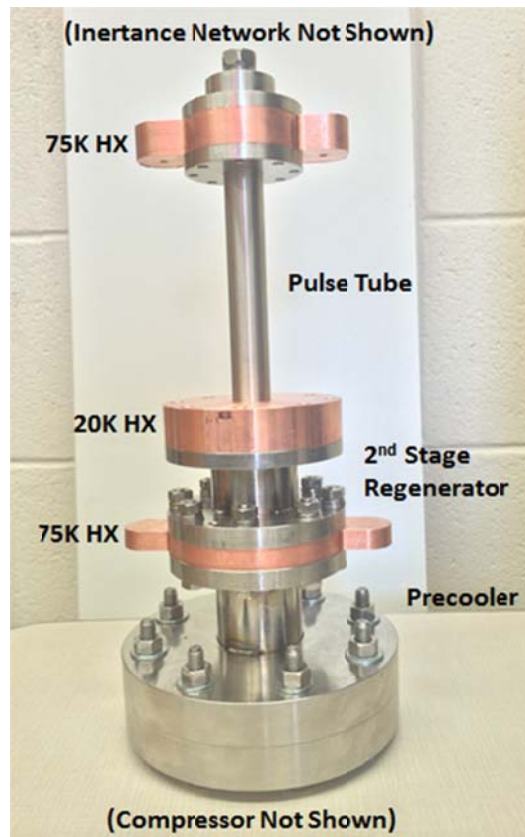


Figure 4.1: 2nd stage PTC

4.2 Preliminary Testing

In order to make sure the cryocooler is safe and leak-tight, each custom component was hydrostatically pressure tested and the entire system was leak tested before actual testing took place.

4.2.1 Hydrostatic Pressure Testing

To ensure that the cryocooler can be safely pressurized to 400psi, the cooler was hydrostatically pressure tested with methanol. This method is much safer than pressure testing with a gas because if a component fails then it will spray methanol rather than blow-up, which could happen if pressurized with a compressible fluid like air or helium. Methanol was used because it evaporates at room temperature and therefore, after the test, the methanol evaporates. The hydrostatic pressure testing system is shown in Figure 4.2. The hydrostatic pressure testing system uses a hydraulic jack to pressurize the cooler. The line connecting the jack to the cooler has a pressure transducer, which is connected to a 10V power supply and a multimeter to measure the voltage output. Each component was tested to 800psi which ensures a factor of safety of two for the cooler. The hydrostatic pressure test also made large leaks easy to find. When the system was hydrostatically pressure tested, some of the indium seals had leaks which were fixed by either adding more indium to the seals or smoothing the seal. After a few iterations of testing and fixing leaks, the cooler was successfully pressurized to 800psi for 20 minutes. Once the cooler passed this test, a helium leak test was performed.



Figure 4.2: Hydrostatic pressure test

4.2.2 Leak Testing

Helium has a thermal conductivity of $0.1513 \text{ W/m}\cdot\text{K}$ which makes it about six times as conductive as air ($0.025 \text{ W/m}\cdot\text{K}$). Therefore, if the cryocooler is not leak tight, helium will leak into the Dewar and spoil the insulation provided by the vacuum.

There were two different leak tests done to ensure that the cooler was leak tight. The first leak test was done by creating a vacuum inside the cooler and sustaining the vacuum with the leak detector. Very small amounts of helium were then sprayed on the joints on the outside of the cooler. If there was a leak, then the helium would be sucked into the vacuum and the leak detector would quantify how large it was. This method allows the leaks to be easily pinpointed and fixed using a variety of methods.

Since the cooler will operate in a vacuum and have an internal peak pressure of 400psi, the cooler needs to be tested for leaks under these conditions. Therefore, the final test to ensure that the cooler was leak tight was to place it in a vacuum chamber that was connected to the leak detector. The cooler was then filled with helium to 400psi. If there was a leak, then the

leak detector would pick it up. This method makes it very difficult to find leaks unlike the previous method because the cooler is in the Dewar. However, to be certain that the cooler will not leak, it must pass this test.

4.3 Experimental Setup and Data Collection

The following section outlines the method used to test the 2nd stage PTC. This includes information about how the 2nd stage hot heat exchangers were kept at 75K, how heat transfer from the pulse tube to its surroundings was minimized, instrumentation, data acquisition, and post processing.

4.3.1 Keeping the 2nd Stage Hot Heat Exchangers at 75K

The two 75K heat exchangers on the 2nd stage PTC were kept at 75K using a commercial GM cryocooler. Therefore, accurate cooling data for the GM cooler is required. The GM cooler was tested at the four conditions shown in Table 4.1. Since the 2nd stage of the GM cooler was not used, the tests were run with no load on the 2nd stage.

Table 4.1: GM Cooling Curve

Voltage [V]	Load [W]	Temperature [K]
0	0	35
48	30	50
59	45	53
68	60	73

To test the first stage of the GM cooler, a variable voltage power supply was used in parallel with two 100W heaters and a multimeter was used to measure voltage. The equivalent resistance (R_e) of the two heaters is 77.75Ω . The required voltage (V_e) is calculated using equation [4.1] for different values of power (P_e).

$$P_e = V_e^2 R_e^{-1} \quad [4.1]$$

The GM cooler was placed in a vacuum chamber to reduce conduction and covered with two sheets of aluminized Mylar to reduce the heat load due to radiation. Heat was applied to the cooler and temperature data was taken once the cooler reached steady state. Once the cooler was tested, a thermal bus from the GM cooler to the 75K heat exchangers was designed.

The SAGE model predicts that the bottom 75K heat exchanger dissipates 35.8W and the top 75K heat exchanger dissipates 10.9W. Therefore, the connection between the heat exchangers and the GM cooler must be able to conduct 46.7W. To size the thermal bus, cooling data was used from the GM cooler. The GM cooler can handle 46.7W at about 60K.

The thermal bus from the GM cooler to the bottom 75K heat exchanger consists of a 12" x 4" x 0.75" copper 101 bar that connects at the 1st stage of the GM cooler. Then, four copper straps, each with a cross-sectional area of 0.3927 in², were bolted from the large copper bar to two 2" x 2" x 0.5" copper bars. Each small bar was connected to opposite ends of the bottom heat exchanger. All the straps were bolted using the part shown in Figure 4.3. The straps are soldered to the large hole and bolted through the small hole.

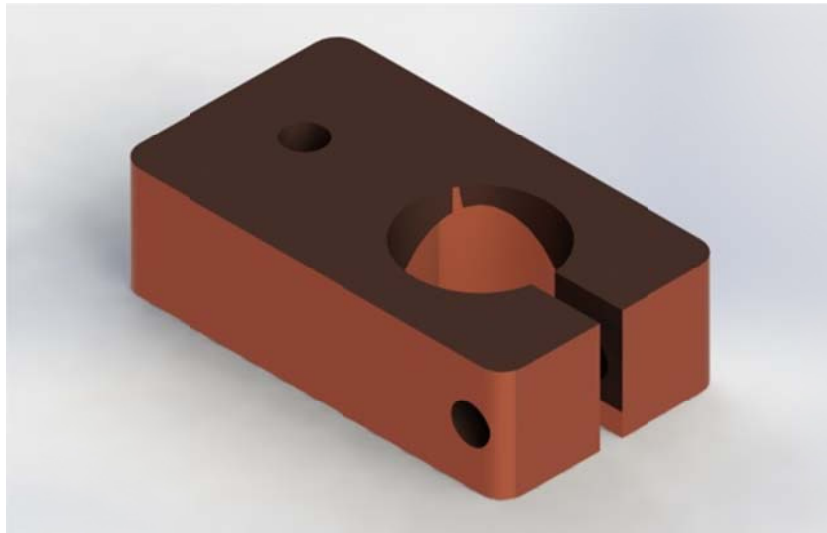


Figure 4.3: Part used to attach copper straps to other components

A 100W heater was also attached to the small copper bar in case the heat exchanger drops below 75K. To calculate the amount of heat that this design conducts from the heat exchanger to the GM cooler, a 1D steady state conduction model with varying thermal conductivity was created. This was done by breaking the bus into n nodes and then analyzing the heat transfer between each node using equation [4.2].

$$q = \frac{(T_i - T_{i-1})}{R_i} \quad [4.2]$$

In equation 4.2, T_i is the temperature of the nodes, T_0 is the temperature of the GM cooler (60K), T_n is the desired temperature of the heat exchanger (75K), q is the heat transfer from the heat exchanger to the GM cooler, and R_i is the resistance from node $i-1$ to i . R_i is calculated with equation [4.3].

$$R_i = \frac{l}{k_i * A} \quad [4.3]$$

Where l is the length of the components ($l_{bar}=12''$, $l_{strap}=4''$ and $l_{connection}=1.5''$) and A is the cross-sectional area ($A_{bar}=3 \text{ in}^2$, $A_{strap}=0.3927 \text{ in}^2$ and $A_{connection}=1 \text{ in}^2$). The conductivity, k_i , was selected using the thermal conductivity of copper as a function of temperature. This simulation shows that this arrangement will transfer 36.7W to the GM cooler and the temperature distribution as a function of position through the bus bar is shown in blue in Figure 4.4.

The thermal bus from the GM cooler to the top 75K heat exchanger has the same design as the bus discussed previously. However, the large bus bar is $12'' \times 1'' \times 0.75''$ and it has two $5''$ straps with a cross sectional area of 0.1963 in^2 used to connect the bar to the heat exchanger. This arrangement will result in a heat transfer of 12.5W and the temperature distribution

shown in Figure 4.4. The EES code used to size the thermal bus is shown in Appendix B: ESS and MATLAB Code and the thermal bus is shown in Figure 4.5.

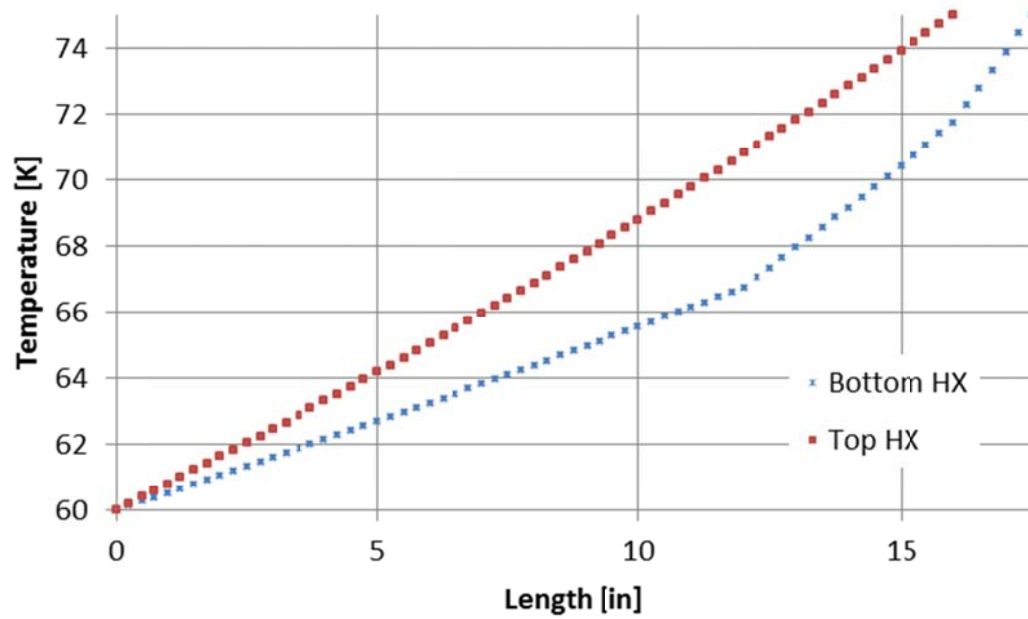


Figure 4.4: Temperature distribution in thermal buses

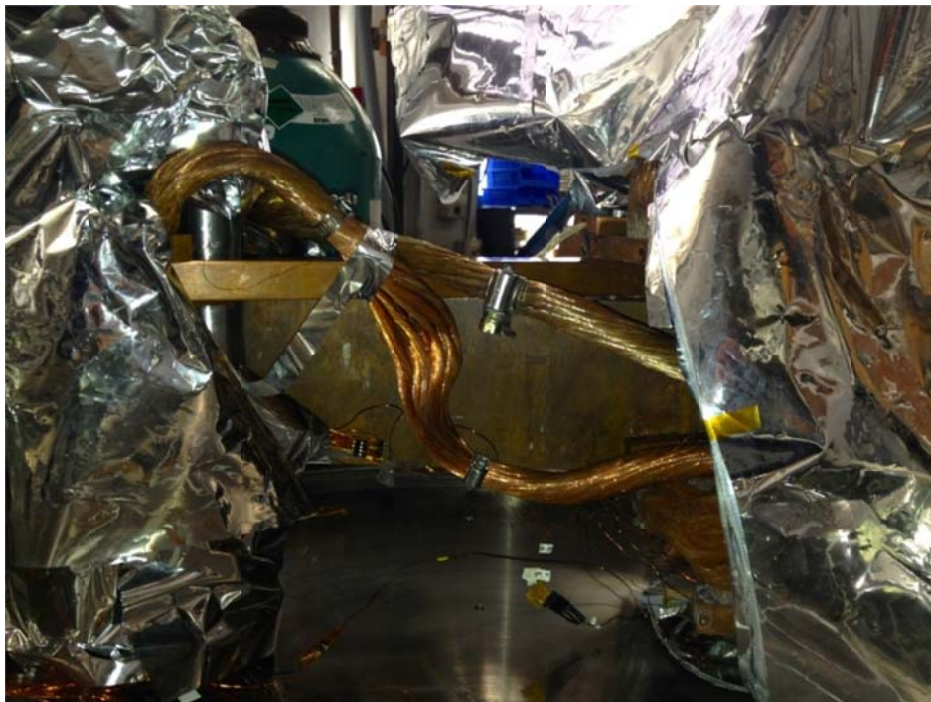


Figure 4.5: Top and bottom thermal buses

4.3.2 Reducing Heat Transfer to the Surroundings

The experiment was placed in a Dewar, shown in Figure 4.6, in order to isolate it from the atmosphere. A vacuum space was created in the Dewar to significantly reduce conductive and convective heat loads. The conductivity of air as a function of pressure in a vacuum is shown in Figure 4.7. A sub 10^{-3} torr vacuum is created using a roughing pump and a turbo pump in series. The Dewar is sealed with a rubber O-ring between the base and lid. There are many KF-40 and conflat ports around the base for connecting the vacuum pump, instrumentation, and other equipment that is necessary to carry out the test. The ports that are not in use were sealed using KF-40 and conflat blanks. Once the vacuum within the Dewar is below 10^{-3} torr, the GM cooler and PTC are turned on.



Figure 4.6: Cryogenic Dewar

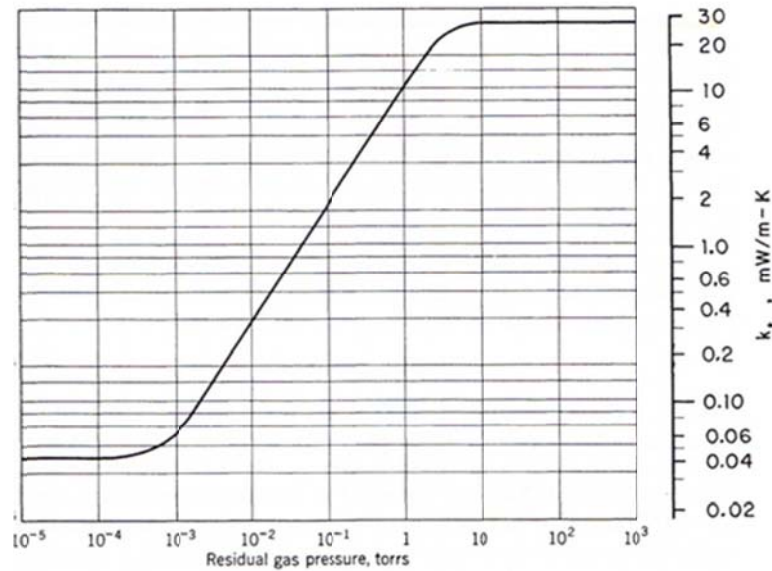


Figure 4.7: Conductivity of air in a vacuum (Barron 1985)

Heat loads due to radiation can be greatly reduced by using radiation shields around the different components that reach cryogenic temperatures. These components include the GM cooler, the thermal bus, and the parts of the pulse tube that go below 300K. Radiation shields use surfaces with very low emissivity to reduce heat transfer due to radiation between surfaces of different temperature. The radiation shields around the 75K components, the bus bar, and the GM cooler are made using multi-layer insulation (MLI), which consists of aluminized Mylar and a thin polyester fabric between the aluminized Mylar to eliminate conduction between the Mylar sheets. The emissivity of aluminized polyester foils is approximately $\varepsilon_{MLI}=0.017$ (Musilova 2004). The heat transfer from the surroundings ($T_H=300K$, $\varepsilon_1=0.1$) to the pulse tube ($T_c=75K$, $\varepsilon_2=0.5$) can be calculated as a function of the number of sheets of aluminized Mylar using equation [4.4] (Jahromi 2011). This equation was solved for 1 to 100 Mylar sheets. As shown in Figure 4.8, the usefulness of each sheet greatly decreases after 10 sheets. Therefore, the pulse tube is covered with 10 sheets of

aluminized Mylar. Since the heat load on the thermal bus and the GM cooler can be larger than the load on the pulse tube, only two sheets of aluminized Mylar were used for these components. The full experimental setup covered in MLI is shown in Figure 4.9.

$$\dot{q} = \frac{\sigma(T_H^4 - T_c^4)}{\left(\frac{1}{\varepsilon_1} + \frac{1}{\varepsilon_2} - 1\right) + N\left(\frac{2}{\varepsilon_{MLI}} - 1\right)} \quad [4.4]$$

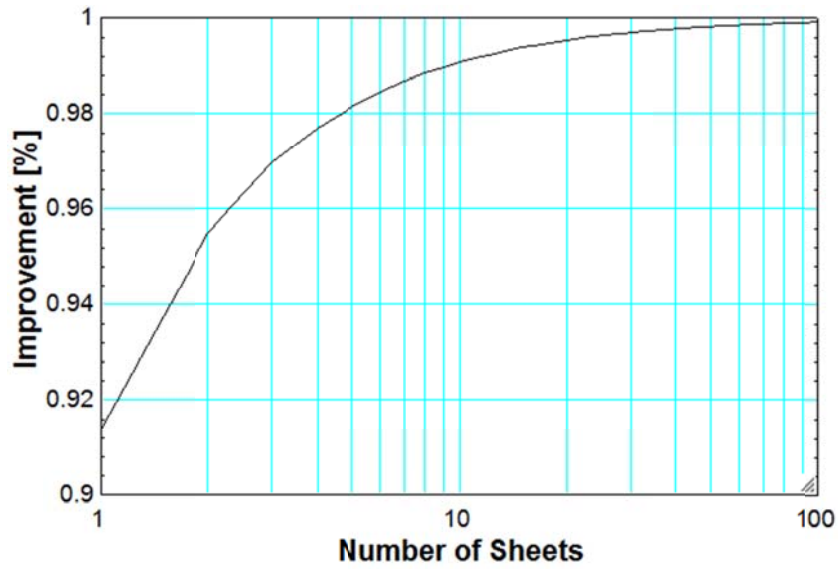


Figure 4.8: Percent improvement due to number of Mylar sheets

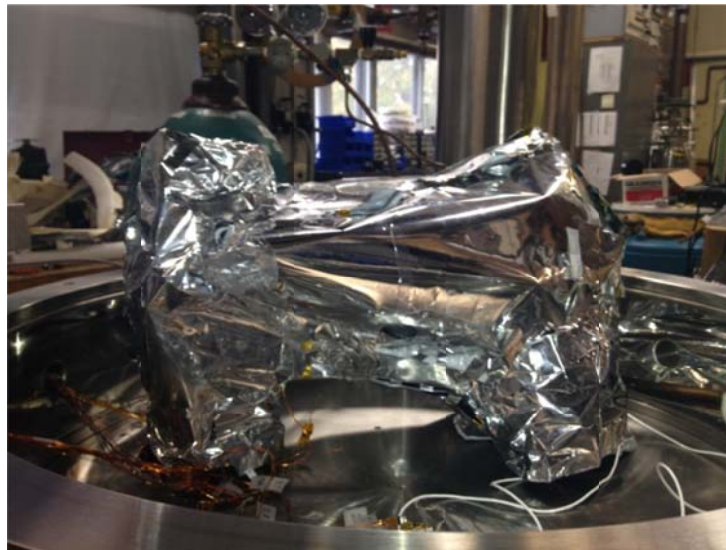


Figure 4.9: Experiment covered in MLI

The two 75K heat exchangers on the pulse tube were connected with a cylindrical aluminum shield, shown in Figure 4.10a. Thus, the 20K heat exchanger only sees radiation from a 75K source. MLI is significantly less effective at reflecting radiation from a 75K source. This is because the wavelength of the majority of the radiation from a surface at 75K is of the same order or larger than the thickness of the aluminum layer on the MLI ($th_{al}=60\mu\text{m}$). The wavelength of radiation at different temperatures can be found using Planck's law (Nellis 2009), shown in equation [4.5].

$$E_{b,\lambda} = \frac{C_1}{\lambda^5 \left[\exp\left(\frac{C_2}{\lambda T}\right) - 1 \right]} \quad [4.5]$$

λ is the wavelength in microns, $C_1=3.742 \times 10^8 \text{ W}\cdot\mu\text{m}^4/\text{m}$ and $C_2=14,388 \mu\text{m}\cdot\text{K}$. The spectral distribution for 75K is shown in Figure 4.11. The area in red is radiation blocked by the 60 micron aluminized Mylar and the area in green passes through the Mylar. The percentage of radiation that passes through the Mylar (%R) can be found using equation [4.6].

$$\%R = \frac{\int_t^\infty E_{b,\lambda} d\lambda}{\int_0^\infty E_{b,\lambda} d\lambda} \quad [4.6]$$

This results in 43.3% of the radiation passing through 60micron aluminized Mylar sheets. Therefore, the 20K heat exchanger is covered with an aluminum radiation shield with a thickness of 381 microns as shown in Figure 4.10b. Using this shield allows only 0.5% of the radiation to pass through.

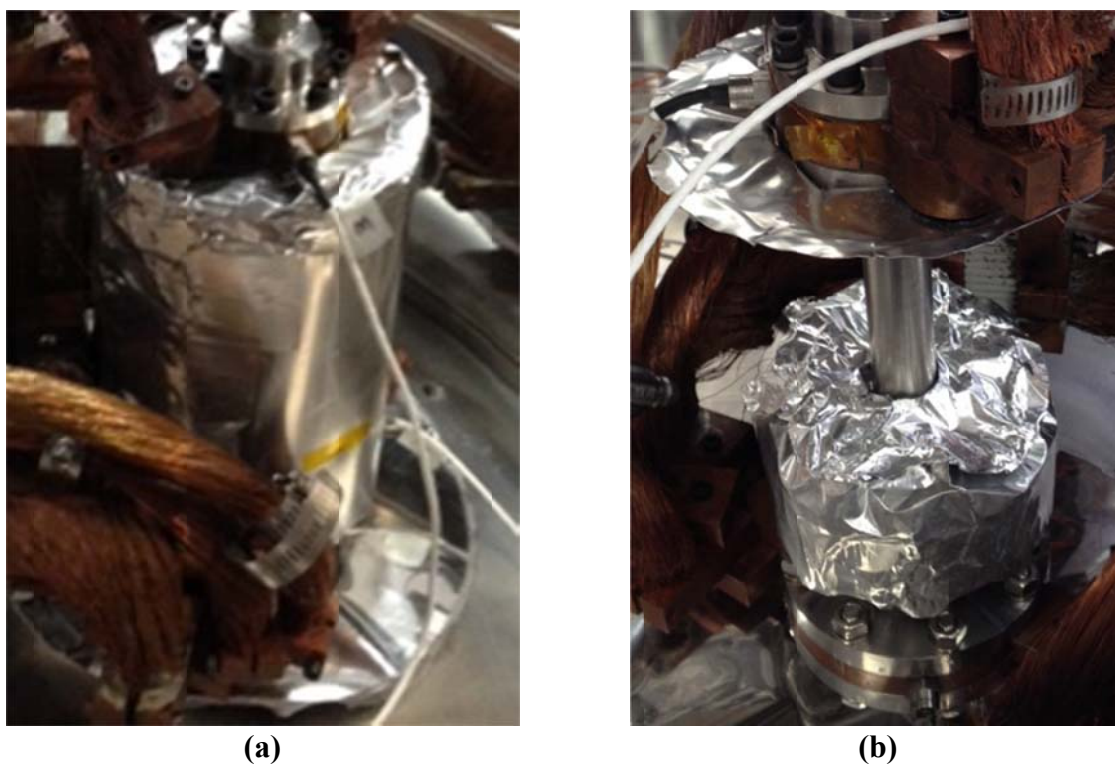


Figure 4.10: Shielding of 20K HX

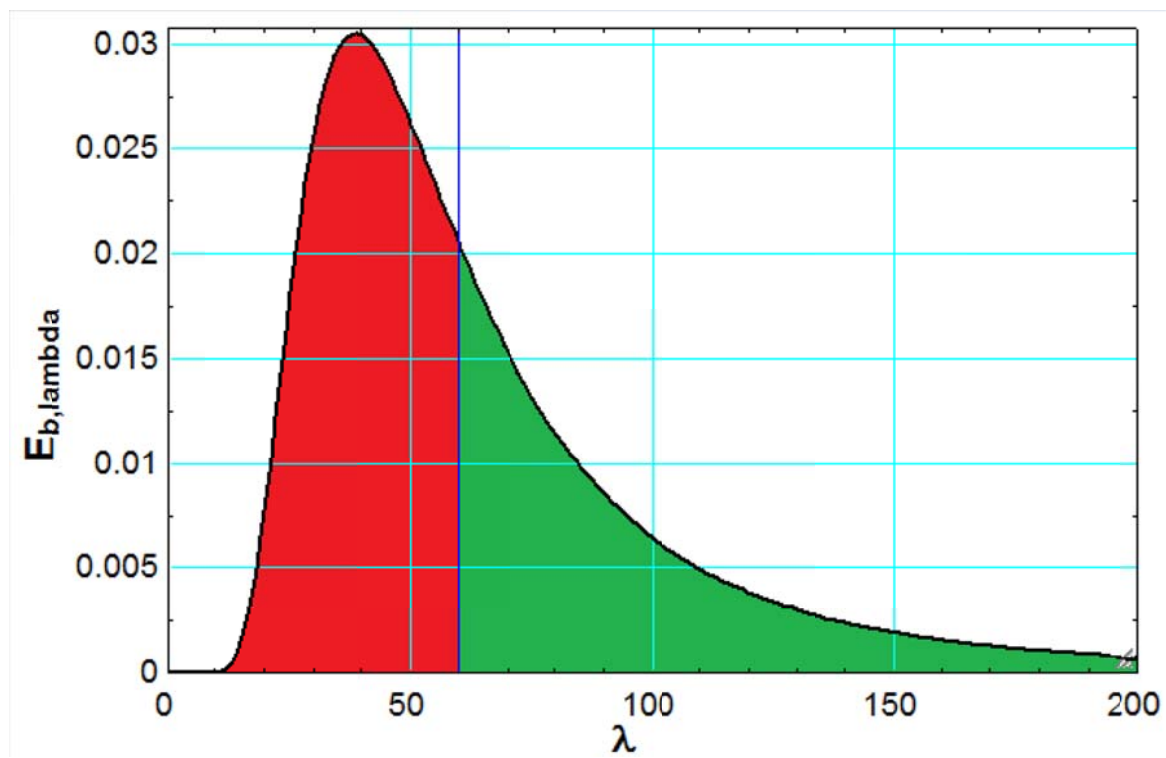


Figure 4.11: Spectral Distribution at 75K

4.3.3 Instrumentation

It is important to have all the components of the test well instrumented. This includes both the GM cooler and the 2nd stage PTC. The majority of the temperature measurements were done using eleven type E thermocouples, which are reliable from 73K to 1173K (NIST 2014). Since the thermocouples are not reliable below 73K, three LakeShore DT-400 series silicon diodes, which are accurate from 10K to 325K (Lake Shore 2015), were employed, two on the 20K heat exchanger and one on the GM cooler. One Endevco 8530B-500 pressure transducer is used to take pressure measurements at room temperature and three Kulite CTL-190 pressure transducers (accurate from 77.65K to 393.15K) are used to take pressure measurements at cryogenic temperatures (Kulite 2015). The mass flow rate through the pulse tube was found by measuring the displacement of the pistons in the compressor. This was done using two Hydrastar HS 1000 position sensors and two SP200A signal processors. The location of each sensor is shown below in Table 4.2; the sensors are wired to a NI SCXI-1100 data acquisition system. The eleven thermocouples, three Kulite pressure transducers, and three diodes are wired from the inside of the Dewar through two KF-40 feedthroughs.

Table 4.2: Location of Each Sensor

Location	Sensor
Compressor	Endevco Transducers P1 and Hydrastar position sensors R and L
Halfway up the precooler	Thermocouples T1, T2, T3 and T4
Bottom 75K HX	Thermocouples T5, T6 and Kulite Pressure Transducer P2
20K HX	Diode 20K T1 and 20K T2
Top 75K HX	Thermocouples T7, T8 Kulite Pressure Transducer P3
Surge Volume	Thermocouples T9, T10 Kulite Pressure Transducer P4
GM cooler (1 st Stage)	Thermocouples T11 and Diode GM T

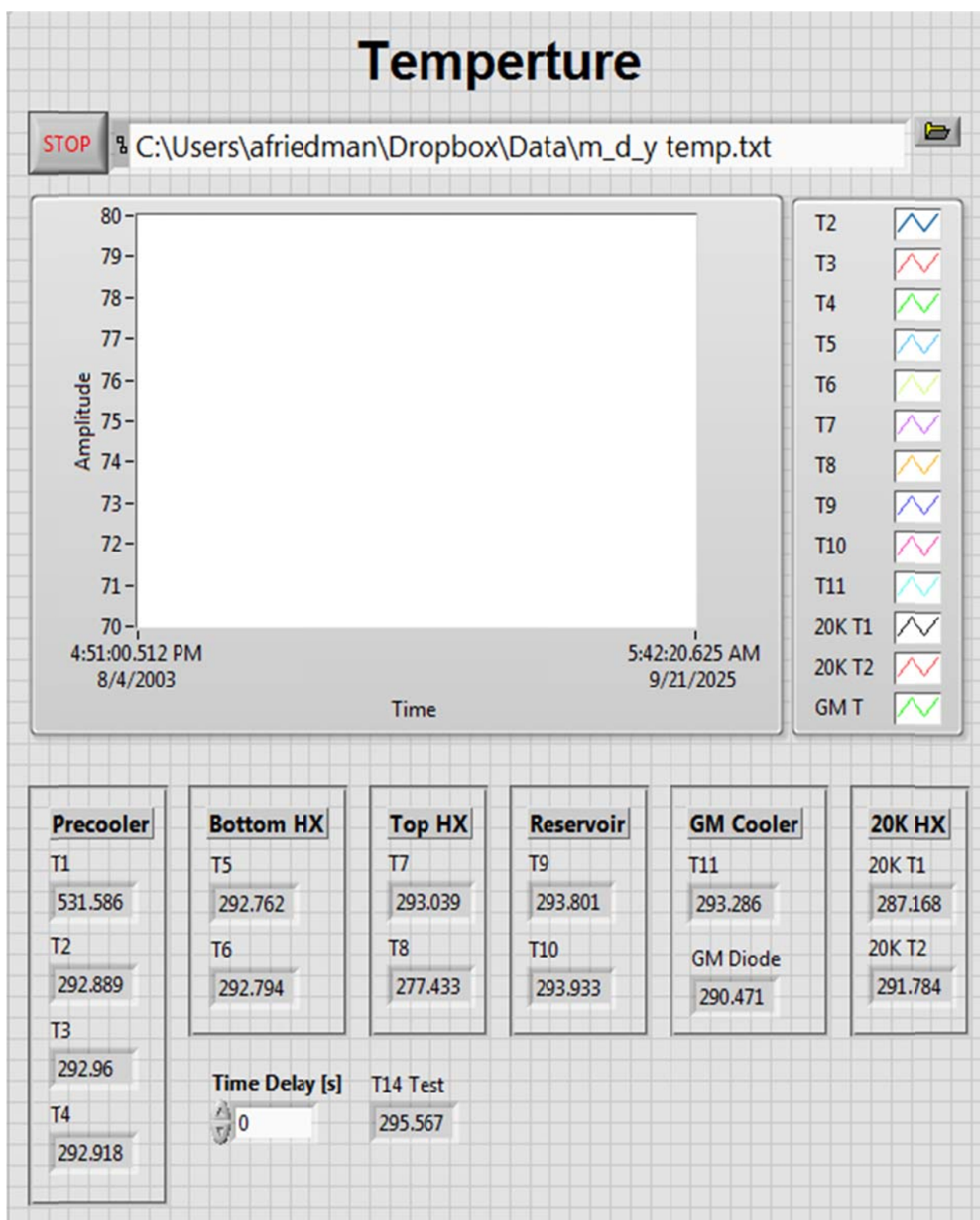
Three heaters were used to test the 2nd stage PTC. This includes one 100W on the thermal bus from the GM cooler to the top 75K heat exchanger, one 100W on the thermal bus from the GM cooler to the bottom 75K heat exchanger and one 7.5W heater on the 20K heat

exchanger. The two 100W heaters are used to keep the 75K heat exchangers at a constant temperature. These heaters are controlled by a variable voltage power supply. The 7.5W heater was used to measure the cooling power of the pulse tube at different temperatures and is connected to a XFR 35-35 DC power supply that measures both current and voltage. To take an accurate voltage measurement over the 7.5W heater a volt meter is wired in parallel at the heater. The power of the heater can then be calculated using $P=VI$.

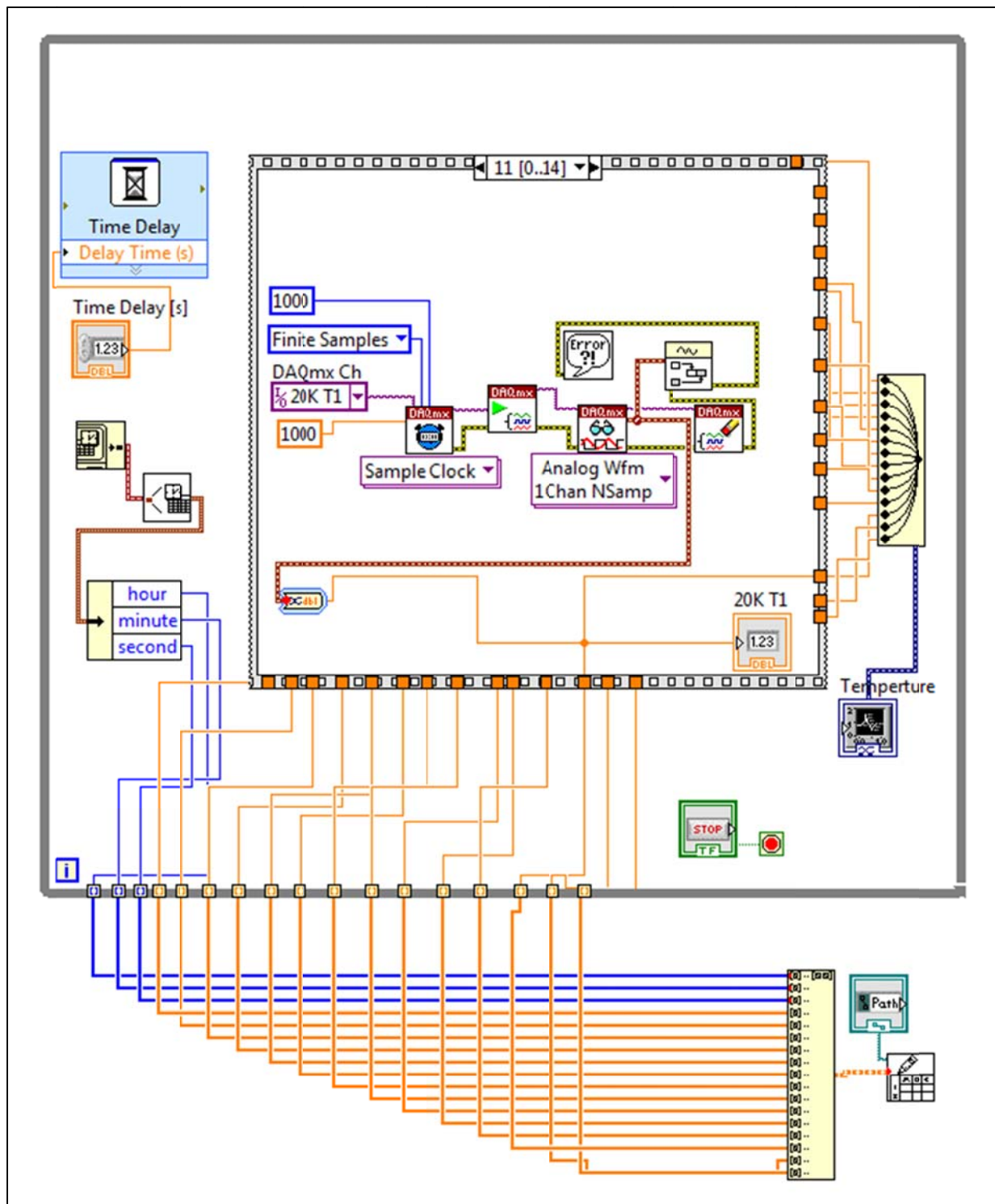
4.3.4 Data Acquisition

The sensors are wired to a NI SCXI-1100, which is connected to a computer. A LabVIEW program was used for thermal (temperature) and mechanical (pressure and displacement) data acquisition, which was then further analyzed in Excel.

Temperature data was acquired using the LabVIEW program shown in Figure 4.12a (the front panel) and Figure 4.12b (the block diagram). This program takes a temperature reading from each temperature sensor sequentially every second starting at T1. Once done with all the temperature sensors, it pauses for the specified time delay minus the time it takes to take all of the temperature measurements (14 s), then repeats. This cycle continues until the stop button on the front panel is pressed. When STOP is pressed the program finishes the current cycle and then records the data and corresponding time in a text document with the name and location specified in the file path. The data was then further analyzed in Excel. It is important to note that the time provided in the text document is the time at the start of each cycle and, therefore, the actual time for each measurement is a few seconds off (depending on the measurement). However, this time change is negligible because it is very small compared to the amount of time it takes the cryocooler to significantly change in temperature.



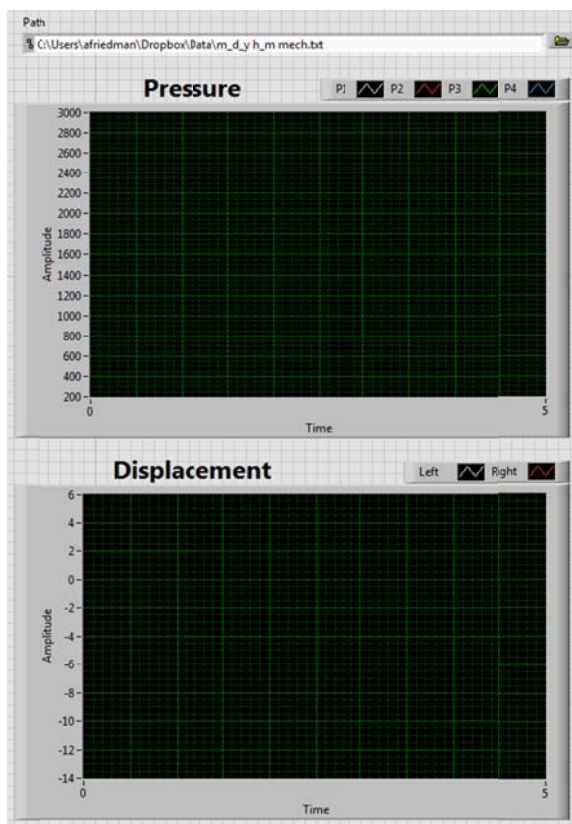
(a)



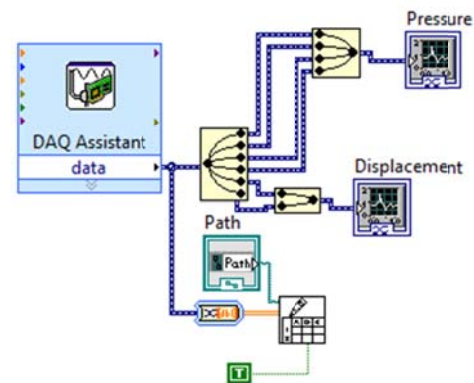
(b)

Figure 4.12: Thermal Program: (a) the front panel (b) the block diagram

Pressure and piston displacement data was taken using the LabVIEW program shown in Figure 4.13a (the front panel) and Figure 4.13b (the block diagram). This is a separate program from the thermal one and works by taking pressure and displacement data sequentially at a rate of 4.5kHz for 5 seconds (22.5k data points for each parameter). After 5 seconds, the program records the time and data to the specified file path and name. As with the thermal program there is a time delay in-between each reading, however, since the program takes data at 4.5kHz, the time difference between the first and last reading must be less than 0.22ms. Since one full period of the parameters being measured takes 100 times as long as the maximum time difference this lag is negligible when analyzing the signal.



(a)



(b)

Figure 4.13: Mechanical program: (a) the front panel (b) the block diagram

4.4 Data Analysis

In conjunction with setting up the data acquisition system, programs to analyze the data were also created. The following section outlines the development of the MATLAB code used to analyze the pressure and mass flow in the cooler.

4.4.1 Determining the Mass Flow

The mass flow rate (\dot{m}) through the cooler can be found using the signals from the displacement sensors on the left and right pistons. The displacement (s) of the pistons follows equation [4.7]. The equation for velocity (v) of the pistons can be derived by taking the derivative of equation [4.7]. This is shown in equation [4.8], where the subscript 0 relates to the maximum displacement.

$$s = s_0 \sin(\omega t) \quad [4.7]$$

$$v = \frac{ds}{dt} = \omega s_0 \cos(\omega t) \quad [4.8]$$

The density (ρ) of the working fluid, helium, can be found by using the ideal gas law shown in equation [4.9], where P_m is mean pressure, R is the gas constant for helium, and T is the temperature of the helium in the compressor.

$$\rho = \frac{P_m}{RT} \quad [4.9]$$

Finally, the mass flow can be derived using the equations for density and velocity, in equation [4.10] where A_p is the area of the piston.

$$\dot{m} = 2\rho v A_p \quad [4.10]$$

Increasing the current supplied to the compressor causes the compressor to have a larger stroke, which creates a higher mass flow rate. A test was run on the system to correlate the

current supplied to the compressor to the mass flow rate in the pulse tube. This was done by taking displacement data of the left and right pistons for current values from 0 to 10A. Using equations [4.8]-[4.10] the mass flow rate can be found. This correlation is shown in Figure 4.14. The mass flow rate through the cooler needs to be 26.95g/s (according to the SAGE model), which corresponds to a current of 6.3A.

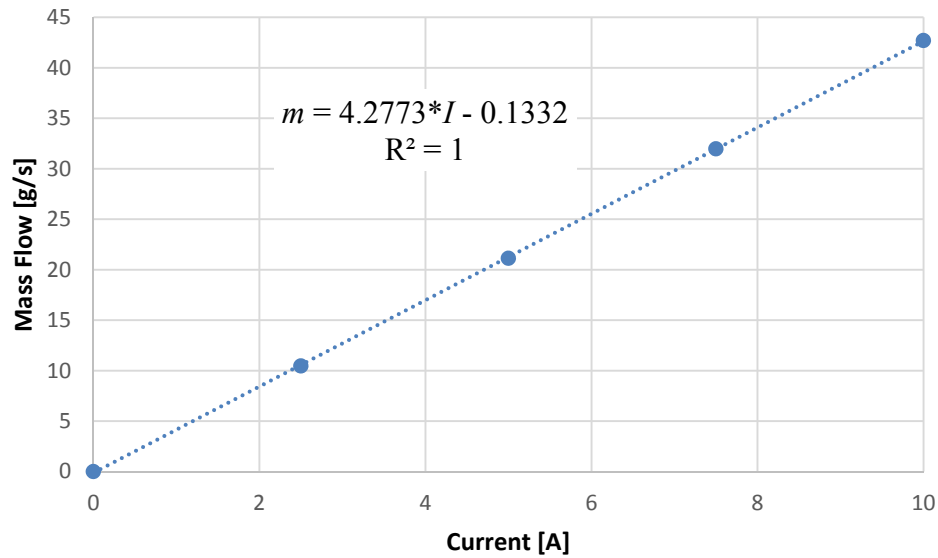


Figure 4.14: Mass flow in the 2nd stage PTC as a function of the current

4.4.2 Phase Angle between Mass Flow and Pressure

From the mechanical data acquired from the LabVIEW code discussed in section 4.3.4

Data Acquisition, the phase, magnitude, and frequency of the pressure and displacement were extracted using the MATLAB code in Appendix B: ESS and MATLAB Code. This code accepts matrix A. Matrix A consist of six columns, one for each mechanical sensor (P1, P2, P3, P4, L and R), and 22,500 rows, each corresponding to a measurement taken at a rate of 4.5kHz. Using the MATLAB command ‘fourier1’ a single term Fourier series was developed for each sensor giving an equation in the form shown in equation [4.11] (the DC offset is neglected in equation [4.11]). After some algebraic and trigonometric

manipulation it can be shown that equation [4.11] is equivalent to equation [4.12] where the magnitude, c , and the phase angle, ϕ , are shown in equations [4.13] and [4.14] respectively.

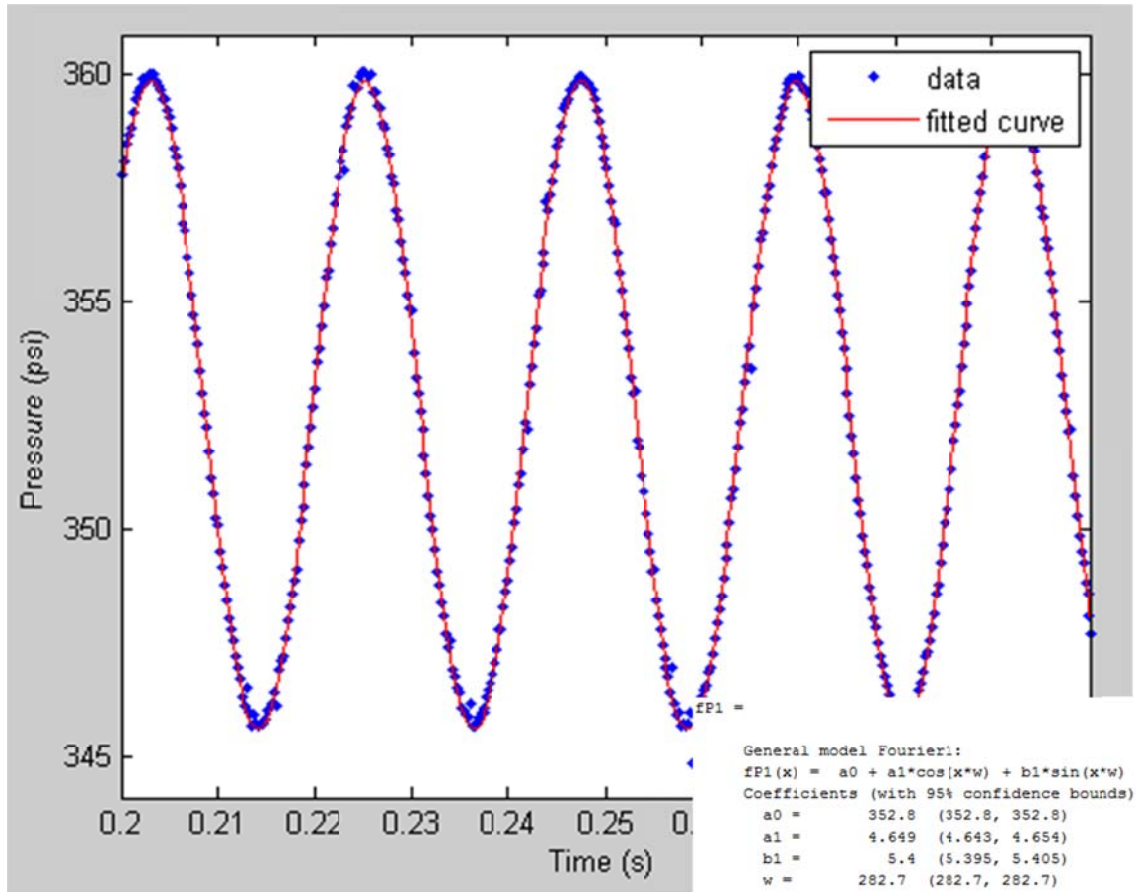
$$F = a * \cos(\omega t) + b * \sin(\omega t) \quad [4.11]$$

$$F = c * \cos(\omega t - \phi) \quad [4.12]$$

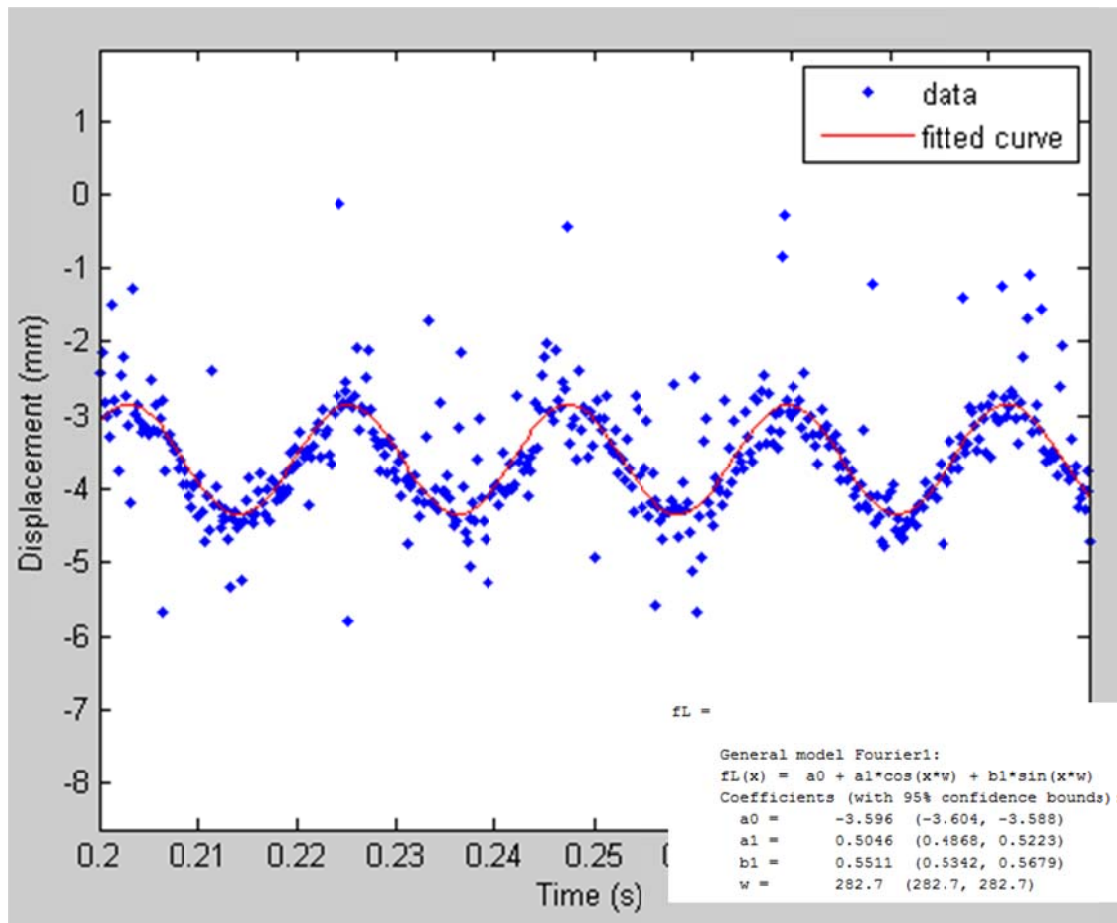
$$c = \sqrt{a^2 + b^2} \quad [4.13]$$

$$\phi = \tan^{-1}(b/a) \quad [4.14]$$

An example of this analysis for the pressure sensor (P1) and the displacement sensor (L) is shown in Figure 4.15.



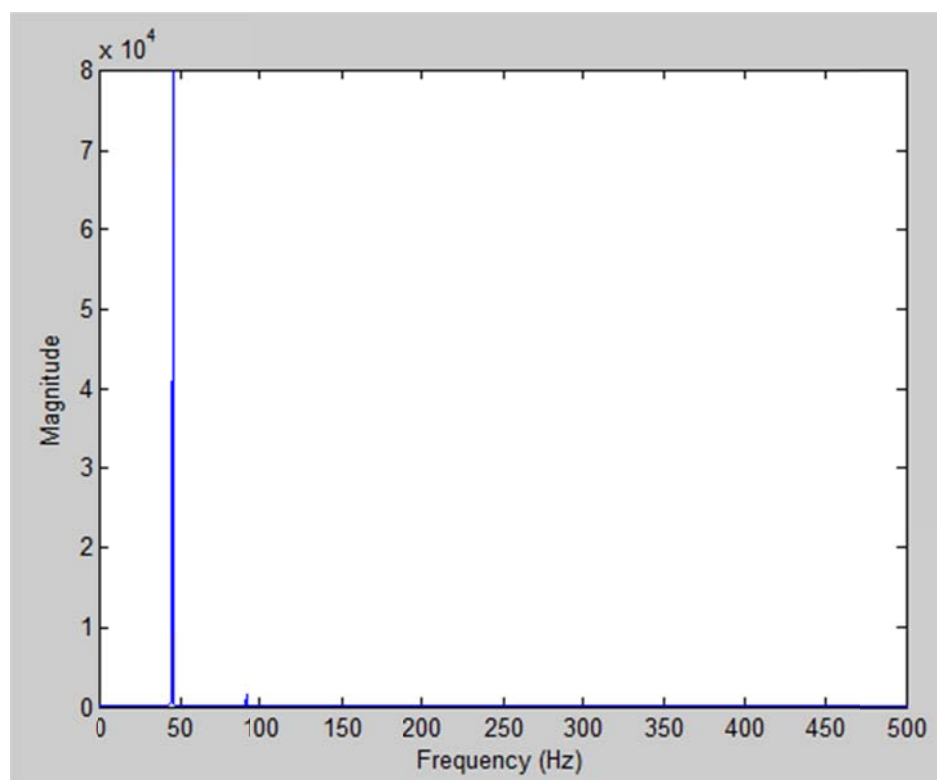
(a)



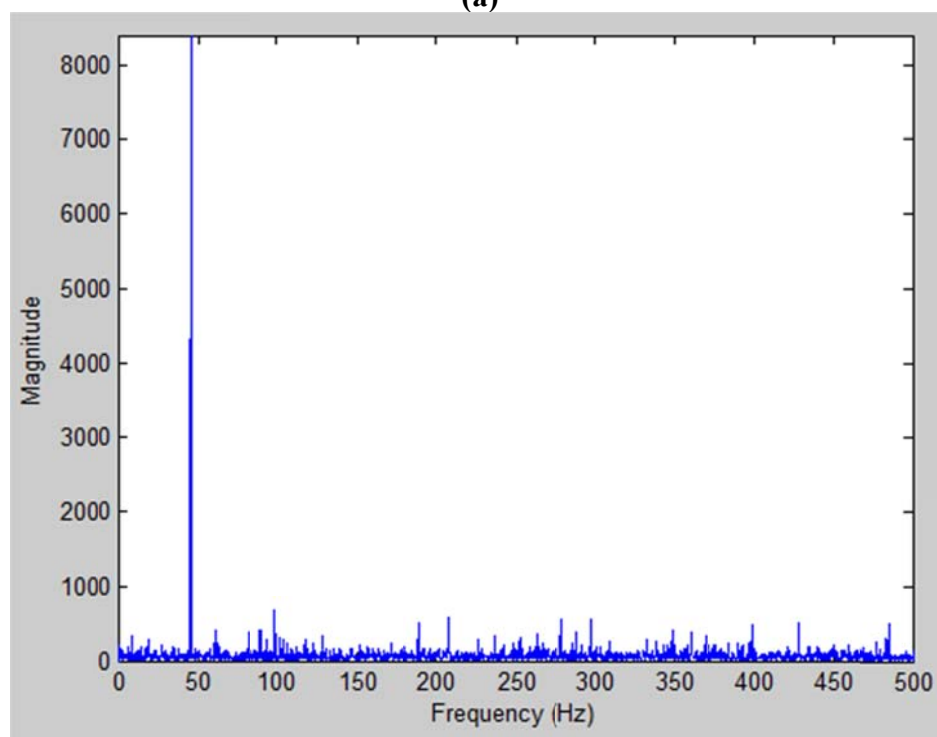
(b)

Figure 4.15: Data and corresponding Fourier series (a) P1 (b) L

As shown in Figure 4.15 the displacement sensors are a lot noisier than the pressure sensors. To determine the source of the noise, a Fast Fourier Transform was added to the Matlab code using the 'fft' command. This transforms the sensor's signals from the time domain to the frequency domain, which displays the frequency of the noise affecting the signal. Figure 4.16 shows the pressure and displacement readings corresponding to Figure 4.15 in the frequency domain. From these plots, it can be seen that there is some noise at most frequencies but it is very small compared to the signal at 45Hz and therefore the 45Hz signal is reliable. To ensure that the data is consistent, five sets of mechanical data were collected, analyzed, and compared.



(a)



(b)

Figure 4.16: Fourier transform (a) P1 (b) L

4.5 Results, Troubleshooting, and Conclusions

Once the preliminary tests were done, data acquisition and analysis programs were developed, the bus bar was put in place, and the cooler was instrumented and covered with MLI, initial testing of the 2nd stage PTC began. The first set of tests were run with the compressor at 5A (mass flow rate of 21.13 g/s), a mean pressure of 360psi and a frequency of 45Hz. The results of this test are shown below in Figure 4.17. The top and bottom 75K heat exchangers reached steady state at (75K±1K). The 20K heat exchanger reached 65.5K with no load.

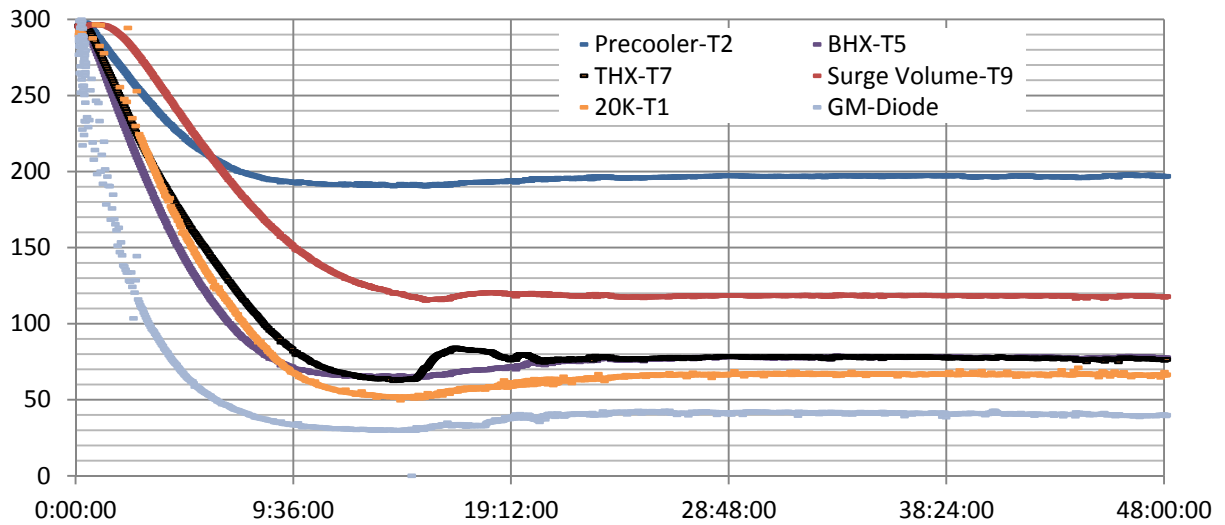


Figure 4.17: Cool down of the 2nd stage PTC

Careful analysis and consideration of all parameters indicate that the failure to reach the design low temperature is due to a few flaws in the system. The main contributing factor to the underperformance of the 2nd stage PTC appears to be the low pressure ratio (PR) produced by the compressor, defined in equation [4.15], where P_a is the pressure amplitude and P_m is the mean pressure.

$$PR = \frac{P_m + P_a}{P_m - P_a} \quad [4.15]$$

Since the performance of the compressor is related to the frequency, a test was run where the frequency was varied and both the stroke of the pistons in the compressor and the pressure ratio was measured. For this test the 2nd stage cooler with a 5.8m long inertance tube was on top of the compressor and the current supplied to the compressor was 10A (RMS) as reported by the power supply running the compressor. The test was run at eight different frequencies, and to ensure accuracy five sets of data were taken at each frequency. The results of this test are shown in Figure 4.18. This data shows that there may be a mismatch between the compressor and the 2nd stage cooler which does not occur when the two stage PTC is attached to the compressor. In order to account for this difference, the SAGE model was rerun with only the 2nd stage cooler.

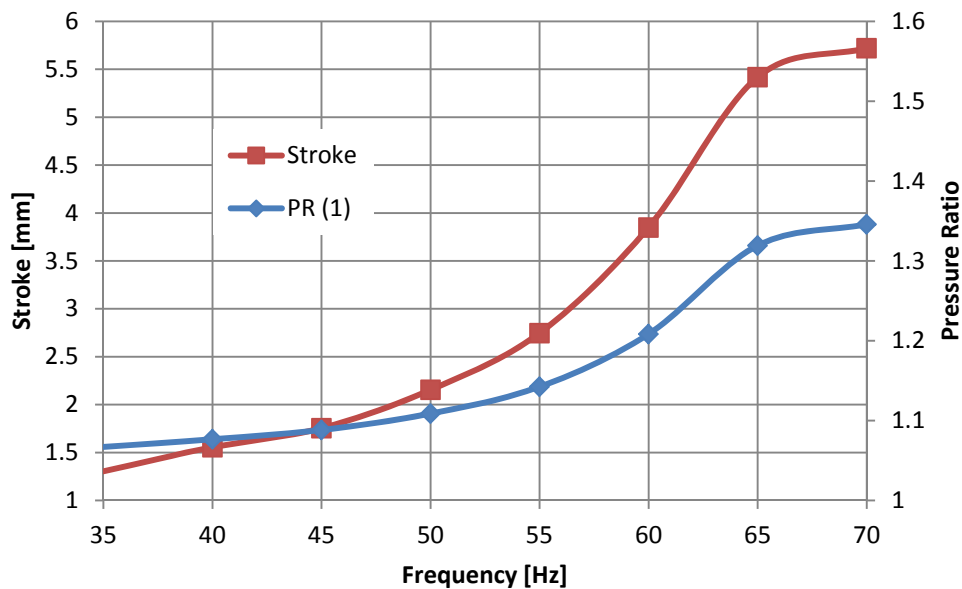


Figure 4.18: Pressure ratio and stroke as a function of frequency

After the SAGE model was rerun with just the 2nd stage cooler, it predicted that the cooler would need a pressure ratio of 1.88 to reach 20K, which this compressor cannot reach. Therefore, there is a mismatch between the compressor and the PTC. The compressor

mismatch can be remedied by adding a transfer-line, which is a second inertance tube, shown in Figure 4.19, between the compressor and the aftercooler. A transfer-line downstream of the cooler but upstream of the compressor would cause the compressor to appear like it had a larger impedance without affecting the entire impedance of the system, as changing the inertance tube would do. The transfer-line was designed but never developed due to time constraints and the objective of the research being to develop the two stage PTC.



Figure 4.19: The transfer-line

Another issue that the data indicated was that there was a significant gap between the precooler's screens and its shell. This could result in the helium flowing predominantly on the outside of the precooler, which would reduce its effectiveness. To check if this was the case the experimental pressure drop from the top of the compressor to the bottom 75K heat

exchanger was compared to the SAGE model's predicted mass flow and pressure drop as shown in Table 4.3. The data show that there was a significant amount of helium blowing around the edge of the precooler, so the inner diameter of the precooler and the outer diameter of the screens were re-measured. This measurement showed that there is a gap of 0.004" due to the shell being 0.0015" above tolerance and the screens being 0.0025" below tolerance. Therefore, the precooler used in the two stage PTC was made to account for the screens being small.

Table 4.3: Pressure Drop and Mass Flow over the Precooler

	Experimental	SAGE
Mass Flow (g/s)	17.9	10.8
Pressure Drop (KPa)	13	13

Due to time constraint, it was decided to continue with the manufacturing and testing of the two stage PTC.

5. Full PTC Testing

5.1 Introduction

The modular design of the standalone 2nd stage PTC enabled the entire 2nd stage to be reused when building the two stage PTC. The rest of the two stage PTC was built and assembled according to the design specifications laid out in Chapter 2. The 2nd stage PTC, the 1st stage of the two stage PTC, and the two stage PTC are shown in Figure 5.1. The following chapter outlines the experimental setup, testing and results of the two stage PTC.

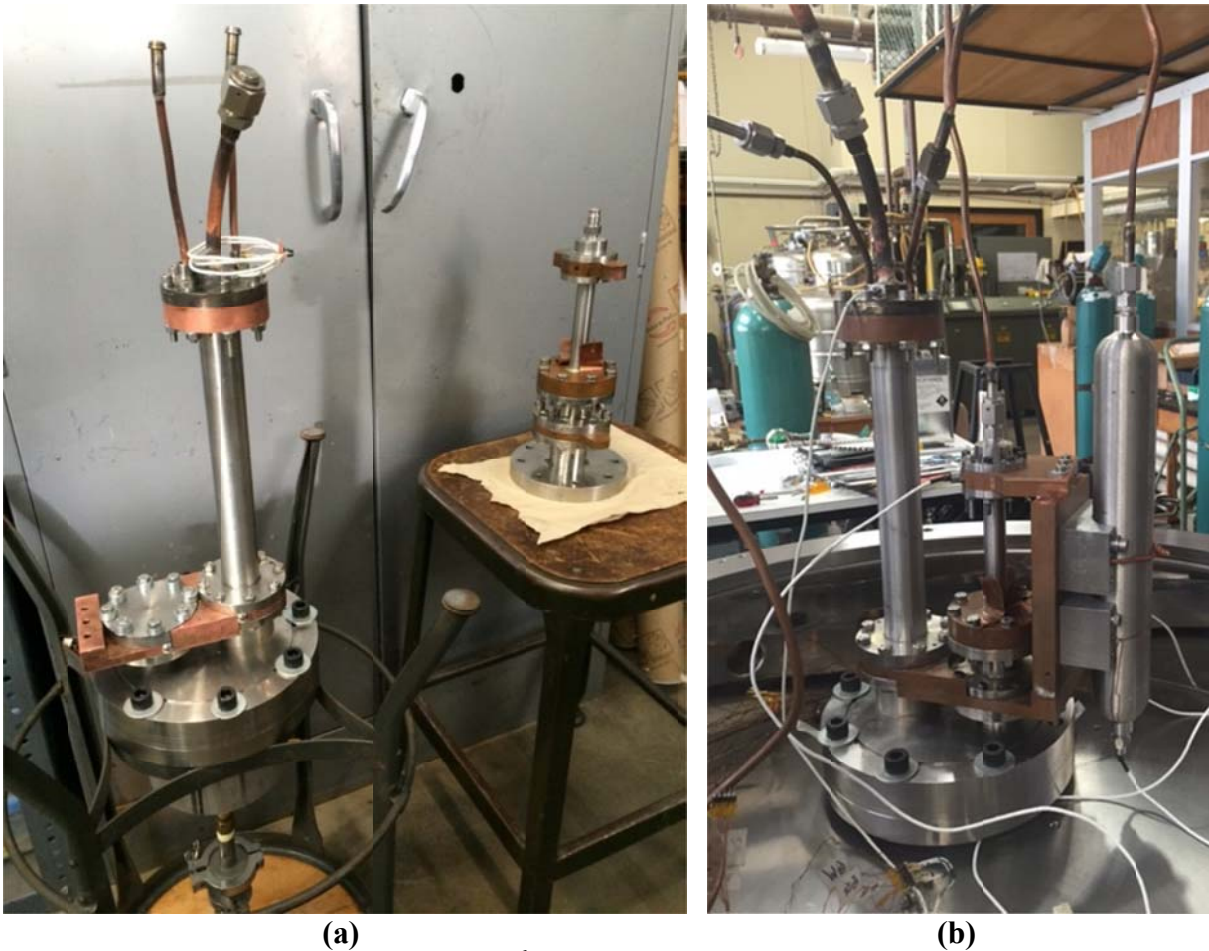


Figure 5.1: (a) Separate 1st stage and 2nd stage PTC (b) two stage PTC

5.2 Experimental Setup and Data Collection

Before the cooler was run it was hydrostatically pressure tested and leak tested to ensure that it was safe and would not leak in a high vacuum environment. This was done using the same methods outlined in section 4.2 Preliminary Testing.

Once the cooler passed the pressure and leak test, it was instrumented as shown in Figure 5.2. The same type of instrumentation that was used for the 2nd stage PTC was used when testing the two stage PTC. The compressor has sensors P1, L, and R as it did when the 2nd stage PTC was being tested. Therefore, dynamic measurements of the mass flow and the pressure are available at this location. Also, two current transformers were added to the compressor so dynamic current information would be available. The current sensors are read using the same LabVIEW program used to read the pressure and displacement sensors. The conical adaptor has two thermocouples (T1 and T2) to ensure that the copper screens transfer the heat from the precooler and 1st stage regenerator to the aftercooler, instead of trapping heat in the conical adaptor. There are three thermocouples (T3, T4, and T6) on the common heat exchanger and one (T5) on the 75K bus bar. The common heat exchanger has a pressure transducer (P2) between the precooler and 2nd stage regenerator, which along with P1, allows for the pressure drop over the precooler to be determined. Phase information at the end of the precooler can be extrapolated from P2 and the pressure ratio into the 2nd stage regenerator can be found. The 20K heat exchanger has two diodes (D1 and D2) to ensure accurate temperature measurements at low temperatures. There is also a 7.5W heater so a cooling curve can be developed for the two stage PTC. The top 75K hot heat exchanger has two thermocouples (T7 and T8) and a pressure transducer (P3). This pressure transducer provides phase information and in conjunction with P2 gives the pressure drop over the 2nd stage

regenerator, since the pulse tube and the heat exchangers have a negligible pressure drop relative to the 2nd stage regenerator. The 2nd stage reservoir has two thermocouples (T9 and T10) along with a pressure transducer (P4). Assuming that the reservoir acts as a pure capacitance, the mass flow into the reservoir can be found using P4 and equation [1.1]. T11 and T12 are on the 300K heat exchanger, to ensure that the water to helium heat exchanger is working properly. P5 is an Endevco pressure transducer located on the 1st stage transition region which provides phase information and the pressure drop over the 1st stage regenerator. The 1st stage reservoir has no thermometry on it because it is meant to stay at room temperature and it is located outside of the vacuum.

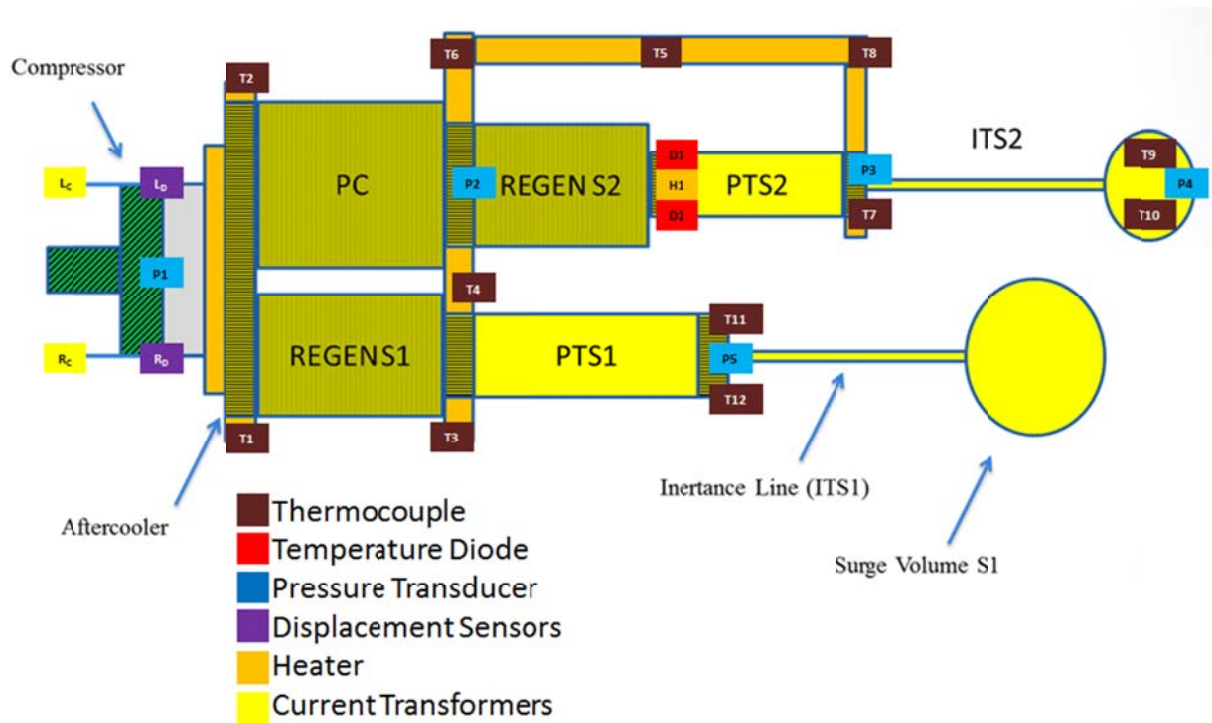


Figure 5.2: Locations of instrumentation used for the two stage PTC

After the cooler was instrumented, it was covered with radiation shields using the same approach as was used when covering the 2nd stage PTC (outlined in section 4.3.2). The 20K

heat exchanger was covered in an aluminum radiation shield with a thickness of 381microns. Then, the precooler, both regenerators, and both pulse tubes were covered with five layers of aluminized Mylar with polyester between each layer. Lastly, the entire 75K section of the cooler was covered with ten layers of aluminized Mylar with polyester between each layer.

5.3 Results

The first set of tests were run on the two stage PTC to determine the correct current at which to run the compressor to ensure that the pressure ratio and stroke provided by the SAGE model matched the experiment. This test was performed by running the compressor at a variety of different currents with the two stage PTC mounted. The compressor was run at 5A, 10A, 15A and 20A while taking displacement and pressure data (using the L, R, and P1 sensors). The corresponding pressure ratio and stroke for each current setting is shown in Figure 5.3 (Note: this test was done at 45Hz).

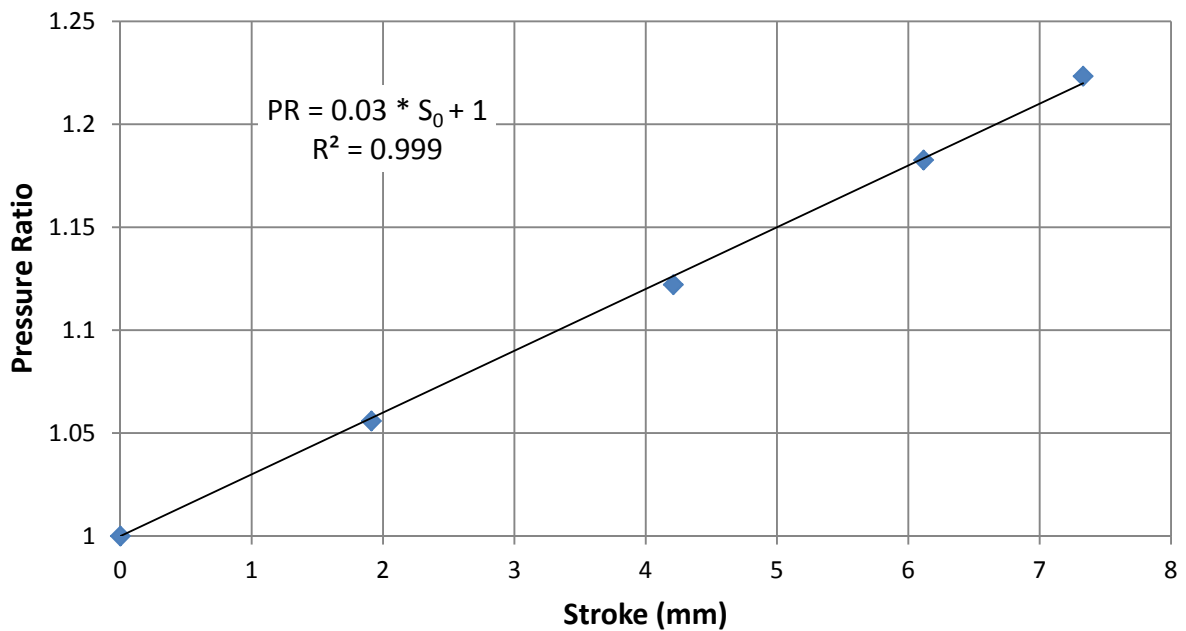


Figure 5.3: Stroke and pressure ratio of the compressor with two stage PTC mounted

When matching the SAGE models stroke (9.6mm) to the experimental trend, the error between the experimental and the model's pressure ratio (1.267) is 1.66%. Unfortunately, the current required to accommodate this input is 25.5A and the compressor can run at a maximum current of 16A. Therefore, the two stage PTC was run at 15.5A, which corresponds to a pressure ratio of 1.16 and a stroke of 5.51mm. Once at steady state, a cooling curve was developed for the two stage PTC. The curve was created by having no load on the 1st stage, while the 2nd stage was tested at 0W, 1W, and 2W as shown in Figure 5.4: Cooling Curve for the two stage PTC.

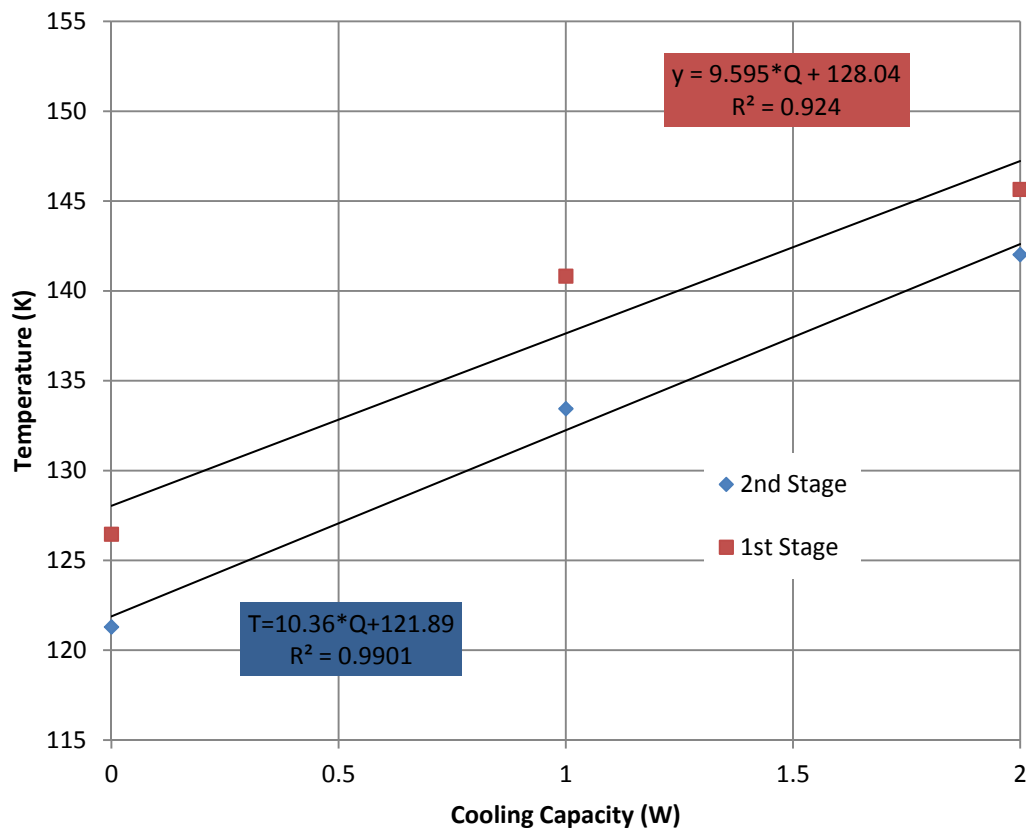


Figure 5.4: Cooling Curve for the two stage PTC

5.4 Conclusions and Recommendations

It is clear from Figure 5.5 that the two stage PTC did not meet the project's target of 3W at 20K. After further investigation, it appears that there are two main issues responsible for the poor performance of the cooler. The first is that due to the 16A limitation of the compressor, the mass flow into the compressor (.112 kg/s) and the pressure amplitude at the compressor (28.2 psi) are lower than what the SAGE model specified ($\dot{m}=0.134$ kg/s and $P=40.8$ psi). This results in a loss of acoustic power. According to equation 5.1, acoustic power is a function of the magnitude and phase, of the mass flow and pressure (Swift 2002). Since the experimental phase angle is only 4.5° greater than the model's predicted phase angle, the 52.5% reduction in acoustic power ($\dot{E}_e=847$ W $\dot{E}_{SAGE}=1783$ W) must be predominantly due to the low magnitude of the pressure and mass flow.

$$\dot{E} = \frac{1}{2\rho} |P| |\dot{m}| \cos(\phi_{P\dot{m}}) \quad [5.1]$$

Since the performance of the compressor is tightly linked to its operating frequency, changing the frequency increases the acoustic power. Therefore, the mass flow and pressure at the compressor was measured as a function of frequency as shown in Figure 5.5. It is clear from Figure 5.5 that running at a frequency above 45Hz will increase the mass flow and the pressure into the cooler, which will result in a large increase of acoustic power. (Note: from 40Hz to 55Hz, the phase between the mass flow and pressure changed by 5.3° so it doesn't have a large effect on acoustic power.) The lack in acoustic power is likely the explanation of why the 1st stage PTC fell significantly short of its 75K goal, since both the phase angle at the inlet of the cooler and the pressure drop over the 1st stage regenerator match the SAGE model. However, it does not explain why the 2nd stage PTC is only 5.2K below the 1st stage.

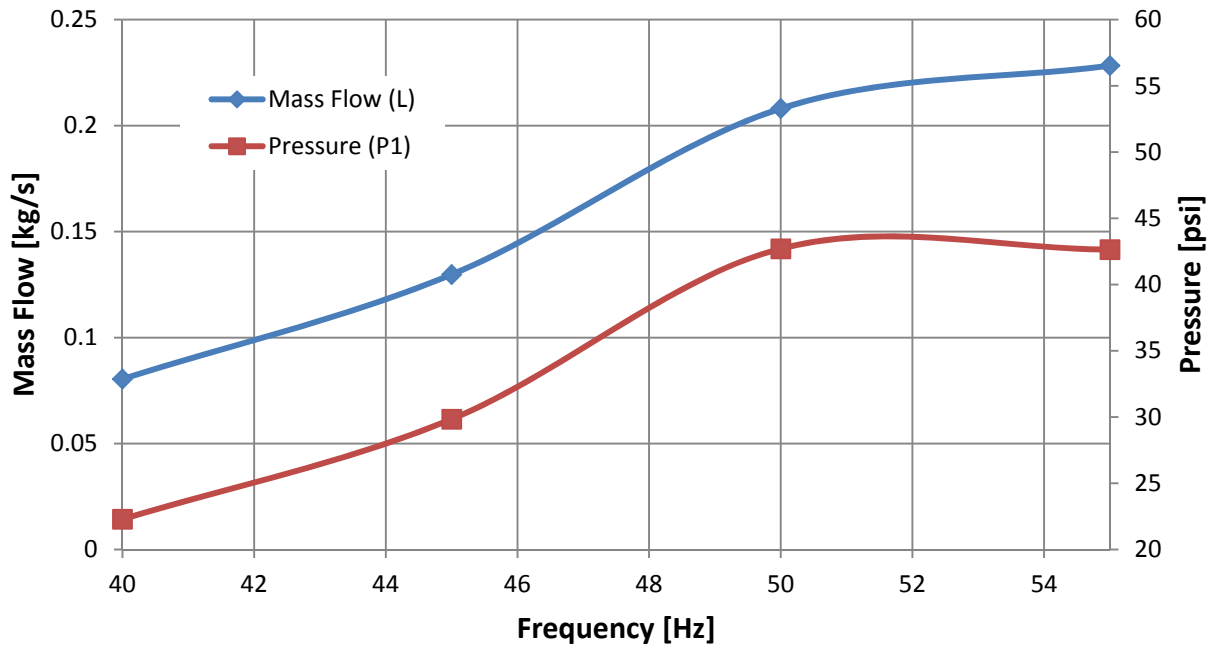


Figure 5.5: Pressure and mass flow as a function of frequency

The second large issue that explains the poor performance of the two stage PTC is that the 2nd stage regenerator is not functioning properly. The pressure drop over the 2nd stage regenerator is only 48.8% of what the SAGE model predicts. Since the mass flow through the regenerator is constant and the density of helium increases as temperature decreases, the actual pressure drop would become farther from the predicted pressure drop when the regenerator is operated at lower temperatures. Therefore, the regenerator must have not been packed to meet the specifications of the SAGE model. Thus, the 2nd stage of the two stage PTC is doing very little to contribute to the overall performance of the cooler and the 2nd stage regenerator needs to be repacked.

References

ASME Pressure Vessel Code, Section VIII, Division I.

"Cryogenic Propellant Storage & Transfer." NASA. NASA, 30 Oct. 2013.

Swift, G. W. Thermoacoustics: A Unifying Perspective for Some Engines and Refrigerators. Melville, NY: Acoustical Society of America through the American Institute of Physics, 2002. Print.

Alar, Eric. A Test Facility for New Non-Rare-Earth Pulse Tube Cryocooler Regenerator Plates. Thesis. UNIVERSITY OF WISCONSIN – MADISON, 2013. N.p.: n.p., n.d. Print.

Klein, Sanford A., and Gregory Nellis. Thermodynamics. New York: Cambridge UP, 2012. Print.

Heat Transfer, G.F. Nellis and S.A. Klein, Cambridge University Press, 2009

Sanchez, N. "Cryogenic Properties of Copper." Cryogenic Properties of Copper, July 1990.

Clearman, William M. Measurement and Correlation of Directional Permeability and Forchheimer's Inertial Coefficient of Micro Porous Structures Used in Pulse-Tube Cryocoolers. Thesis. Georgia Institute of Technology, 2007.

Fluent Inc. "User Inputs for Porous Media." FLUENT 6.3 Documentation. ANSYS FLUENT, 20 Sept. 2006.

Musilova, V., Hanzelka, P., Kralik, T., Srnka, A., "Low temperature radiative properties of materials used in cryogenics", Cryogenics, Vol. 45 (2004) Pg. 529-536

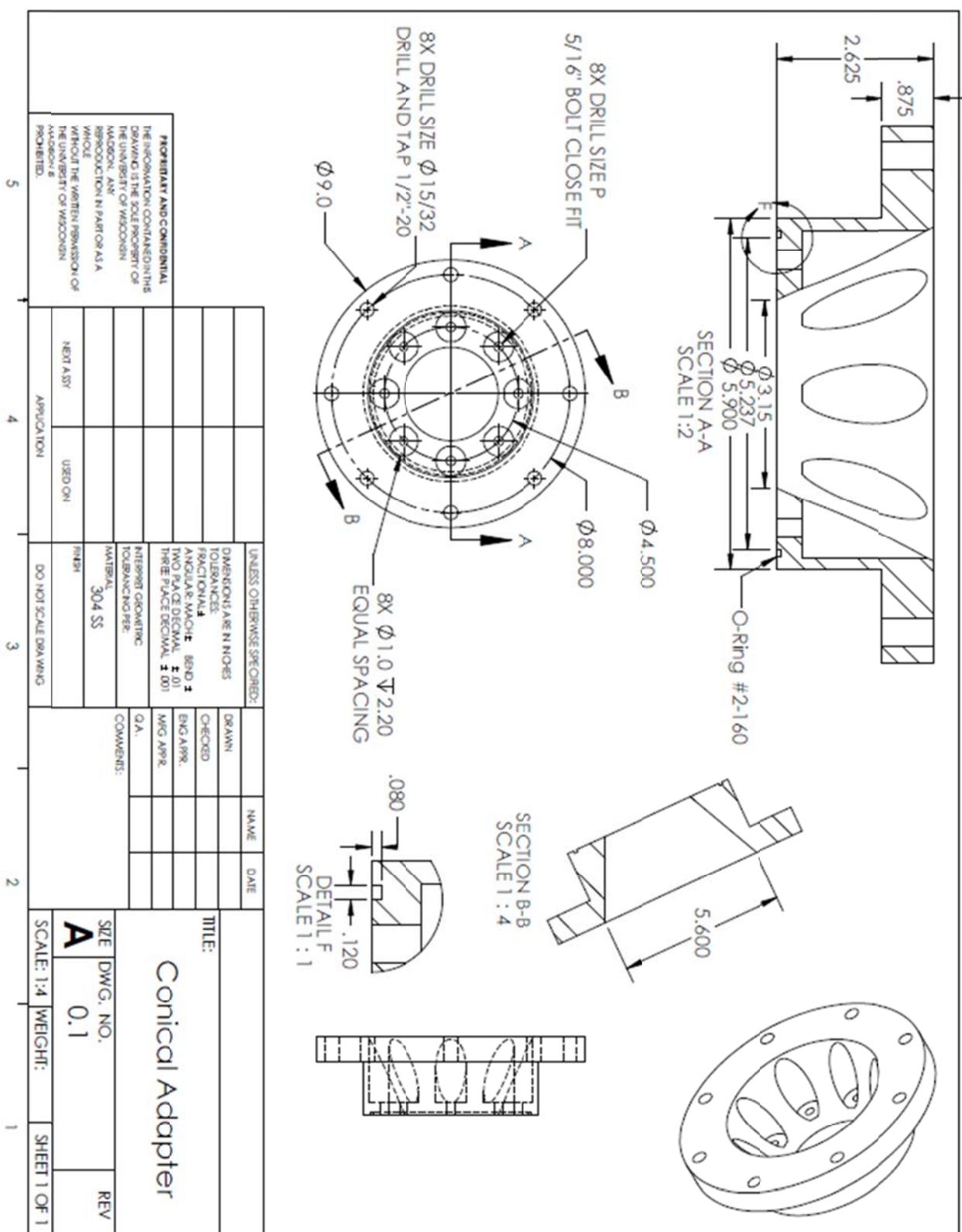
Jahromi, Amir E. Development of a 1K Facility and Modeling of a Superfluid Magnetic Pump with No Moving Parts. Thesis. University of Wisconsin-Madison, 2011.

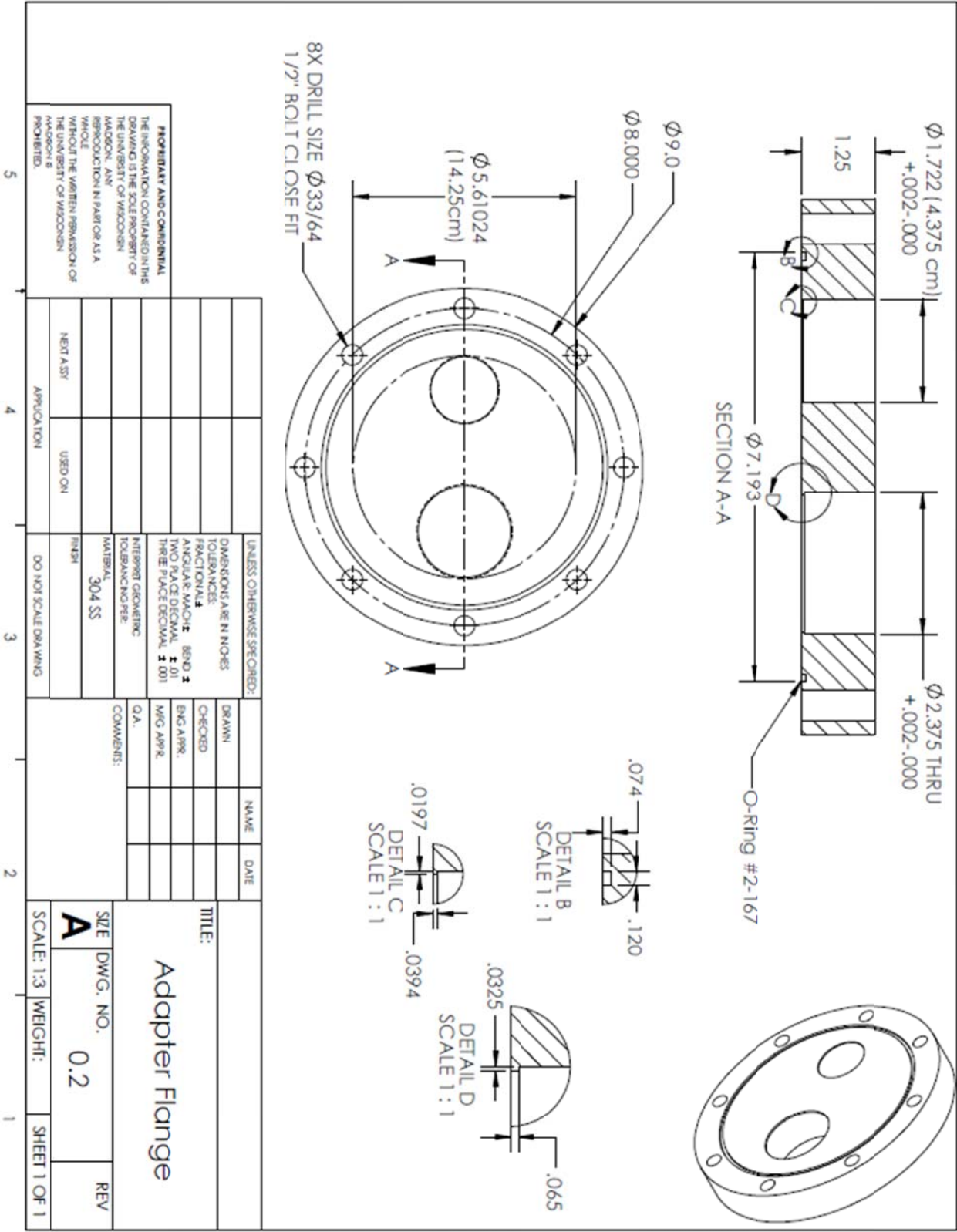
"ITS-90 Thermocouple Database." ITS-90 Thermocouple Database. NIST 2014

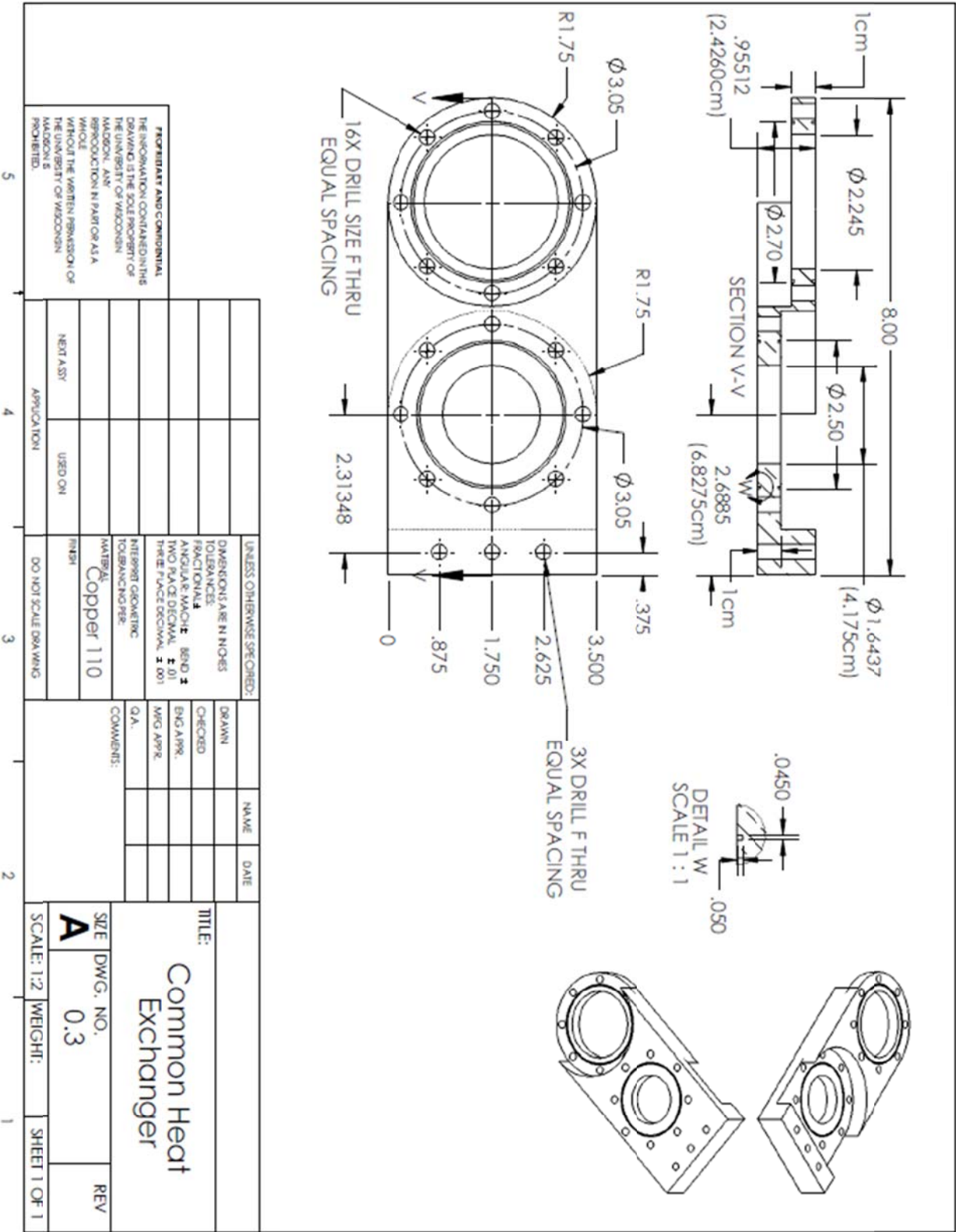
"DT-400 Series Silicon Diodes." Lake Shore 2015

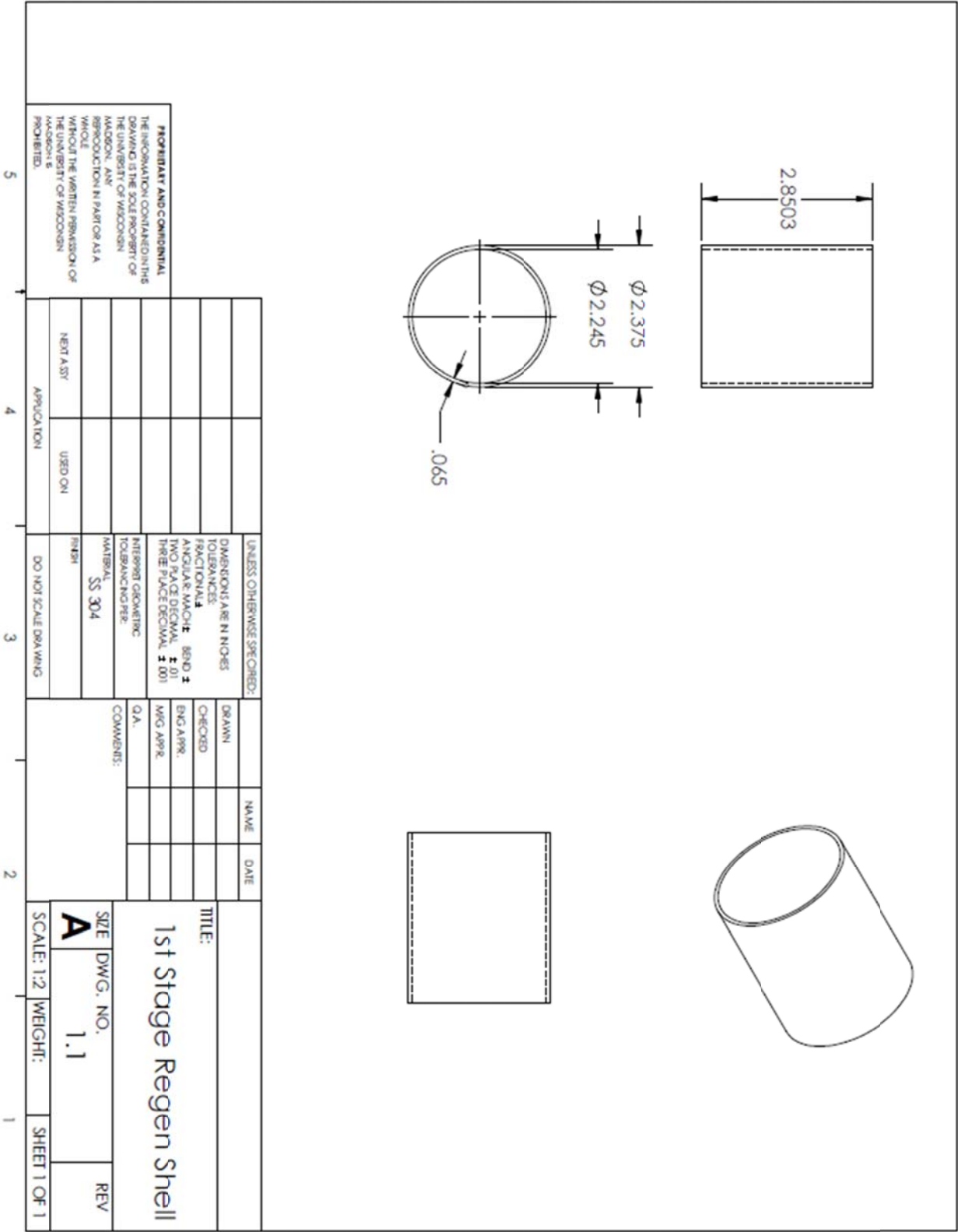
Kulite "Cryogenic Miniature Ruggedized Pressure Transducer" (2015)

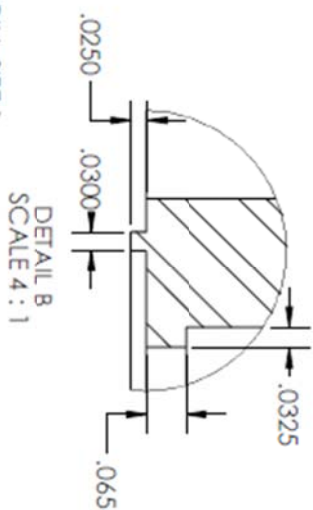
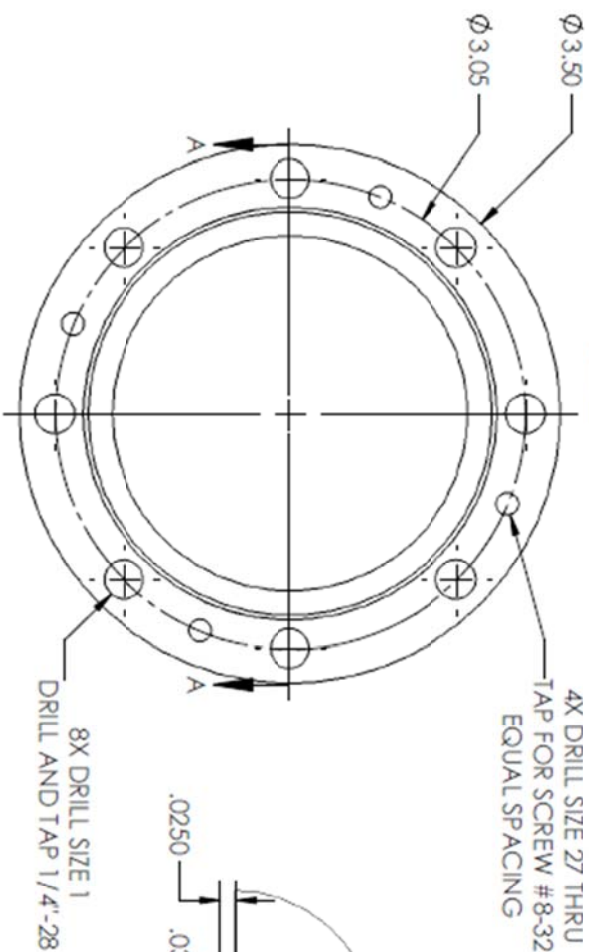
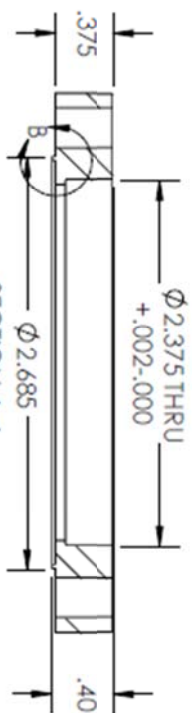
Barron, Randall F. Cryogenic Systems. 2nd ed. New York: Oxford UP, 1985. Print.











PROPERTY AND CONFIDENTIAL
THE INFORMATION CONTAINED IN THIS
DRAWING IS THE SOLE PROPERTY OF
THE UNIVERSITY OF WISCONSIN
MADISON. ANY REPRODUCTION IN
WHOLE OR IN PART WITHOUT THE
WRITTEN PERMISSION OF THE
UNIVERSITY OF WISCONSIN MADISON
IS PROHIBITED.

5

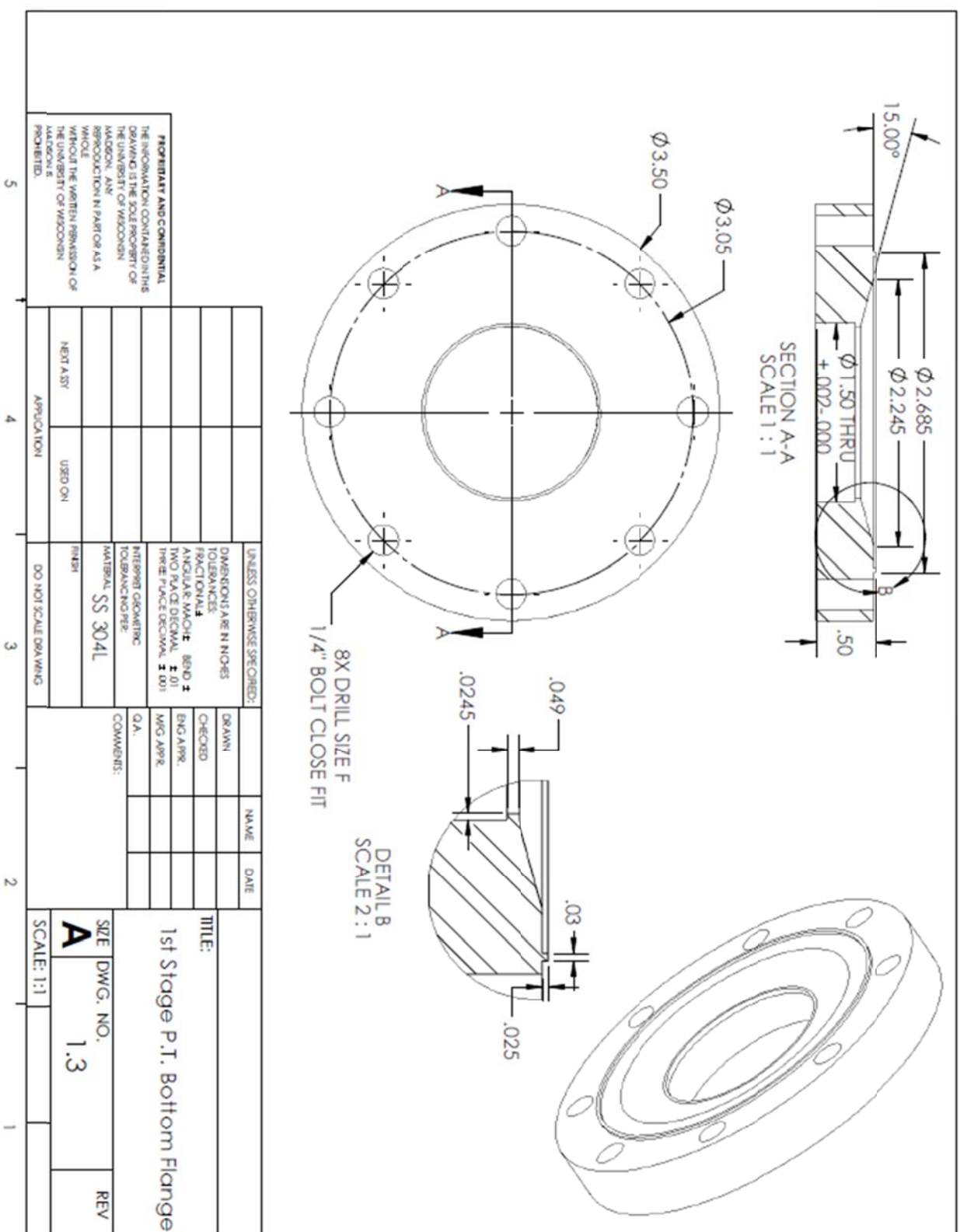
4

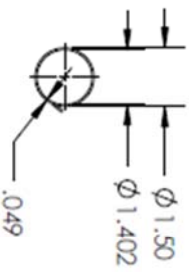
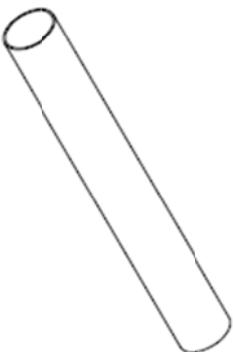
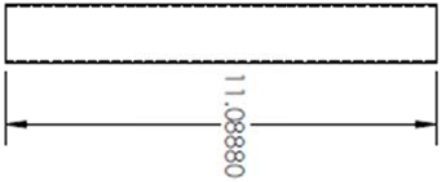
3

2

1

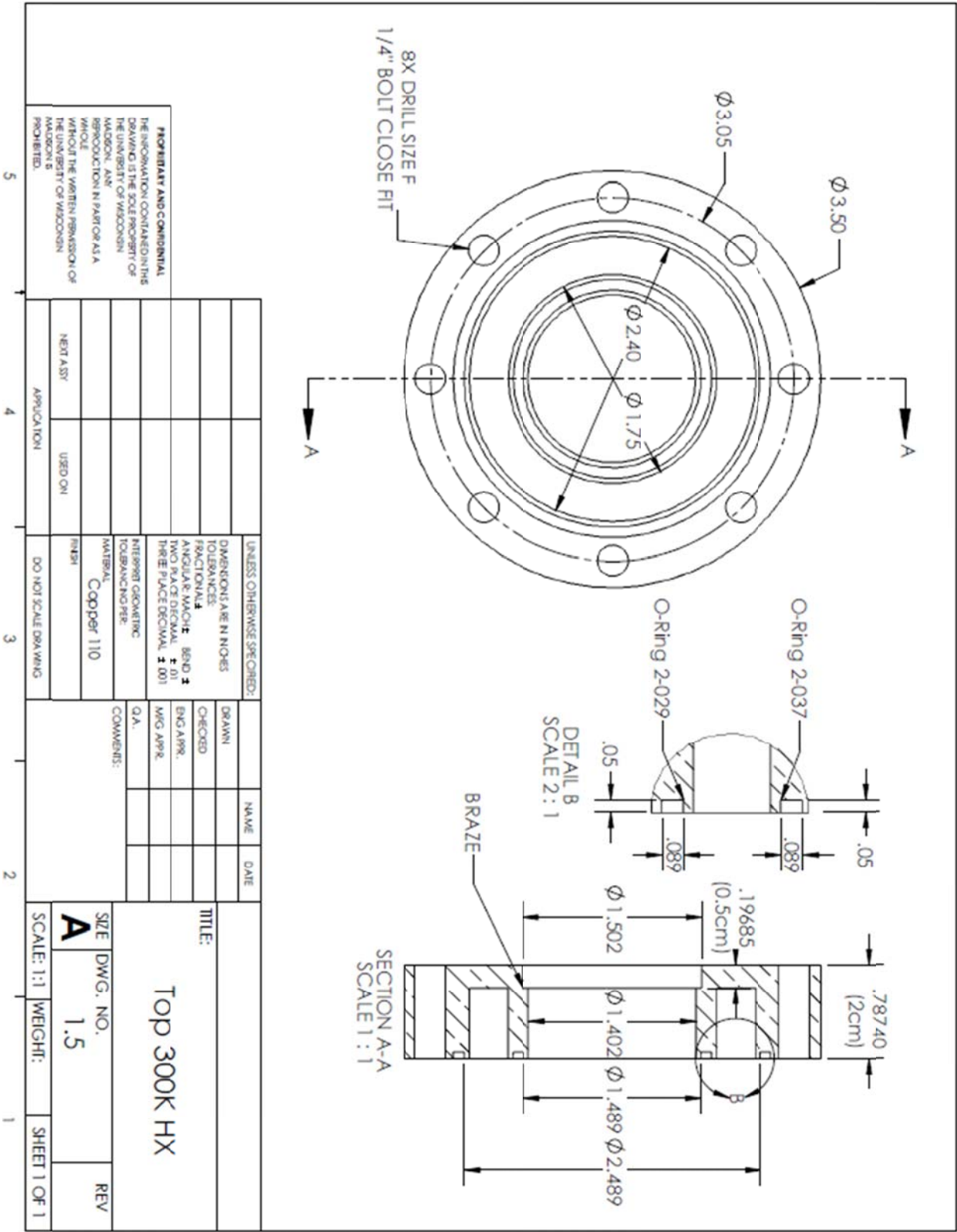
UNLESS OTHERWISE SPECIFIED:				NAME		DATE	
DIMENSIONS ARE IN INCHES				DRAWN			
TOLERANCES				CHECKED			
FRACTIONAL				ENG APPR.			
ANGULAR MATCH				W/C APPR.			
TWO PLACE DECIMAL $\pm .01$				Q.A.			
THREE PLACE DECIMAL $\pm .001$				COMMENTS:			
INTERPRET DIMENSIONS							
TOLERANCING PER							
MATERIAL							
SS 304							
FINISH							
NEUTRALITY							
USED ON							
APPLICATION							
DO NOT SCALE DRAWING							
TITLE:				1st Stage Regen Top Flange			
SIZE DWG. NO.				A 1.2			
SCALE: 1:1				REV			
SHEET 1 OF 1							

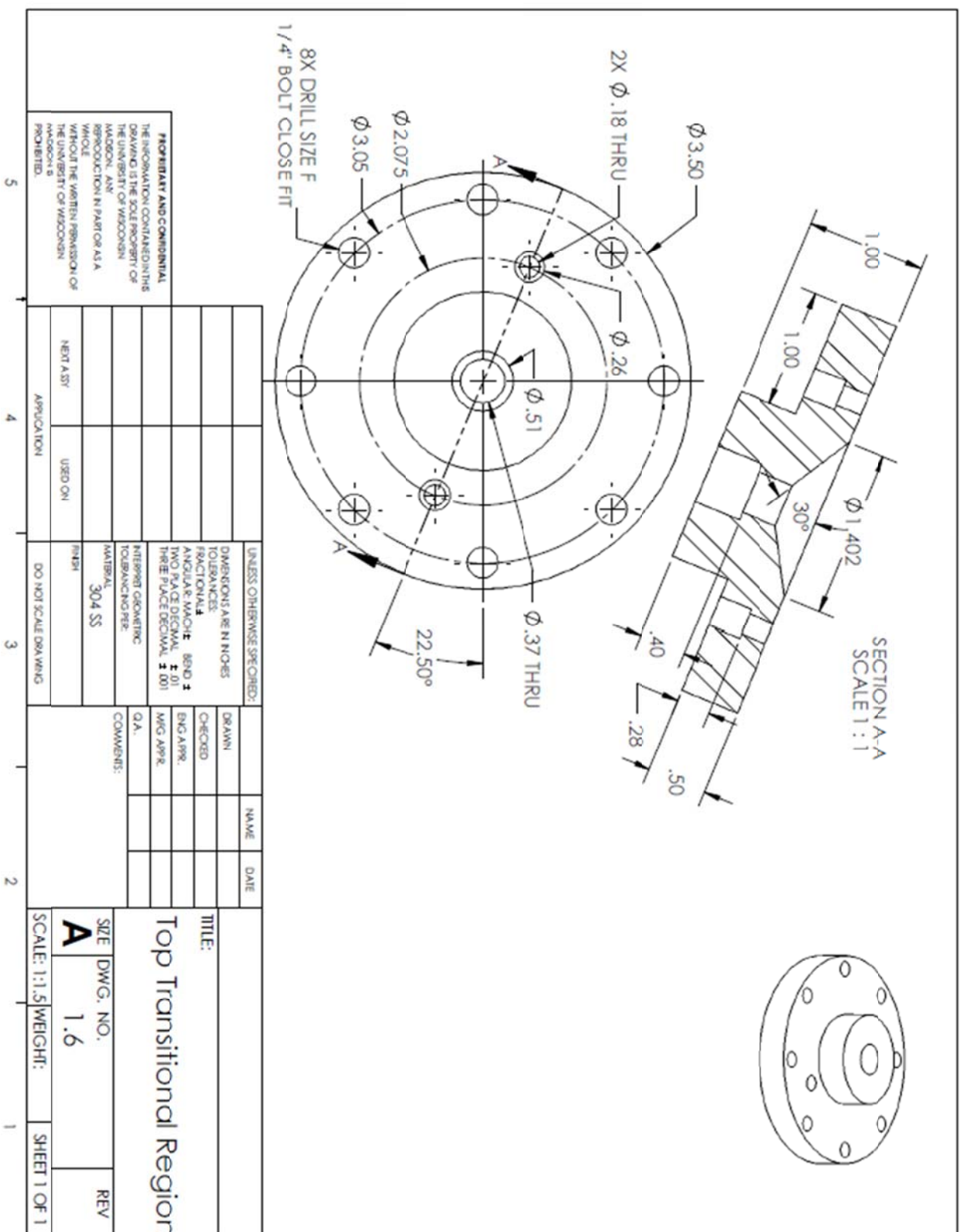


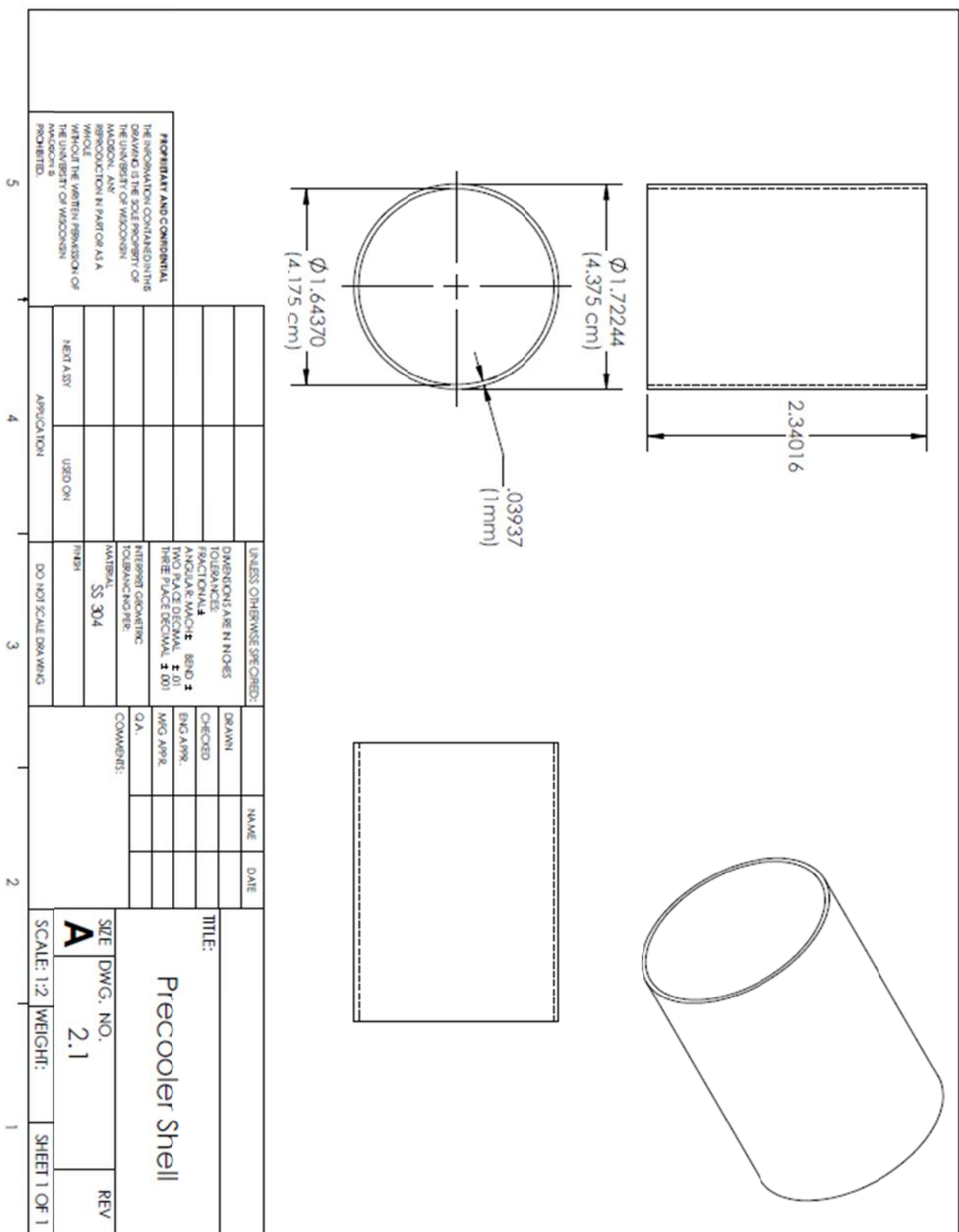


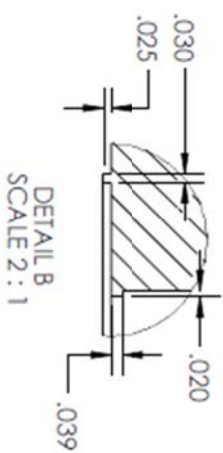
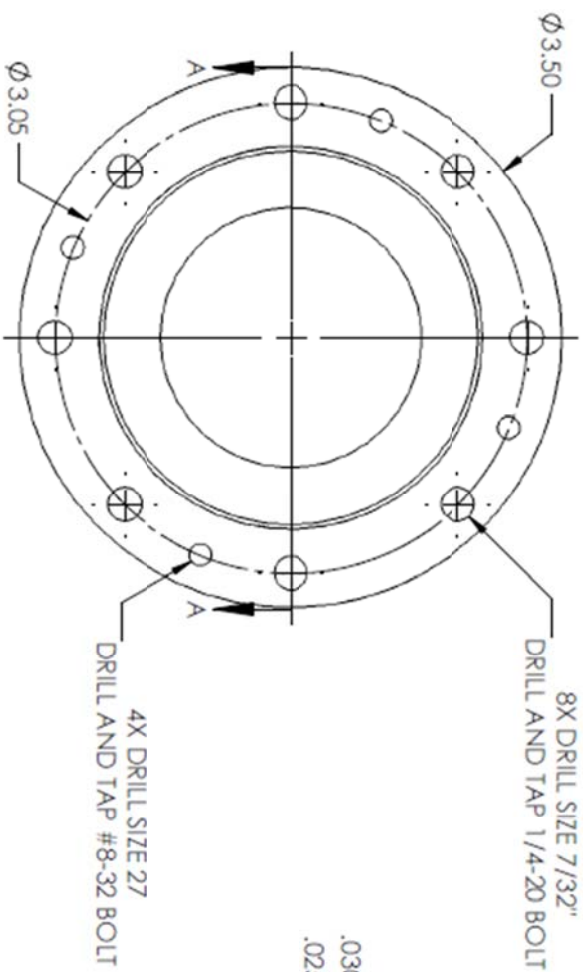
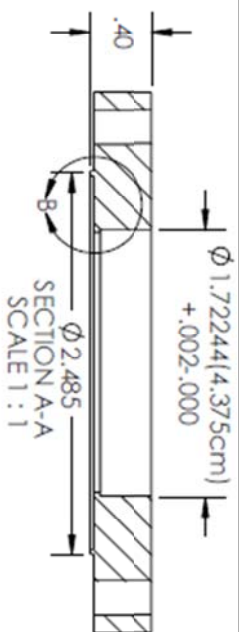
UNLESS OTHERWISE SPECIFIED: DIMENSIONS ARE IN INCHES TOLERANCES: FRACTIONAL ± .005 DECIMAL ± .001 ANGULAR MACHINE ± .01 TWO PLACE DECIMAL ± .01 THREE PLACE DECIMAL ± .001		DRAWN	NAME	DATE	TITLE: 1st Stage P.T. Shell
		CHECKED			
		ENG APPR.			
		MFG APPR.			
		Q.A.			
INTERPRET GEOMETRIC TOLERANCING PER: MATERIAL: SS 304 FINISH:		COMMENTS:			SIZE: DWG. NO. 1.4 SCALE: 1:4 WEIGHT: SHEET 1 OF 1
DO NOT SCALE DRAWING		NEXT ASSY USED ON:			
APPLICATION		5			
4		3			
1		2			

PROPRIETARY AND CONFIDENTIAL
 THE INFORMATION CONTAINED IN THIS
 DRAWING IS THE SOLE PROPERTY OF
 THE UNIVERSITY OF WISCONSIN
 MADISON. ANY
 REPRODUCTION IN PART OR AS A
 WHOLE
 WITHOUT THE WRITTEN PERMISSION OF
 THE UNIVERSITY OF WISCONSIN
 MADISON IS
 PROHIBITED.





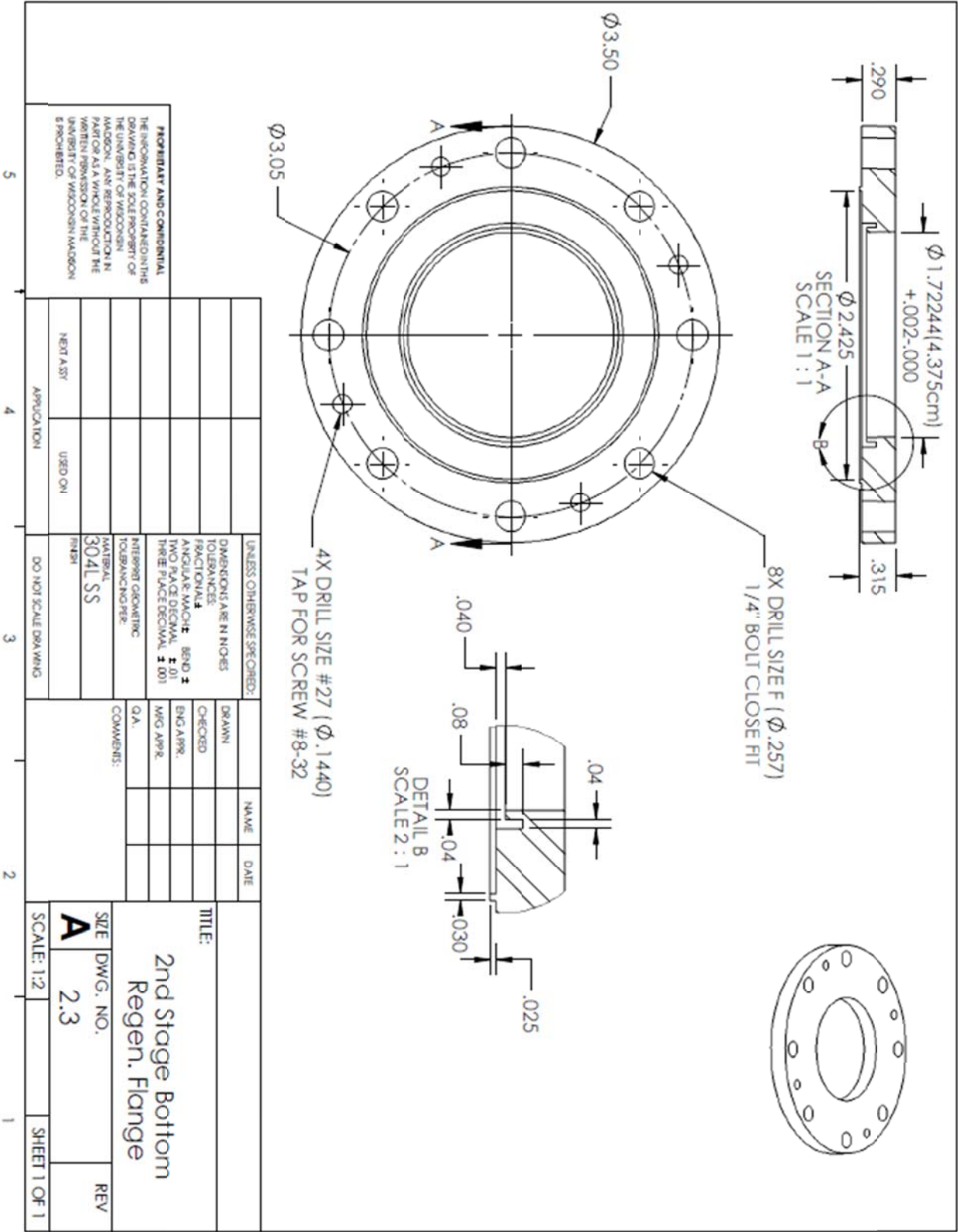




PROPRIETARY AND CONFIDENTIAL
THE INFORMATION CONTAINED IN THIS
DRAWING IS THE SOLE PROPERTY OF
THE UNIVERSITY OF WISCONSIN
MADISON. ANY REPRODUCTION IN
PART OR AS A WHOLE WITHOUT THE
WRITTEN PERMISSION OF THE
UNIVERSITY OF WISCONSIN MADISON
IS PROHIBITED.

5 4 3 2 1

UNLESS OTHERWISE SPECIFIED:				TITLE:	
DIMENSIONS ARE IN INCHES	DRAWN	NAME	DATE	Precooler Top Flange	
TOLERANCES	CHECKED				
FRACTIONS	ENG APPR.				
ANGULAR MATCH: .880 ±	W/C APPR.				
TWO PLACE DECIMAL: ±.01	Q.A.			SIZE DWG. NO. 2.2 REV	
THREE PLACE DECIMAL: ±.001	COMMENTS:				
INTERPRET DIMENSIONS					
TOLERANCES PER MATERIAL					
SS 304				SCALE: 1:1 SHEET 1 OF 1	
FINISH					
DO NOT SCALE DRAWING					
USED ON					
NEXT ASSY					
APPLICATION					



2nd Stage Regen. Shell

SCALE: 1:1

TITLE:

DWG. NO. 2.4

REV

SHEET 1 OF 1

DATE: 10/10/2010

UNLESS OTHERWISE SPECIFIED:

DIMENSIONS ARE IN INCHES

TOLERANCES:

FRACTIONAL ±

ANGULAR MAJOR ± BOND ±

TWO PLACE DECIMAL ± 0.01

THREE PLACE DECIMAL ± 0.001

INTERPRET DRAWING:

TOLERANCE PER:

MATERIAL:

FINISH:

COMMENTS:

QA:

DATE:

NAME:

DRAWN:

CHECKED:

ENG APPR:

MFG APPR:

DO NOT SCALE DRAWING

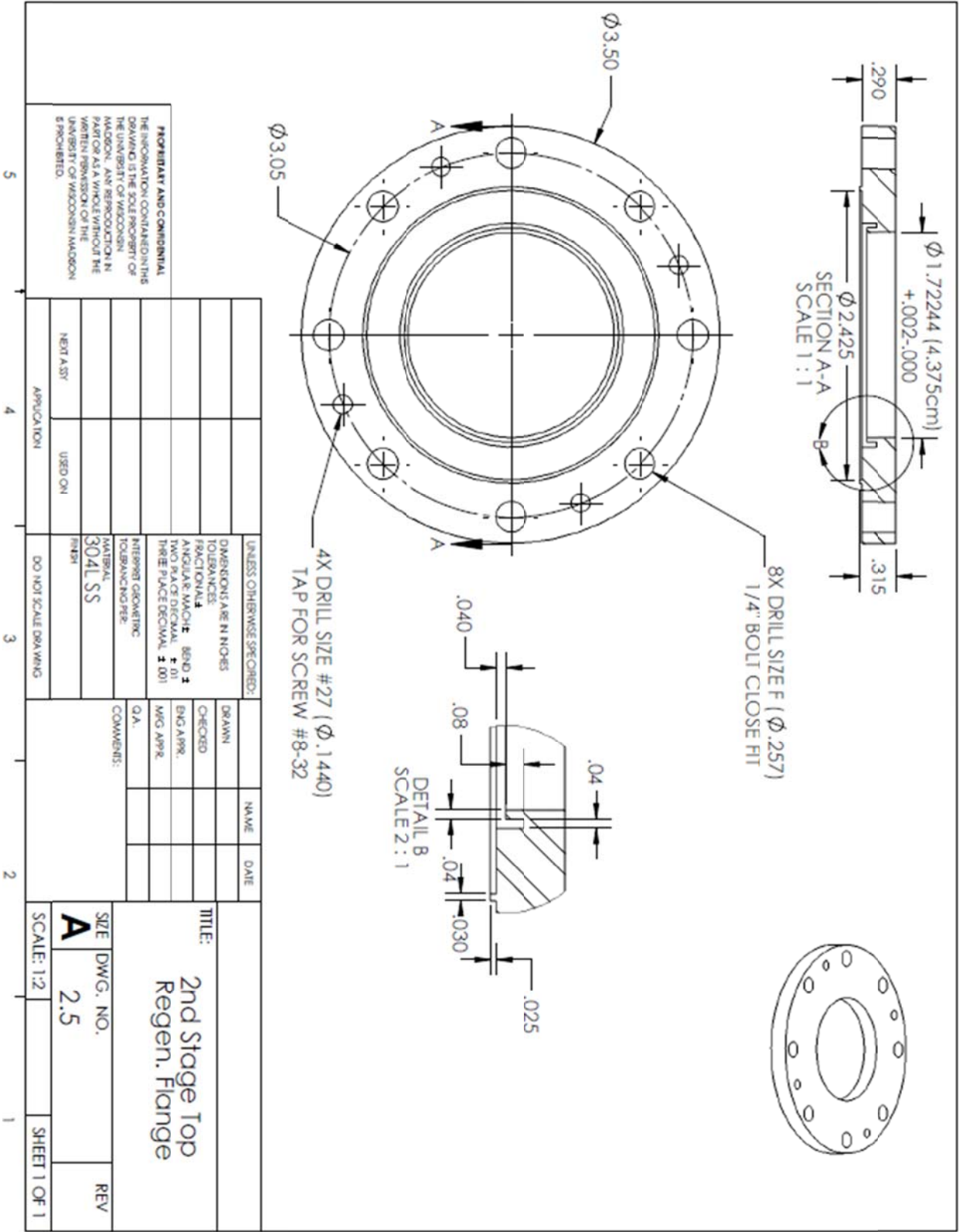
USED ON:

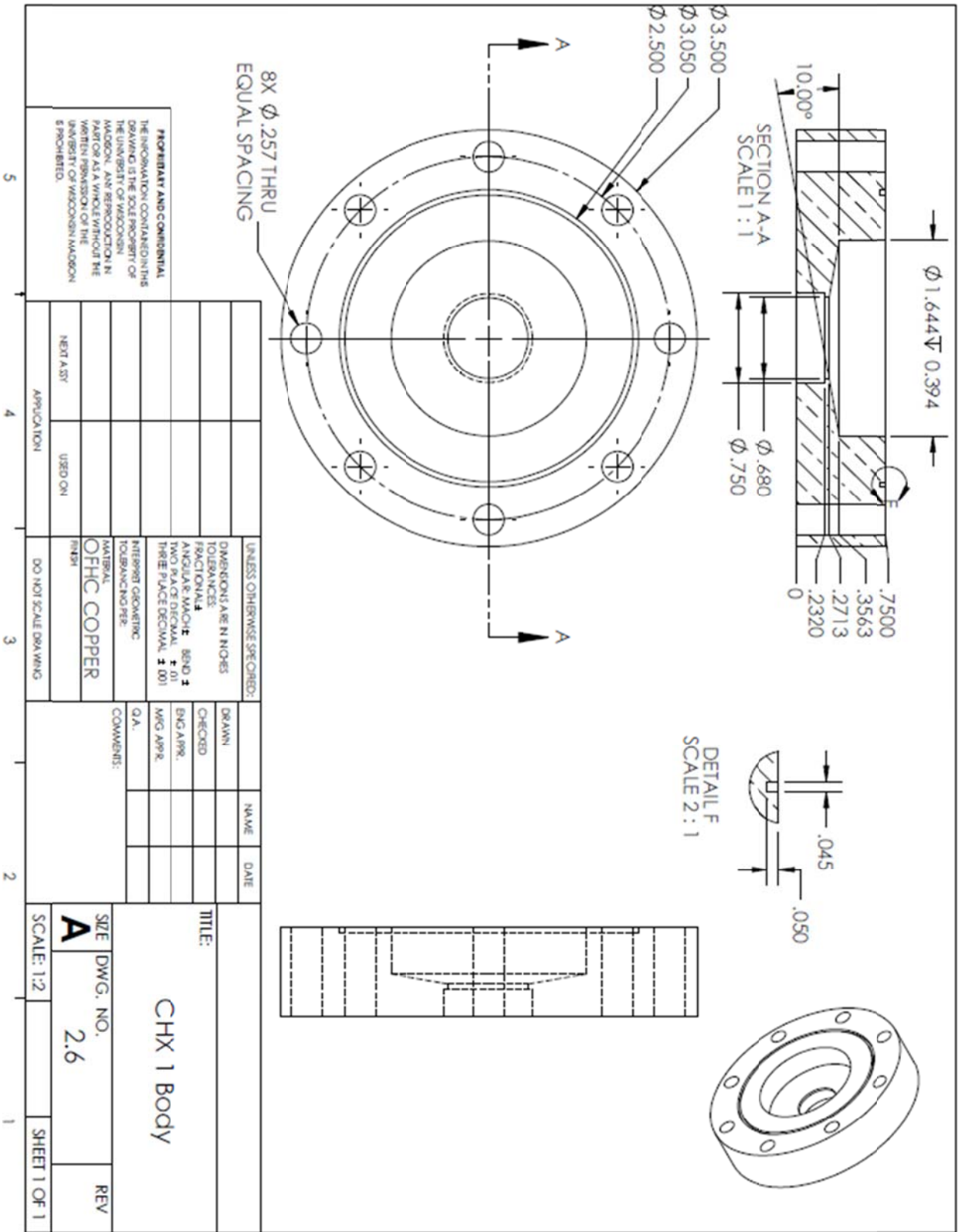
NEXT ASSY:

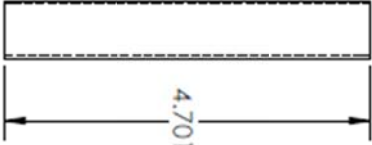
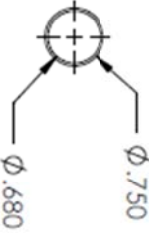

APPLICATION:

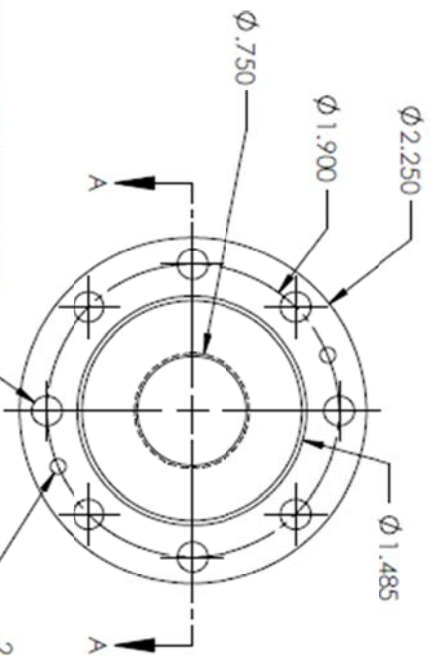
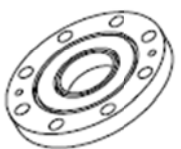
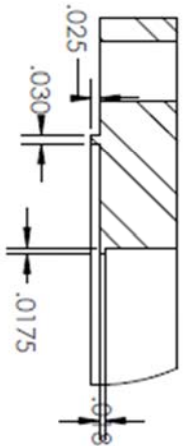
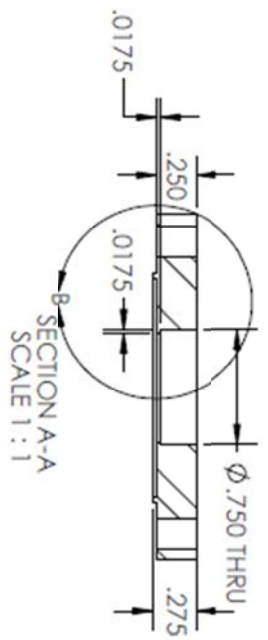
PROPERTY AND CONFIDENTIAL

THE INFORMATION CONTAINED IN THIS DRAWING IS THE SOLE PROPERTY OF THE UNIVERSITY OF WISCONSIN-MADISON. ANY REPRODUCTION IN WHOLE OR IN PART WITHOUT THE WRITTEN PERMISSION OF THE UNIVERSITY OF WISCONSIN-MADISON IS PROHIBITED.





					
<p>PROPERTY AND CONFIDENTIAL</p> <p>THE INFORMATION CONTAINED IN THIS DRAWING IS THE SOLE PROPERTY OF MADISON. ANY REPRODUCTION IN PART OR AS A WHOLE WITHOUT THE WRITTEN PERMISSION OF THE UNIVERSITY OF WISCONSIN MADISON IS PROHIBITED.</p>					
<p>UNLESS OTHERWISE SPECIFIED:</p>		<p>DIMENSIONS ARE IN INCHES</p>		<p>TOLERANCES</p>	
<p>FRACTIONS</p>		<p>DECIMALS</p>		<p>ANGULAR WORK: BEND ± TWO PLACE DECIMAL ± .01</p>	
<p>THREE PLACE DECIMAL ± .001</p>		<p>INTERPRET GOING INTO TOLERANCE</p>		<p>INTERPRET GOING INTO TOLERANCE</p>	
<p>MATERIAL</p>		<p>304 SS</p>		<p>COMMENTS:</p>	
<p>NEST ASY</p>		<p>USED ON</p>		<p>Q.A.</p>	
<p>APPLICATION</p>		<p>DO NOT SCALE DRAWING</p>		<p>DATE</p>	
<p>5</p>		<p>4</p>		<p>2</p>	
<p>1</p>		<p>2</p>		<p>1</p>	
<p>TITLE:</p>		<p>2nd Stage P.T. Shell</p>		<p>SCALE: 1:2</p>	
<p>SIZE</p>		<p>DWG. NO.</p>		<p>REV</p>	
<p>A</p>		<p>2.7</p>		<p>SHEET 1 OF 1</p>	

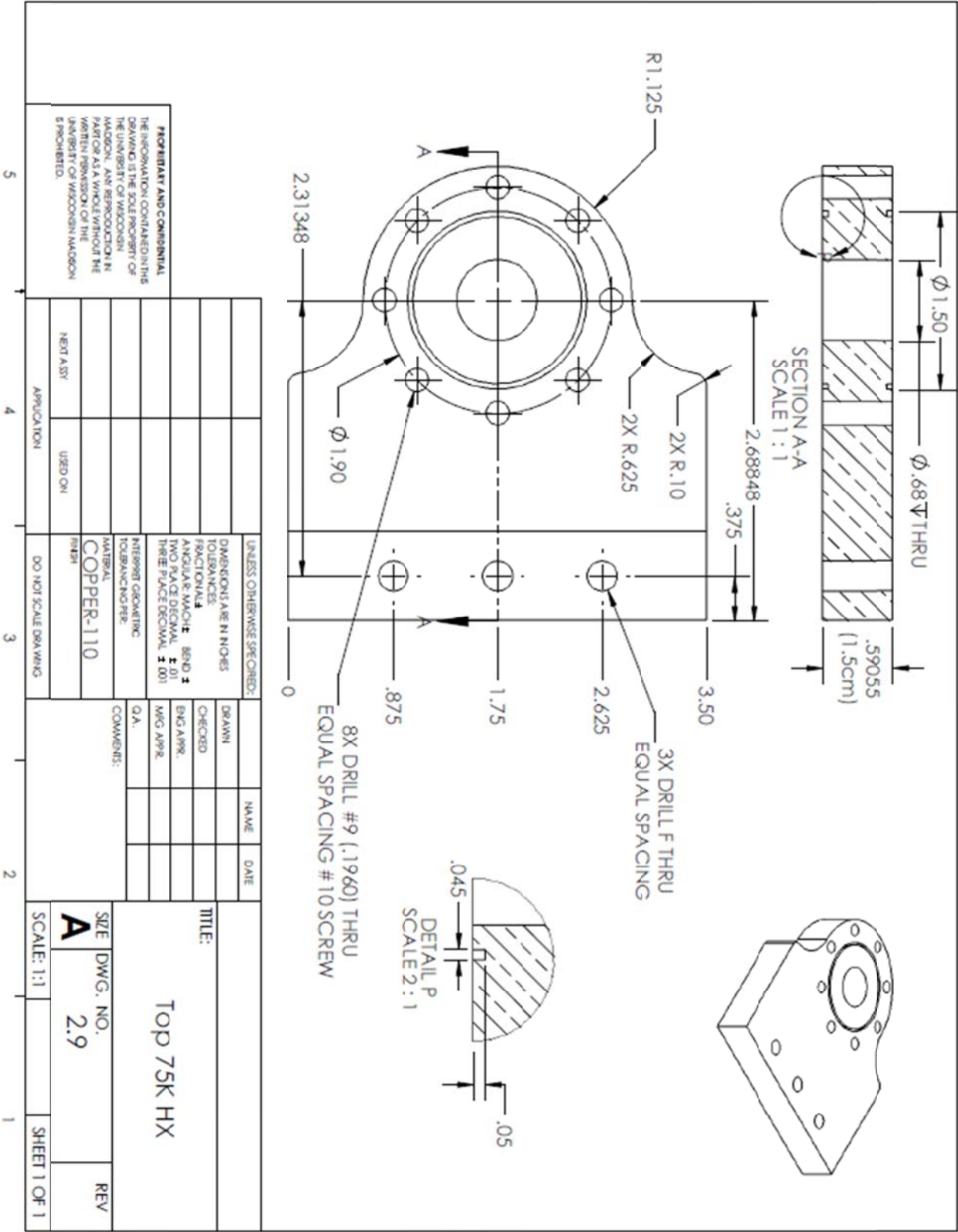


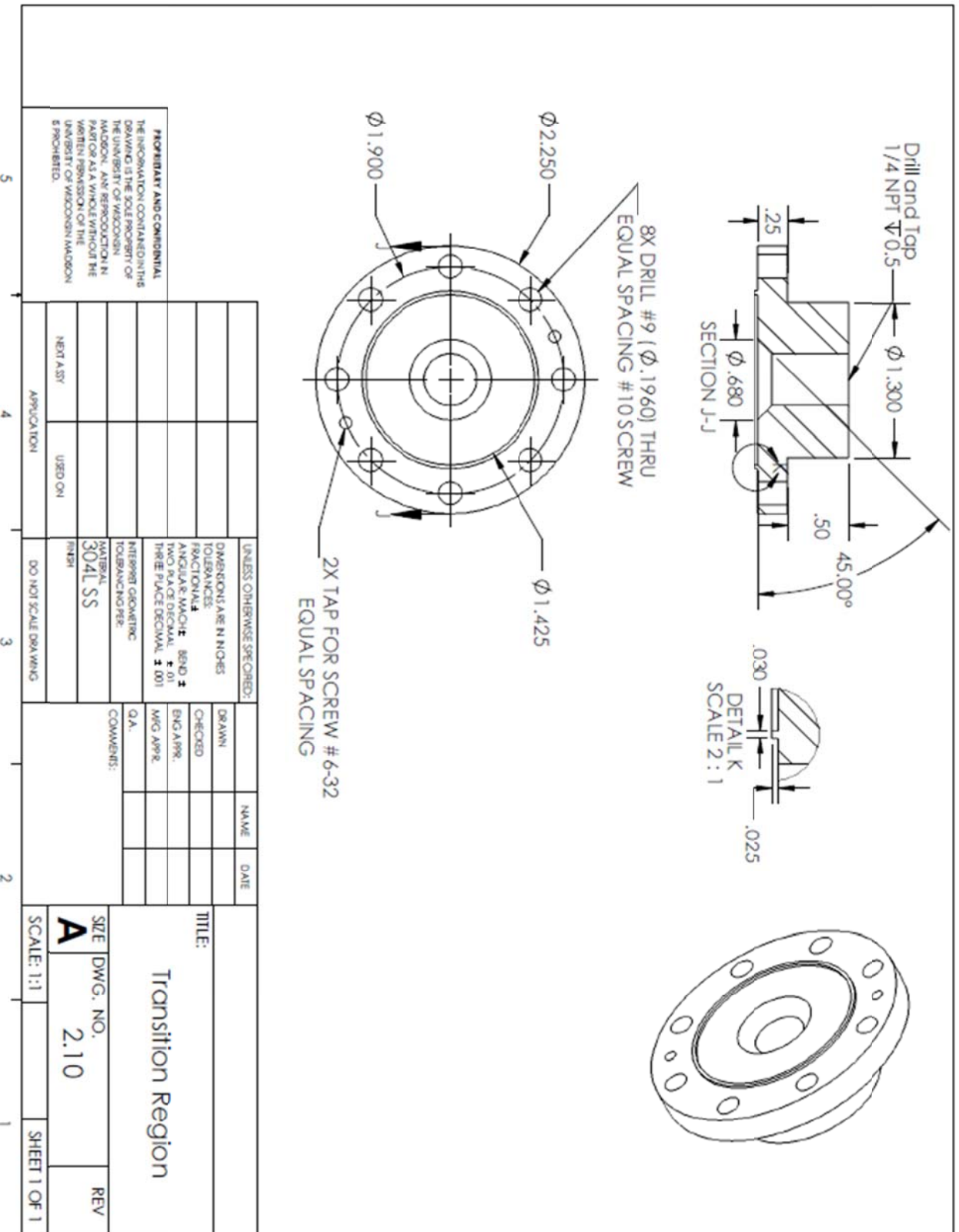
8X DRILL #9 (.1960) THRU
EQUAL SPACING #10 SCREW

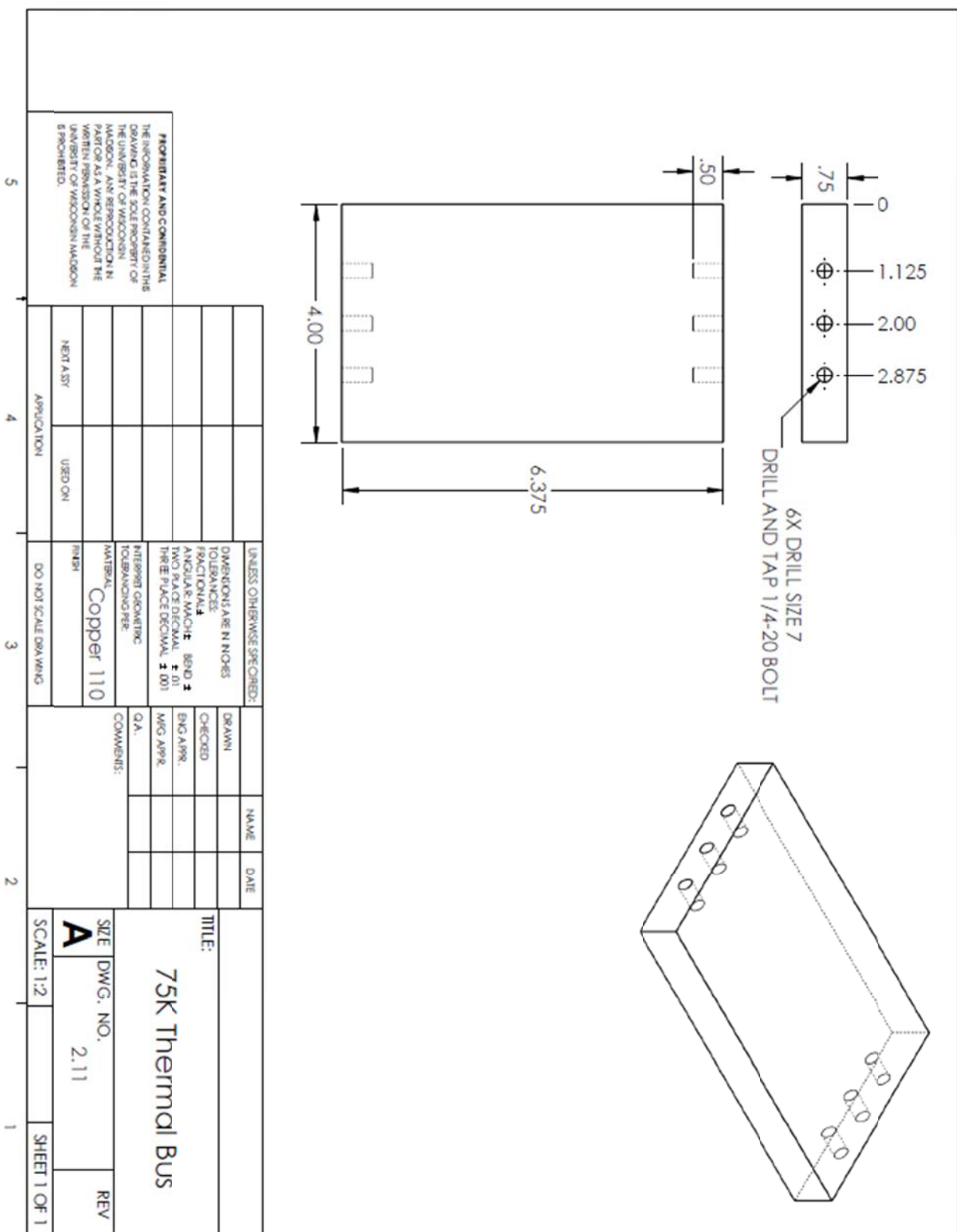
2X DRILL SIZE #40 (0.0980)
TAP FOR SCREW #4-48
EQUAL SPACING

PROPRIETARY AND CONFIDENTIAL
THE INFORMATION CONTAINED IN THIS
DRAWING IS THE SOLE PROPERTY OF
THE UNIVERSITY OF WISCONSIN
MADISON. ANY REPRODUCTION IN
WHOLE OR IN PART WITHOUT THE
WRITTEN PERMISSION OF THE
UNIVERSITY OF WISCONSIN MADISON
IS PROHIBITED.

--	--	--	--	--	--	--	--	--	--	--	--	--	--	--	--	--	--	--	--	--	--	--	--	--	--	--	--	--	--	--	--	--	--	--	--	--	--	--	--	--	--	--	--	--	--	--	--	--	--	--	--	--	--	--	--	--	--	--	--	--	--	--	--	--	--	--	--	--	--	--	--	--	--	--	--	--	--	--	--	--	--	--	--	--	--	--	--	--	--	--	--	--	--	--	--	--	--	--	--	--	--	--	--	--	--	--	--	--	--	--	--	--	--	--	--	--	--	--	--	--	--	--	--	--	--	--	--	--	--	--	--	--	--	--	--	--	--	--	--	--	--	--	--	--	--	--	--	--	--	--	--	--	--	--	--	--	--	--	--	--	--	--	--	--	--	--	--	--	--	--	--	--	--	--	--	--	--	--	--	--	--	--	--	--	--	--	--	--	--	--	--	--	--	--	--	--	--	--	--	--	--	--	--	--	--	--	--	--	--	--	--	--	--	--	--	--	--	--	--	--	--	--	--	--	--	--	--	--	--	--	--	--	--	--	--	--	--	--	--	--	--	--	--	--	--	--	--	--	--	--	--	--	--	--	--	--	--	--	--	--	--	--	--	--	--	--	--	--	--	--	--	--	--	--	--	--	--	--	--	--	--	--	--	--	--	--	--	--	--	--	--	--	--	--	--	--	--	--	--	--	--	--	--	--	--	--	--	--	--	--	--	--	--	--	--	--	--	--	--	--	--	--	--	--	--	--	--	--	--	--	--	--	--	--	--	--	--	--	--	--	--	--	--	--	--	--	--	--	--	--	--	--	--	--	--	--	--	--	--	--	--	--	--	--	--	--	--	--	--	--	--	--	--	--	--	--	--	--	--	--	--	--	--	--	--	--	--	--	--	--	--	--	--	--	--	--	--	--	--	--	--	--	--	--	--	--	--	--	--	--	--	--	--	--	--	--	--	--	--	--	--	--	--	--	--	--	--	--	--	--	--	--	--	--	--	--	--	--	--	--	--	--	--	--	--	--	--	--	--	--	--	--	--	--	--	--	--	--	--	--	--	--	--	--	--	--	--	--	--	--	--	--	--	--	--	--	--	--	--	--	--	--	--	--	--	--	--	--	--	--	--	--	--	--	--	--	--	--	--	--	--	--	--	--	--	--	--	--	--	--	--	--	--	--	--	--	--	--	--	--	--	--	--	--	--	--	--	--	--	--	--	--	--	--	--	--	--	--	--	--	--	--	--	--	--	--	--	--	--	--	--	--	--	--	--	--	--	--	--	--	--	--	--	--	--	--	--	--	--	--	--	--	--	--	--	--	--	--	--	--	--	--	--	--	--	--	--	--	--	--	--	--	--	--	--	--	--	--	--	--	--	--	--	--	--	--	--	--	--	--	--	--	--	--	--	--	--	--	--	--	--	--	--	--	--	--	--	--	--	--	--	--	--	--	--	--	--	--	--	--	--	--	--	--	--	--	--	--	--	--	--	--	--	--	--	--	--	--	--	--	--	--	--	--	--	--	--	--	--	--	--	--	--	--	--	--	--	--	--	--	--	--	--	--	--	--	--	--	--	--	--	--	--	--	--	--	--	--	--	--	--	--	--	--	--	--	--	--	--	--	--	--	--	--	--	--	--	--	--	--	--	--	--	--	--	--	--	--	--	--	--	--	--	--	--	--	--	--	--	--	--	--	--	--	--	--	--	--	--	--	--	--	--	--	--	--	--	--	--	--	--	--	--	--	--	--	--	--	--	--	--	--	--	--	--	--	--	--	--	--	--	--	--	--	--	--	--	--	--	--	--	--	--	--	--	--	--	--	--	--	--	--	--	--	--	--	--	--	--	--	--	--	--	--	--	--	--	--	--	--	--	--	--	--	--	--	--	--	--	--	--	--	--	--	--	--	--	--	--	--	--	--	--	--	--	--	--	--	--	--	--	--	--	--	--	--	--	--	--	--	--	--	--	--	--	--	--	--	--	--	--	--	--	--	--	--	--	--	--	--	--	--	--	--	--	--	--	--	--	--	--	--	--	--	--	--	--	--	--	--	--	--	--	--	--	--	--	--	--	--	--	--	--	--	--	--	--	--	--	--	--	--	--	--	--	--	--	--	--	--	--	--	--	--	--	--	--	--	--	--	--	--	--	--	--	--	--	--	--	--	--	--	--	--	--	--	--	--	--	--	--	--	--	--	--	--	--	--	--	--	--	--	--	--	--	--	--	--	--	--	--	--	--	--	--	--	--	--	--	--	--	--	--	--	--	--	--	--	--	--	--	--	--	--	--	--	--	--	--	--	--	--	--	--	--	--	--	--	--	--	--	--	--	--	--	--	--	--	--	--	--	--	--	--	--	--	--	--	--	--	--	--	--	--	--	--	--	--	--	--	--	--	--	--	--	--	--	--	--	--	--	--	--	--	--	--	--	--	--	--	--	--	--	--	--	--	--	--	--	--	--	--	--	--	--	--	--	--	--	--	--	--	--	--	--	--	--	--	--	--	--	--	--	--	--	--	--	--	--	--	--	--	--	--	--	--	--	--	--	--	--	--	--	--	--	--	--	--	--	--	--	--	--	--	--	--	--	--	--	--	--	--	--	--	--	--	--	--	--	--	--	--	--	--	--	--	--	--	--	--	--	--	--	--	--	--	--	--	--	--	--	--	--	--	--	--	--	--	--	--	--	--	--	--	--	--	--	--	--	--	--	--	--	--	--	--	--	--	--	--	--	--	--	--	--	--	--	--	--	--	--	--	--	--	--	--	--	--	--	--	--	--	--	--	--	--	--	--	--	--	--	--	--	--	--	--	--	--	--	--	--	--	--	--	--	--	--	--	--	--	--	--	--	--	--	--	--	--	--	--	--	--	--	--	--	--	--	--	--	--	--	--	--	--	--	--	--	--	--	--	--	--	--	--	--	--	--	--	--	--	--	--	--	--	--	--	--	--	--	--	--	--	--	--	--	--	--	--	--	--	--	--	--







Appendix B: ESS and MATLAB Code

Thermal Bus for Two Stage PTC (discussed in 2.4.2)

```
SubProgram FindLimit(T_T:k_int)
    T_B=76[K]                                "Temperature of Bottom HX"
    k=Conductivity(Copper, T=T)              "Conductivity of Copper"
    k_int=INTEGRAL(k,T,T_B,T_T)             "Integrated conductivity from T_B to T_T"
end
```

```
T_B=76[K]                                "Temperature of Bottom HX"
q=11[W]                                "Heat load from top 75K HX"
L=20.13400659*convert(cm,m)             "Length of Thermal Bus"
A=A_in2*convert(in^2,m^2)               "Area of Thermal Bus"
k_int=q*L/A                             "Equation to find area"
Call FindLimit(T_T:k_int)
DELTAT=T_T-T_B                          "Temperature between top and bottom HX"
```

Top 300K Heat Exchanger ESS Code (discussed in 2.5.4)

```
rho=1000[kg/m^3]                        "Density of H2O"
mu=Viscosity(Water,T=300[K],P=101300[Pa]) "Viscosity of H2O"
cp=Cp(Water,T=300[K],P=101300[Pa])      "Cp of H2O"
k_H2O=Conductivity(Water,T=300[K],P=101300[Pa]) "Conductivity of H2O"
k=Conductivity(Copper, T=300[K])         "Conductivity of Copper"
```

```
V_dot_cc=(0.0035/11)                   "Volumetric flow rate experimentally measured"
D_cc=.5*convert(in,m)                   "ID of tube from T to sink"
A_cc=.375*convert(in,m)*1.5*convert(cm,m) "Area of Tube"
```

```
r_1=(1.402/2)*convert(in,m)             "ID of Copper"
r_2=(1.75/2)*convert(in,m)             "OD of Copper"
l=1.5*convert(cm,m)                     "Thickness of Copper"
T_inf=293.7[K]                          "Measured value of cooling water"
```

```
Re_h=rho*u_inf*2*r_2/mu                  "Re number"
Pr_h=cp*mu/k_H2O                         "Pr number"
```

```
Call External_Flow_Cylinder_ND(Re_h,Pr_h: Nusselt_h,C_d)
Nusselt_h=h*2*r_2/k_H2O                  "Nu number"
T=q*((ln(r_2/r_1)/(2*pi*l*k)))+(1/(2*pi*l*k))+T_inf "Temp of He"
```

Thermal Bus from GM Cooler to 2nd Stage PTC

//Heat Transfer to Bottom 75K HX (Target Q=35.8[W])

T[0]=60[K]

T[A+B+C]=75[K]

"Temperature of GM cooler"
"Temperature of bottom 75K HX"

L_bar=12*convert(in,m)

L_strap=4*convert(in,m)

L_con=1.5*convert(in,m)

A_bar=3*convert(in^2,m^2)

A_strap=4*0.3927*convert(in^2,m^2)

A_con=1*convert(in^2,m^2)

"Length of large bar"

"Length of straps"

"Length of small bar"

"Area of large bar"

"Area of straps"

"Area of small bar"

A=48

B=16

C=6

DELTAx=L_bar/A

DELTAy=L_strap/B

DELTAz=L_con/C

"Nodes in large bar"

"Nodes in straps"

"Nodes in small bar"

"Step size in large bar"

"Step size in straps"

"Step size in small bar"

Duplicate i=1,A+B+C

k[i]=Conductivity(Copper, T=(T[i]+T[i-1])/2)

end

"Conductivity at each node"

Duplicate i=1,A

R[i]=DELTAx/(k[i]*A_bar)

Q=(T[i]-T[i-1])/R[i]

end

"Resistance in large bar"

"Fourier's law"

Duplicate i=A+1,A+B

R[i]=DELTAy/(k[i]*A_strap)

Q=(T[i]-T[i-1])/R[i]

end

"Resistance in straps"

"Fourier's law"

Duplicate i=1+A+B,C+A+B

R[i]=DELTAz/(k[i]*A_con)

Q=(T[i]-T[i-1])/R[i]

end

"Resistance in small bar"

"Fourier's law"

A_s=2*0.1963*convert(in^2,m^2)

L_s=2*convert(ft,m)

k_s=Conductivity(Copper, T=T_s)

Q_s=(A_s/L_s)*Integral(k_s,T_s,60,75)

"Area of extra strap"

"Length of extra strap"

"Conductivity through strap"

"Fourier's law"

Q_T_b=Q_s+Q

"Total heat transfer"

//Heat Transfer to Top 75K HX (Target Q=10.9[W])

T[0]=60[K]

"Temperature of GM cooler"

T[A+B]=75[K]

"Temperature of top 75K HX"

L_bar=12*convert(in,m)

"Length of bar"

L_strap=2*convert(in,m)

"Length of strap"

A_bar=.75*convert(in^2,m^2)

"Area of bar"

A_strap=2*0.1963*convert(in^2,m^2)

"Area of strap"

A=48

"Nodes in bar"

B=16

"Nodes in strap"

DELTAx=L_bar/A

"Step size in bar"

DELTAy=L_strap/B

"Step size in strap"

Duplicate i=0,A+B

"Conductivity at each node"

k[i]=Conductivity(Copper, T=T[i])

end

Duplicate i=1,A

R[i]=DELTAx/(k[i]*A_bar)

"Resistance in bar"

Q=(T[i]-T[i-1])/R[i]

"Fourier's law"

end

Duplicate i=A+1,A+B

R[i]=DELTAy/(k[i]*A_strap)

"Resistance in strap"

Q=(T[i]-T[i-1])/R[i]

"Fourier's law"

Phase angle Matlab code (Only the method for P1 and L are shown)

```

clear
uiimport                                     %import mechanical data
pause                                       %pause until any key is pressed

time=(0:0.0002222:4.9997)';               %Time vector (data taken for 5s at 4.5Hz)
C=[time A];                               %creates matrix: time P1 P2 P3 P4 P5 P6 L R L_C R_C

P1=C(:,2);                                %Pressure Vectors
fP1=fit(time,P1,'fourier1');              %Fourier Transform
a0P1=fP1.a0+15;                           %Define Fourier series values
a1P1=fP1.a1;
b1P1=fP1.b1;
freqP1=fP1.w/(2*pi)                       %Frequency
phiP1d=atan2d(b1P1,a1P1);                 %Find phi in degrees
magP1=sqrt(a1P1^2+b1P1^2)                 %Magnitude
phiP1drel=0;                              %Set Phi_P1=0
plot(fP1,time,P1)                         %Plot of data and Fourier series fit
xlabel('Time (s)')
ylabel('Pressure (psi)')
axis([0.2,0.25,-inf,inf])
PR1=(a0P1+magP1)/(a0P1-magP1)
pause

fs=4500;                                  % sample rate [Hz]
n=length(P1);                             % number of points
f = (0:n-1)*(fs/n);                       % conversion from bins to Hz
P1fft = fft(P1);                          % DFT of signal
P1ABS=abs(P1fft);                          % magnitude of DFT
P1ABS(1)=0;
plot(f,P1ABS)                             % plot Frequency vs magnitude
xlabel('Frequency (Hz)')
ylabel('Magnitude')
axis([0,500,-inf,inf])
pause

%same method for P2 P3 P4 P5 P6 L R L_C and R_C
L=C(:,8);
fL=fit(time,L,'fourier1');
a0L=fL.a0;
a1L=fL.a1;
b1L=fL.b1;
freqL=fL.w/(2*pi);
phiL=atan2d(b1L,a1L);
magL=sqrt(a1L^2+b1L^2);
phiLd=phiP1d-phiL;
plot(fL,time,L);
xlabel('Time (s)')
ylabel('Displacement (mm)')
axis([0.2,0.25,-inf,inf])
pause

```